

Review

Transition Metal–(μ -Cl)–Aluminum Bonding in α -Olefin and Diene Chemistry

Ilya E. Nifant'ev^{1,2}, Ildar I. Salakhov¹ and Pavel V. Ivchenko^{1,2,*}

¹ A.V. Topchiev Institute of Petrochemical Synthesis, Russian Academy of Sciences (RAS), 29 Leninsky Pr., 119991 Moscow, Russia

² Chemistry Department, M.V. Lomonosov Moscow State University, 1-3 Leninskie Gory, 119991 Moscow, Russia

* Correspondence: phpasha1@yandex.ru

Abstract: Olefin and diene transformations, catalyzed by organoaluminum-activated metal complexes, are widely used in synthetic organic chemistry and form the basis of major petrochemical processes. However, the role of M–(μ -Cl)–Al bonding, being proven for certain $>C=C<$ functionalization reactions, remains unclear and debated for essentially more important industrial processes such as oligomerization and polymerization of α -olefins and conjugated dienes. Numerous publications indirectly point at the significance of M–(μ -Cl)–Al bonding in Ziegler–Natta and related transformations, but only a few studies contain experimental or at least theoretical evidence of the involvement of M–(μ -Cl)–Al species into catalytic cycles. In the present review, we have compiled data on the formation of M–(μ -Cl)–Al complexes (M = Ti, Zr, V, Cr, Ni), their molecular structure, and reactivity towards olefins and dienes. The possible role of similar complexes in the functionalization, oligomerization and polymerization of α -olefins and dienes is discussed in the present review through the prism of the further development of Ziegler–Natta processes and beyond.

Keywords: carboalumination; DFT; dienes; hydroalumination; heterobimetallic complexes; metallocenes; methylenealkanes; olefins; oligomerization; polymerization; polyolefins; single-site catalysts; Ziegler–Natta catalysts



Citation: Nifant'ev, I.E.; Salakhov, I.I.; Ivchenko, P.V. Transition Metal–(μ -Cl)–Aluminum Bonding in α -Olefin and Diene Chemistry. *Molecules* **2022**, *27*, 7164. <https://doi.org/10.3390/molecules27217164>

Academic Editor:
Athanassios C. Tsipis

Received: 30 September 2022

Accepted: 20 October 2022

Published: 23 October 2022

Publisher's Note: MDPI stays neutral with regard to jurisdictional claims in published maps and institutional affiliations.



Copyright: © 2022 by the authors. Licensee MDPI, Basel, Switzerland. This article is an open access article distributed under the terms and conditions of the Creative Commons Attribution (CC BY) license (<https://creativecommons.org/licenses/by/4.0/>).

1. Introduction

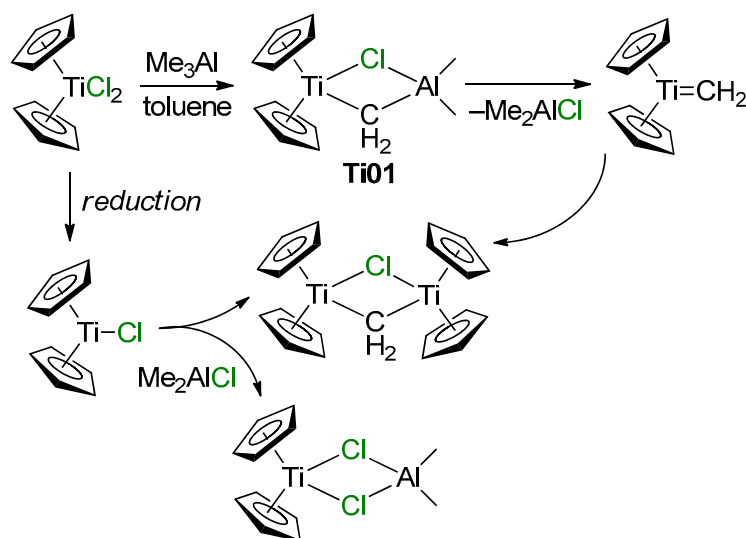
In the past few decades, catalytic transformations of olefins and conjugated dienes have become mainstream processes of the petrochemical industry: polyolefins are major multi-tonnage plastics [1,2]; polydienes are still indispensable in rubber manufacturing [3,4]. Advanced technologies of polyolefins and diene rubbers are based on the coordination polymerization of α -olefins, buta-1,3-diene, and isoprene [1,2,4–11]. Selective coordination di-, tri- and tetramerization of ethylene [12–15] are also industrially important processes. Coordination oligomerization [16,17], as well as the hydro- and carboalumination [18] of higher α -olefins, are currently lab-based processes, even though they show strong industrial prospects.

Supported metal salts (primarily chlorides) or metal complexes as pre-catalysts, and organoaluminum compounds as co-catalysts, are used in the majority of these processes. After activation, the reaction mixtures contain metal alkyls and alkylaluminum chlorides. In coordination polymerization, mechanistic understanding of the reaction mechanism as a coordination/insertion of α -olefin or diene molecule at the metal–alkyl (or metal–hydride) center in stable ligand environments is generally accepted [13,16,19–21]. For group 4 metal polymerization catalysts, the conventional Cossee–Arlman mechanism has been expanded by including interactions between the metal center and bulky counterions (XMAO[−], B(C₆F₅)₄[−], anionic supports, etc.) [22–35], and binuclear Zr₂ complexes [34,36]; however, the direct participation of R₂AlCl in the formation of catalytic species remains hypothetical, even with the results of numerous experimental and theoretical studies [37–43]. It is also an

2. Complexes of Ti

2.1. The Tebbe Reagent and Similar Ti Complexes

The Ti–Al heterobimetallic complex of the formula $\text{Cp}_2\text{Ti}(\mu\text{-Cl})(\mu\text{-CH}_2)\text{AlMe}_2$ (**Ti01**) was first synthesized by Tebbe et al. in 1978; the reaction of Cp_2TiCl_2 with AlMe_3 resulted in the formation of **Ti01** with 80–90% yields [49]. The synthesis of **Ti01** was complicated by side reactions (Scheme 1), making it difficult to isolate the samples suitable for X-ray diffraction (XRD) analysis, and as a result, the molecular structure of **Ti01** was only determined in 2014 [50] (Figure 2a). The difference between interatomic distances ($d(\text{Ti}-\text{CH}_2) < d(\text{Al}-\text{CH}_2)$, $d(\text{Ti}-\text{Cl}) > d(\text{Al}-\text{Cl})$) considers **Ti01** as a complex of $\text{Cp}_2\text{Ti}=\text{CH}_2$ and Me_2AlCl . In this way, in **Ti01**, Me_2AlCl serves as a stabilizing agent for the Ti(IV) carbene complex, that can be removed by Lewis base.



Scheme 1. Synthesis of Tebbe reagent **Ti01** and possible side reactions and products [50].

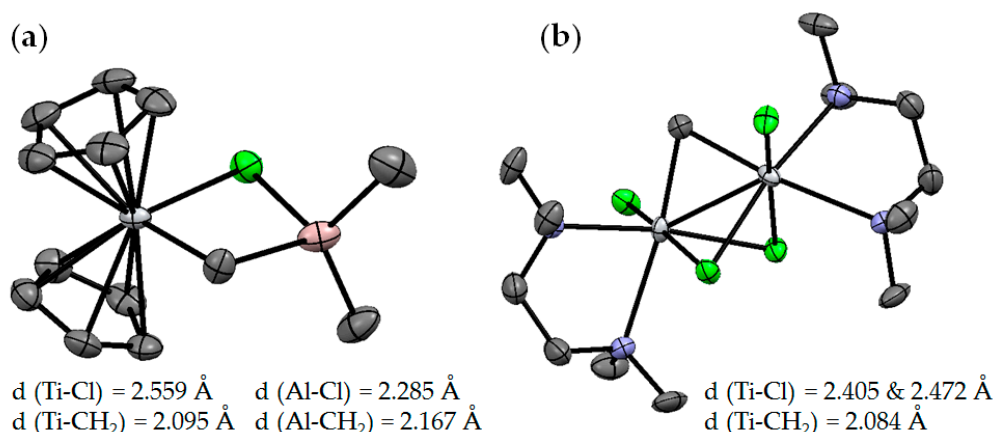
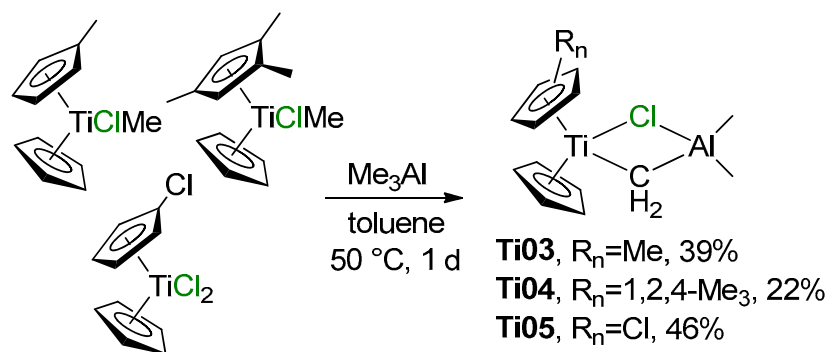


Figure 2. Molecular structures of (a) **Ti01** [50] and (b) **Ti02** [51]. The hydrogen atoms are omitted for clarity.

A structural analog of the Tebbe reagent, **Ti02**, was synthesized by the reaction of the N^1, N^1, N^2, N^2 -tetramethylethane-1,2-diamine (TMEDA) complex $(\text{TMEDA})\text{TiCl}_3(\text{THF})$ with $[(\text{TMEDA})\text{ZnI}]_2\text{CH}_2$ [51]. Analysis of the molecular structure of **Ti02** (Figure 2b) showed that the value of $d(\text{Ti}-\text{CH}_2)$ does not differ from that in **Ti01**. Notably, a series of chlorine-free analogs of Tebbe reagent was described in [52].

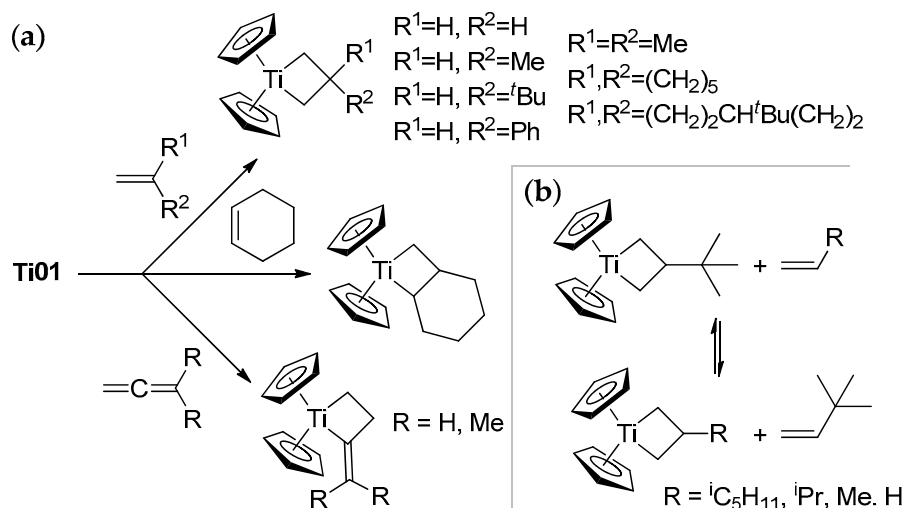
Close structural analogs of **Ti01** were synthesized by the reactions of $(\eta^5\text{-C}_5\text{H}_4\text{Me})\text{CpTiClMe}$ and $(\eta^5\text{-1,2,4-C}_5\text{H}_2\text{Me}_3)\text{CpTiClMe}$ with Me_3Al (Scheme 2, complexes **Ti03** and **Ti04**, respectively) or by the interaction of $(\eta^5\text{-C}_5\text{H}_4\text{Cl})\text{CpTiCl}_2$ with Me_3Al (Scheme 2, complex

Ti05 [53]. Treatment of $\text{Cp}_2\text{TiCl}(\text{CH}=\text{CHMe})$ with ${}^i\text{Bu}_2\text{AlH}$ resulted in the formation of complex $\text{Cp}_2\text{Ti}(\mu\text{-Cl})(\mu\text{-CHEt})\text{Al}{}^i\text{Bu}_2$ [54]; the product was not isolated, but has been identified by NMR spectroscopy. The attempt of Halterman and Ramsey to synthesize the chiral Tebbe reagent from 1,1'-binaphthyl-bridged bis(η^5 -tetrahydroinden-2-yl) Ti(IV) dichloride failed [55].



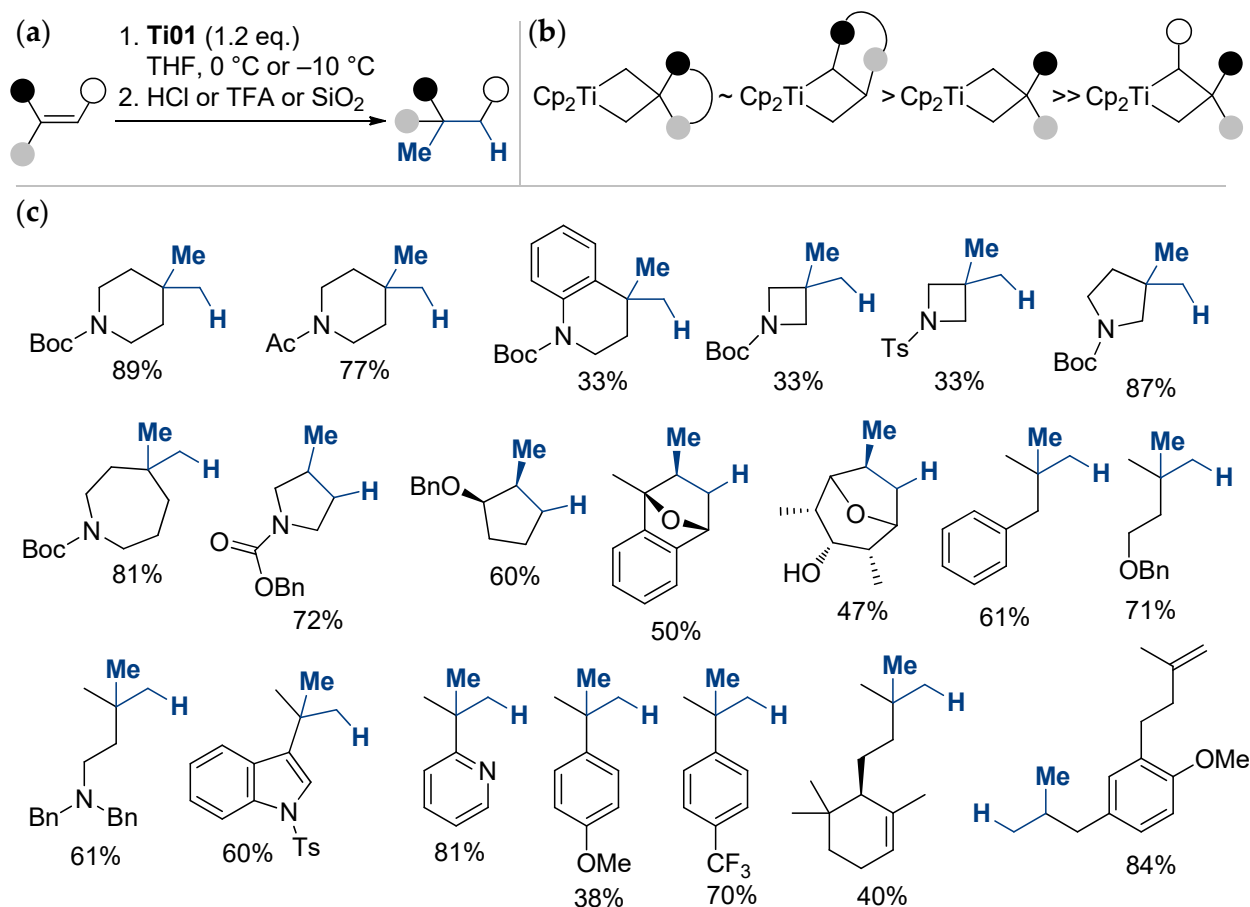
Scheme 2. Synthesis of ring-substituted analogs of the Tebbe reagent [53].

Ti01 has found its main applications for carbonyl methylenation similarly to phosphonium ylides in the Wittig reaction [52]. The reactions of **Ti01** with carbonyl compounds are rapid and selective, even in the presence of other reactive groups (for example, $-\text{COOR}$ [56], $-\text{C}=\text{NOR}$ [57]), but this subject is beyond the scope of our review. However, α -olefins can react with **Ti01**: as shown by Grubbs et al., this reaction resulted in the formation of titanacyclobutanes, and allenes formed titanacyclobutanes with exocyclic C=C bonds (Scheme 3a) [58–60]. Titanacyclobutanes are reactive towards α -olefins, as demonstrated by Grubbs et al.; this reversible process proceeds through the formation of $\text{Cp}_2\text{Ti}=\text{CH}_2$ [61] (Scheme 3b). Ti–Al complexes **Ti03–Ti05** reacted with ${}^t\text{BuCH}=\text{CH}_2$ similarly, with a formation of the mixtures of isomeric titanacyclobutanes [53].



Scheme 3. (a) Formation of titanacyclobutanes [59,60]; (b) reactivity of *tert*-butyl-substituted titanacyclobutane towards α -olefins [61].

A degenerate metathesis reaction between titanium methylenes unveiled from **Ti01** and unactivated alkenes, followed by acid hydrolysis, was recently proposed by Frederick et al. [62] as a direct method for the Markovnikov hydromethylation of alkenes (Scheme 4). The reaction is site-specific; the reactivity of olefins decreases in the order α -olefins > methylenealkanes > trisubstituted alkenes.

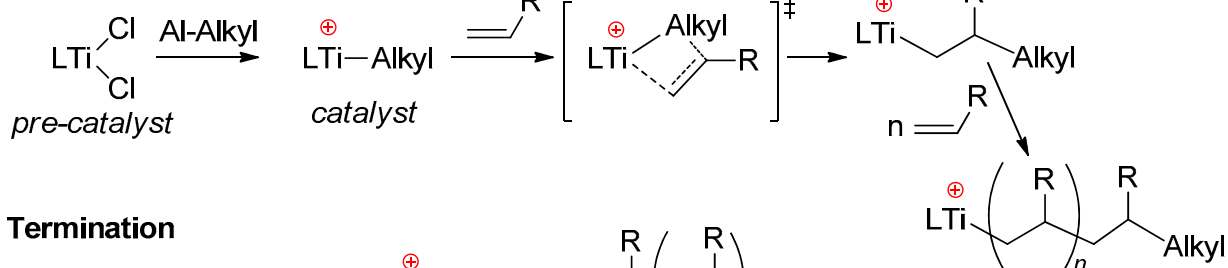


Scheme 4. (a) General reaction scheme; (b) relative stability of titanacyclobutane intermediates; (c) scope and limitations of the titanium-mediated hydromethylation of alkenes [62].

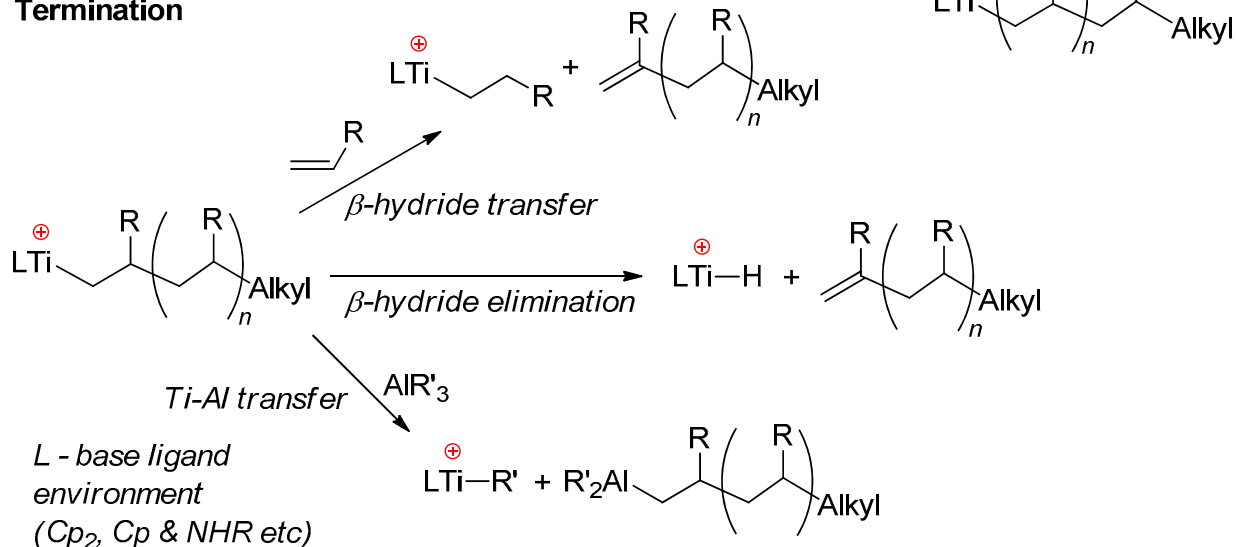
2.2. Single-Site Ti Catalysts of the Polymerization and Oligomerization of α -Olefins

In early experiments on the single-site polymerization of ethylene, conducted by Shilov's group, the occurrence of cationic species during the reaction of Cp_2TiCl_2 with Et_2AlCl was regarded as an experimental criterion of the rapid catalytic process [63,64]. In the opinion of Shilov, after the intermediate formation of complex $\text{Cp}_2\text{TiClEt} \cdot \text{EtAlCl}_2$, partial dissociation of the complex occurs, and Cp_2TiEt^+ is active in polymerization. For the most part, this view has not fundamentally changed in terms of the reaction mechanism, and for sandwich and half-sandwich complexes of Ti(IV), the polymerization of α -olefins includes stages of π -coordination of alkene at the Ti-Alkyl cation and insertion of the alkene via the four-membered Cossee-Arlman transition state. Possible termination events for the growing polyolefin chain are β -hydride transfer to monomer, β -hydride elimination, and Ti \rightarrow Al alkyl transfer (Scheme 5) [65,66]. The main problems arising during the use of Ti(IV) sandwich complexes derive from side reactions that deactivate the active titanocene catalyst via reduction of the Ti(IV) cationic center [65]. Stabilization of the active Ti(IV) species was achieved via ligand design, with the development of half-sandwich constrained-geometry complexes (CGCs) [67–70] and different Ti(IV)-based post-metallocene catalysts [5,71].

Initiation and propagation

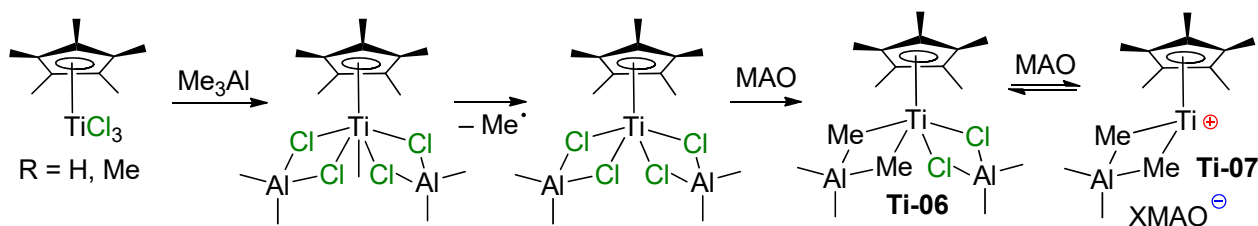


Termination



Scheme 5. Conventional mechanism of α -olefin polymerization, catalyzed by sandwich and half-sandwich Ti(IV) complexes [65].

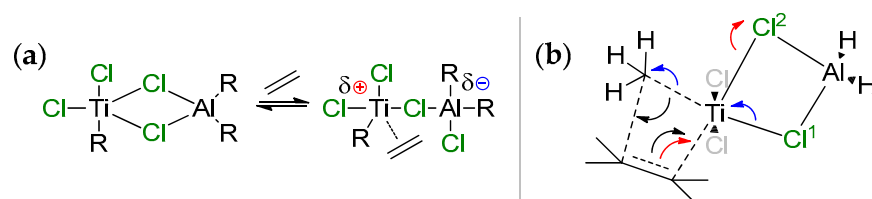
In the following model experiments on activation of Ti(IV) chloro complexes by aluminum alkyls, Ti-(μ -Cl)-Al-containing products were detected by ESR and electronic absorption spectroscopy. Thus, in the 1980s, Mach's group studied the formation and relative stability of Ti-Al half-sandwich complexes with the formula CpTiAl₂Cl_{8-x}Et_x and (η^6 -C₆H₆)TiAl₂Cl_{8-x}Et_x, and demonstrated their reduced stability by increasing the number of Et fragments, x [72,73]. In 2004, Bonoldi et al. studied the activation of CpTiCl₃ and (η^5 -C₅Me₅)TiCl₃ (Cp*TiCl₃) by different aluminum alkyls, MAO and AlMe₃/[CPh₃][B(C₆F₅)₄] [74]. ESR spectral studies have shown that during the reaction of LTiCl₃ with Me₃Al at an Al/Ti ratio of 10:1, after 3 h, Ti(III) complexes are formed with 12% and 8% yields, respectively. This was explained by the more electron-rich nature of Cp* in comparison with Cp, which hindered an increase in the electron density by reduction (Ti(IV) + e⁻ → Ti(III)). In the presence of MAO, complex **Ti06** was formed (Scheme 6). This complex demonstrated moderate catalytic activity in the polymerization of styrene, although it is the cationic complex **Ti07** that was considered as an *active* polymerization catalyst.



Scheme 6. Formation of catalytically active half-sandwich Ti-Al complexes [74].

The hypothesis of the coordination of R₂AlCl (Scheme 7a) with the possibility of the partial ionization of the active center, followed by the coordination/insertion of ethylene, was put forward by Jensen et al. in 1994 [75]. This hypothesis was based on the assumption

that single-site Ziegler–Natta catalysts, obtained by the reaction of TiCl_4 with AlR_3 , contain active Ti(IV) species. Quantum chemical optimization of the model complex $\text{MeCl}_2\text{Ti}(\mu\text{-Cl})_2\text{AlH}_2\cdot\text{CH}_2=\text{CH}_2$ at the DFTG level showed weak coordination of the ethylene molecule ($d(\text{Ti}-\text{C}) > 3 \text{ \AA}$) [76]; no stationary point due to the π -coordination of ethylene was found for this system. Similar results were obtained by the same research group during more thorough theoretical studies [77]; however, the authors have not abandoned the idea of the direct participation of Ti–(μ -Cl)–Al species in the catalytic process. Notably, one year earlier, Sakai reported the results of ab initio studies of the formation and further transformations of exactly the same molecule, $\text{MeCl}_2\text{Ti}(\mu\text{-Cl})_2\text{AlH}_2\cdot\text{CH}_2=\text{CH}_2$, in comparison with the $\text{MeTiCl}_3/\text{CH}_2=\text{CH}_2$ system [78]. First, Sakai was able to find the local minima corresponding to π -complex $\text{MeCl}_2\text{Ti}(\mu\text{-Cl})_2\text{AlH}_2\cdot\text{CH}_2=\text{CH}_2$ (Scheme 7b). Second, even more interestingly, no stationary point was found for π -complex $\text{MeTiCl}_3\cdot\text{CH}_2=\text{CH}_2$, and the activation energy barrier of ethylene insertion for the $\text{MeTiCl}_3/\text{CH}_2=\text{CH}_2$ system was $20.5 \text{ kcal}\cdot\text{mol}^{-1}$ higher than that for $\text{MeCl}_2\text{Ti}(\mu\text{-Cl})_2\text{AlH}_2\cdot\text{CH}_2=\text{CH}_2$. Sakai explained it in this way: in the rate-limiting transition state of the ethylene insertion, the π -electrons in ethylene move to the Ti–C(ethylene) region to form the new Ti–C bond. The electrons, belonging to the Ti–C(methyl) bond, move to the C–C (methyl–ethylene) region to form a new C–C bond (push–pull mechanism, black arrows). In the Ti–(μ -Cl) $_2$ –Al complex, the Ti–Cl 2 bond, opposite to the ethylene coordination side for the Ti center, increases in length with electron transfer to the Cl 2 atom along the reaction pathway (red arrow in Scheme 7b). The original π -electrons move to the new Ti–C bond region (opposite to the Ti–Cl 2 bond) easily (red arrow), this process is similar to $\text{S}_{\text{N}}2$ reaction. At the same viewpoints, the Ti–Cl 1 bond, opposite to Ti–C(methyl), decreases in length, and the electrons move from Cl 1 to Ti and from Ti–C(methyl) bond to C(methyl) (blue arrows). Therefore, the Al–Cl (or Ti–Cl) bonds switching mechanism facilitates the push–pull mechanism of the insertion.



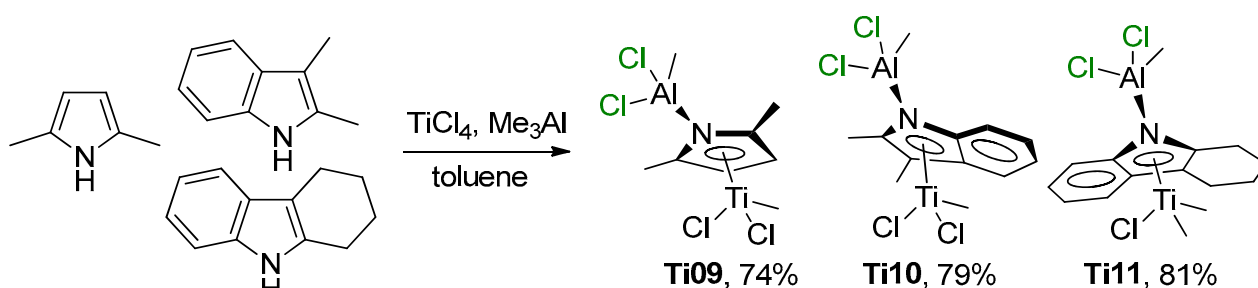
Scheme 7. (a) Suggested scheme for partial ionization of the active center through action of the aluminum cocatalyst [75]; the authors proposed that after the cleavage of one of the Ti–Cl–Al bonds, the vacated position due to partial ionization is occupied through the coordination of ethylene; (b) ab initio modeling [78] showed that Ti–(μ -Cl) $_2$ –Al bonding is retained in the rate-limited transition state, and facilitates the insertion.

It can be assumed that similar single-site catalytic species are formed when using $\text{TiCl}_4/\text{AlCl}_3$ on a SiO_2 support, activated by Et_2AlCl [79,80]. This catalyst was studied in the oligomerization of dec-1-ene, which resulted in the preferential formation of trimers (by wt.%). The authors did not discuss the nature of the catalytic species (including oxidation state of Ti), confining themselves to the analysis of oligomer’s microstructure. However, studies of the impact of AlCl_3/Ti ratio on catalytic activity and oligomer distribution have shown the presence of an optimum, suggesting Ti–(μ -Cl)–Al contacts. Note that dec-1-ene oligomers, obtained with the use of this Ti/Al catalytic system, were regioirregular and contained nonnegligible proportion of tail-to-tail and head-to-head monomer units, differing from structurally homogeneous products of zirconocene-catalyzed oligomerization (see Section 3.2). This fact, and uniform molecular weight distribution (MWD) of the oligomer mixtures, suggest this Ti/Al catalyst to be qualitatively distinct from conventional heterogeneous Ziegler–Natta catalysts (see Section 2.4).

The results of Jensen et al. [75] were augmented with the studies of Ti ether complexes by Bulychev’s group [81]. Here, it has clearly been established that in the presence of ethers, R_2AlCl reduces Ti(IV) to Ti(III). A conventional activator of single-site polymerization catalysts, MAO, was completely inactive towards Ti(III) etherates. In contrast, when using

Et_2AlCl or 3:1 $\text{Et}_2\text{AlCl}/\text{Bu}_2\text{Mg}$ mixture as activators, the ionic complex of Ti(III) [(15-Crown-5) TiCl_2] $^+$ [AlCl_4] $^-$ (**Ti08**) demonstrated moderate activity in ethylene polymerization. The catalytic activity of **Ti08** decreases with the increasing Al/Ti ratio; therefore, it can be assumed that only partial alkylation of the Ti–Cl bonds occurs. However, there was no experimental proof of Ti–(μ -Cl)–Al bonding in catalytic species discussed in [81].

There are limited studies devoted to the participation of Ti–(μ -Cl)–Al complexes with proven structure in catalytic polymerization and oligomerization of α -olefins. In 2012, Duchateau et al. reported the synthesis, structural characterization, and ethylene polymerization performance of heterobimetallic Ti–Al–pyrrolyl complexes (η^5 -2,5-Me $_2$ C $_4$ H $_2$ NAICl $_2$ Me)TiCl $_2$ Me (**Ti09**), (η^5 -2,3-Me $_2$ C $_8$ H $_4$ NAICl $_2$ Me)TiCl $_2$ Me (**Ti10**), and (η^5 -3,4,5,6-C $_{12}$ H $_{12}$ NAICl $_2$ Me)TiClMe $_2$ (**Ti11**) [82]. These complexes were obtained by the treatment of TiCl $_4$ with equimolar amounts of Me $_3$ Al and the corresponding pyrrole ligands (Scheme 8).



Scheme 8. Synthesis of Ti(IV)–Al–pyrrolyl complexes **Ti09**–**Ti11** [82].

Molecular structures of **Ti09**–**Ti11** were determined by XRD analysis (Figure 3). All molecules exhibited a distorted tetrahedral piano stool configuration. The Ti(1)–CEN $_{\text{pyrrole}}$ bond distances (CEN $_{\text{pyrrole}}$ is a centroid of the pyrrole ring) are identical in **Ti09** and **Ti10** ($d(\text{Ti}(1)\text{–CEN}) = 2.062 \text{ \AA}$), but are slightly shorter than the Ti(1)–CEN $_{\text{pyrrole}}$ bond distance in **Ti11** ($d(\text{Ti}(1)\text{–CEN}) = 2.088 \text{ \AA}$). Although formally **Ti09**–**Ti11** were assigned to η^5 -type complexes, in **Ti10** and **Ti11**, titanium has a stronger interaction with the N atom, resulting in an η^4, κ -bonding mode for Al–indolyl and Al–carbazolyl ligands.

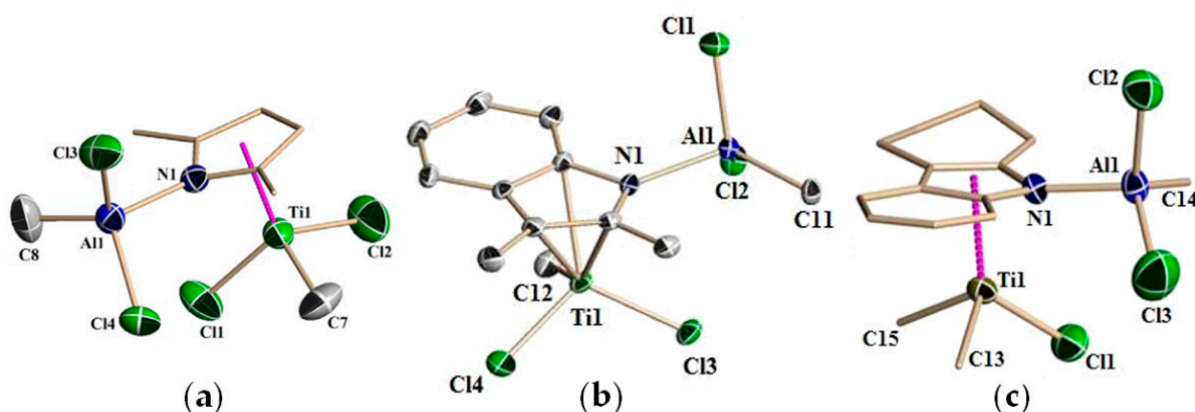
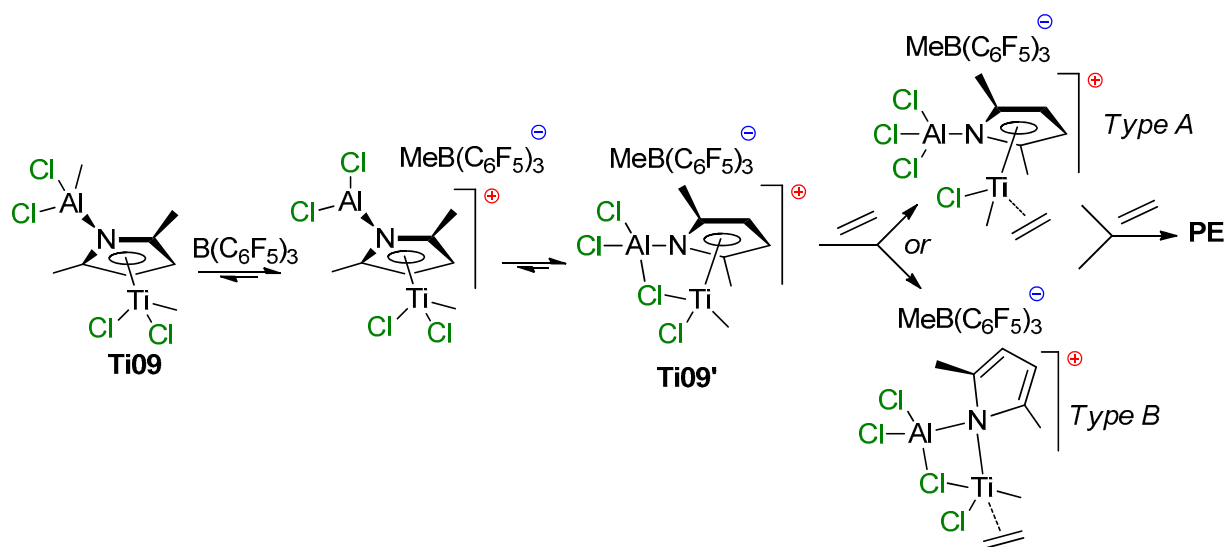


Figure 3. Molecular structures of Ti(IV)–Al–pyrrolyl complexes: (a) **Ti09**; (b) **Ti10**; (c) **Ti11**. Reprinted with permission from [82]. Copyright (2012) American Chemical Society.

Upon activation with MAO at 30 °C, **Ti09** produces a single-site catalyst affording ultra-high-molecular weight polyethylene (UHMWPE, $M_w = 2300 \text{ kDa}$, $D_M = 2.5$). When **Ti09** was activated with $[\text{Ph}_3\text{C}]^+[\text{B}(\text{C}_6\text{F}_5)_4]^-$ and TIBA (50 eq.) at 30 °C, bimodal distribution of the polymer was detected, indicating the formation of two distinct active species. A similar bimodal distribution and significant reduction in M_n were observed when MAO-activated polymerization was carried out at 60 °C. MAO-activated Ti–Al complexes **Ti10** and **Ti11**

displayed higher catalytic activity compared with **Ti09**, and also produced UHMWPE. Complex **Ti10** showed the same bimodal behavior when activated with $[\text{Ph}_3\text{C}]^+[\text{B}(\text{C}_6\text{F}_5)_4]^-$ and TIBA.

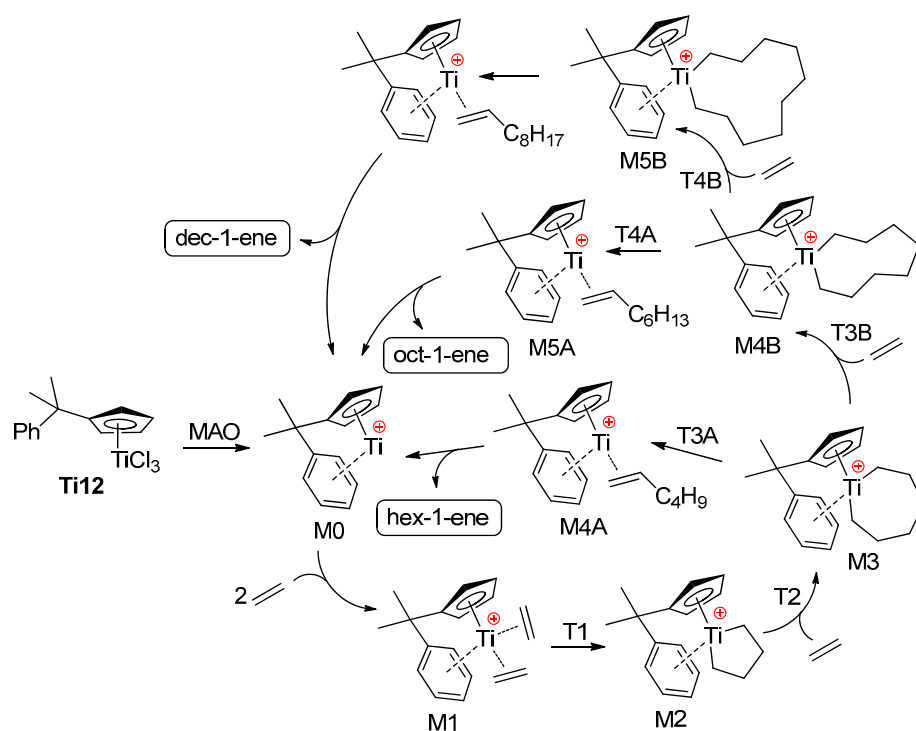
To clarify polymerization mechanism, the reaction of **Ti09** with $\text{B}(\text{C}_6\text{F}_5)_3$ was investigated to determine which of the methyl groups (Ti–Me or Al–Me) would be abstracted. The ^1H NMR spectrum clearly showed that $\text{B}(\text{C}_6\text{F}_5)_3$ selectively abstracts Al–Me group with the formation of a cationic complex **Ti09'**, containing a Ti–(μ -Cl)–Al fragment (Scheme 9). The ability of the supposed cationic species **Ti09'** to polymerize ethylene was tested by treating **Ti09** with $\text{B}(\text{C}_6\text{F}_5)_3$ under ethylene pressure (20 bar) at room temperature, and the rapid formation of polyethylene was detected.



Scheme 9. Proposed pathways of the activation of **Ti09** by $\text{B}(\text{C}_6\text{F}_5)_3$ [82].

DFT optimization of the putative structures of the cationic species and their ethylene adduct showed that a constrained type of geometry with the Ti–(μ -Cl)–Al fragment is the most stable configuration for **Ti09'**. This saturated complex **Ti09'** should not be an active catalyst; either release of the bridged Cl (Type A structure in Scheme 9) or $\eta^5 \rightarrow \mu$ ring slippage of the pyrrole moiety (Type B structure in Scheme 9) may result in a coordinatively unsaturated complex to coordinate and polymerize ethylene. The DFT calculations showed that the formation of a Type A complex requires $12.2 \text{ kcal}\cdot\text{mol}^{-1}$, and no local minima were found for the Type B product of $\eta^5 \rightarrow \mu$ ring slippage.

In this way, intramolecular Ti–(μ -Cl)–Al bonding has a strong impact on the catalytic behavior of Ti complex. The other extreme is weak $\text{Ti}\cdots\text{Cl}\cdots\text{Al}$ coordination; de Bruin et al. [83] carried out a computational study of the influence of ‘chlorinated’ MAO anions on the catalytic behavior of complex **Ti12** which represents an efficient pre-catalyst of the selective trimerization of ethylene with the formation of hex-1-ene [14,15,84]. The key intermediates of the reaction are presented in Scheme 10, although the energetically unfavorable process of but-1-ene elimination from intermediate M2 (see below) is not shown.



Scheme 10. Reaction pathway for the oligomerization of ethylene, catalyzed by Ti12/MAO [83].

For DFT calculations, one of many possible MAO structures [85,86] was selected, namely, the cage $(\text{MeAlO})_6\text{Cl}^-$ model (Figure 4a), negatively charged due to the coordination of one Cl^- , abstracted from Ti12 during activation. Two different potential free energy reaction profiles have been modeled (Figure 4b): the first only takes into account the cationic catalyst (cationic profile), whereas the second describes the energy changes in the presence of a chlorinated MAO (zwitterionic profile). The reaction starts with the activated catalyst M1 (two ethylene molecules coordinated to the cationic Ti(II) center). After oxidative coupling (M2), a third ethylene molecule coordinates and inserts with a formation of the seven-membered metallacycle (M3). This species can undergo a β -hydride transfer followed by reductive elimination (M4A), which, in turn, releases hex-1-ene. Alternatively, a fourth ethylene may coordinate to M3 and insert to yield a nine-membered metallacycle M4B. This latter species can then undergo a ring-opening reaction to yield 1-octene (M5A), or a fifth ethylene coordination and insertion can take place. The calculated barrier for β -hydride elimination in M2 (but-1-ene formation) was $\sim 35 \text{ kcal}\cdot\text{mol}^{-1}$. Based on a comparison of cationic and zwitterionic profiles, it can be concluded that the presence of $(\text{MeAlO})_6\text{Cl}^-$ does not impact the selectivity of ethylene oligomerization. Based on the results of modeling, the authors concluded that the presence of MAO model does not necessarily need to be taken into account, and the cationic system alone is sufficiently representative.

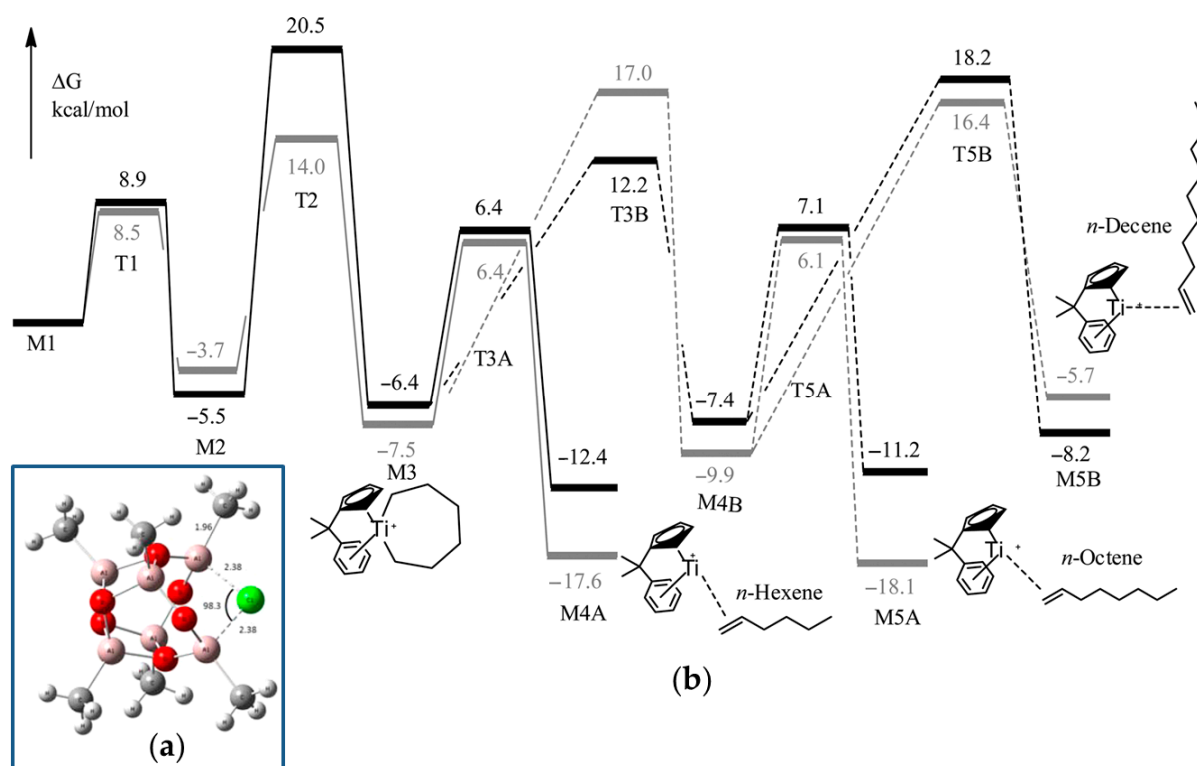


Figure 4. (a) B3LYP-optimized configuration of the $[\text{MAO-Cl}]^-$ anion; (b) comparative reaction profile over the potential energy surface for a cationic (gray) and zwitterionic (black) catalyst. The solid line indicates the main path; the dotted line indicates the less favorable alternative path. Reprinted with permission from [83]. Copyright (2015) American Chemical Society.

As reported by Blakemore et al., the reaction of the Ti(IV) complex $(\eta^6\text{-C}_9\text{H}_7)\text{TiCl}_2(\text{N}=\text{P}^t\text{Bu}_3)$ with Et_3Al resulted in the formation of Ti(III)-Al complex **Ti13** [87]. The molecular structure of **Ti13** is presented in Figure 5a. Both complexes catalyzed the polymerization of ethylene being activated by Et_3Al in the presence of a solid superacid. During subsequent research [88], the complexes **Ti14** and **Ti15** of the formula $(\eta^6\text{-C}_9\text{H}_7)\text{Ti}(\text{N}=\text{P}^t\text{Bu}_3)(\mu\text{-Cl})_2\text{AlR}_2$ ($\text{R} = \text{Me}$ and ^tBu , respectively) were obtained, and the molecular structure of **Ti15** (Figure 5b) was virtually identical to the molecular structure of **Ti13**. However, in experiments on the polymerization of ethylene, catalytic activities of the complexes decreased in the order **Ti15** > **Ti13** > **Ti14**. In this way, the nature of the substituents at Al atoms influenced the catalyst's properties, thus indirectly confirming the presence of Ti-($\mu\text{-Cl}$)-Al bonding in catalytic species.

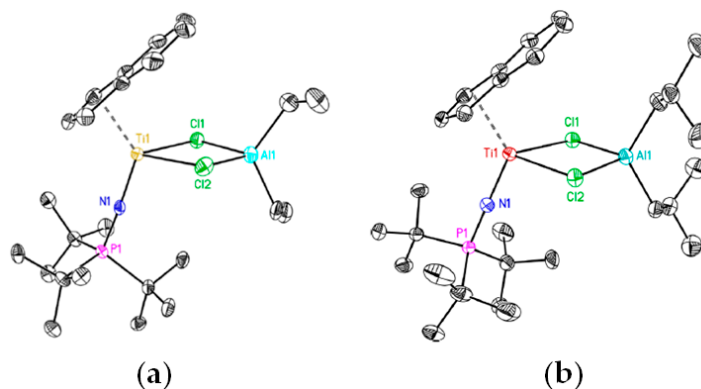
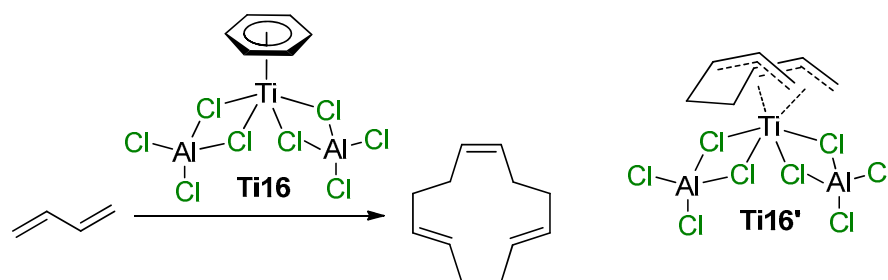


Figure 5. Molecular structure of Ti-Al complexes (a) **Ti13** and (b) **Ti15**. Reprinted with permission from [88]. Copyright (2021) American Chemical Society.

2.3. Single-Site Ti Catalysts of Polymerization of Dienes

Ti(IV) halogenides, activated by aluminum alkyls, represent the first-generation catalysts of coordination polymerization of 1,3-dienes [8,89]. However, despite half a century of research, molecular structure of the catalytic species, formed as a result of the reaction of LTiCl_n with $\text{R}_m\text{AlCl}_{3-m}$, is not entirely clear. In examining the reaction mechanisms of diene polymerization, the ‘pure’ cationic concept is still actual [90].

The participation of Ti-($\mu\text{-Cl}$)-Al species in the coordination polymerization of conjugated dienes was proposed by Mach et al., who studied the catalytic activity of η^6 -arene Ti complexes with AlCl_3 and alkylaluminum chlorides [91–93]. Similar complexes of $(\eta^6\text{-C}_6\text{H}_6)\text{Ti}[(\mu\text{-Cl})_2\text{AlCl}_2]_2$ (**Ti16**) and $(\eta^6\text{-C}_6\text{Me}_6)\text{Ti}[(\mu\text{-Cl})_2\text{AlCl}_2]_2$ (**Ti17**) were obtained and structurally characterized in the late 1970s and early 1980s by Thewalt et al. [94,95]. The molecules of **Ti16** and **Ti17** exhibit square pyramidal geometry, with the titanium atom above the rectangle of the bridging Cl atoms and with the π -bonded arene at the apex. When **Ti16** was used as a single-component catalyst of the oligomerization of buta-1,3-diene, (1*Z*,5*E*,9*E*)-cyclododeca-1,5,9-triene was formed with 92% selectivity (Scheme 11) [91]. The authors assumed that the high stereospecificity of the cyclotrimerization indicates that the reaction proceeds by a sterically controlled coordination mechanism. The experimental results, i.e., the approximate second-order dependence of the reaction rate on buta-1,3-diene concentration, the low concentrations of all the intermediates participating in the catalytic steps and no interaction between the catalyst and final product, suggest that cyclotrimerization may proceed via the replacement of C_6H_6 by two molecules of buta-1,3-diene, followed by the formation of the active species **Ti16'** (Scheme 11). In the presence of EtAlCl_2 , Et_2AlCl , and Et_3Al , catalytic activity of complex **Ti16** increased due to the substitution of non-bridged Cl atoms by Et groups [92]. In the presence of a large excess of Et_3Al , complete deactivation of the catalyst was observed. Complex **Ti17** demonstrated low activity due to higher stability of the $(\eta^6\text{-C}_6\text{Me}_6)\text{-Ti}$ bond in comparison with the $(\eta^6\text{-C}_6\text{H}_6)\text{-Ti}$ bond [93]. However, the substitution of non-bridged Cl atoms by Et groups proceeded stepwise with maximum preservation of the molecular symmetry—by an example of the complex $(\eta^6\text{-C}_6\text{Me}_6)\text{Ti}[(\mu\text{-Cl})_2\text{AlClEt}]_2$ (**Ti17'**), for which XRD analysis was performed. This substitution resulted in a manyfold increase in the catalytic activity [93].

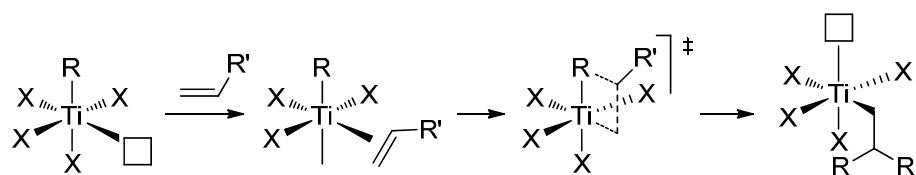


Scheme 11. Selective cyclotrimerization of buta-1,3-diene, catalyzed by **Ti16**, and tentative structure of the intermediate **Ti16'** [91].

In conclusion, we note that Ti complexes are not actually considered as prospective catalysts of the polymerization of conjugated dienes, and further comprehensive studies of the reaction mechanism seem unlikely.

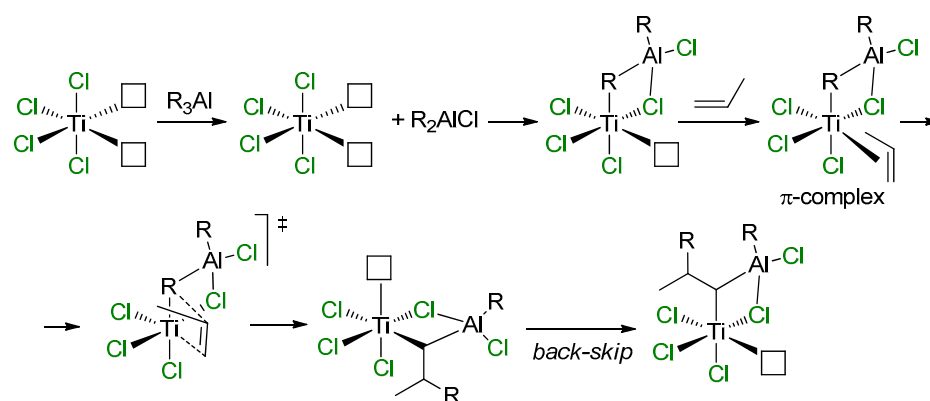
2.4. Heterogeneous Ti Ziegler–Natta Catalysts

The $\text{TiCl}_3/\text{R}_3\text{Al}$ system, called the ‘1st generation Ziegler–Natta catalyst’, was one of the early efficient catalysts of α -olefin polymerization [96]. It is for these catalysts that the common mechanism of the coordination polymerization of α -olefins was proposed by Cossee and Arlman [97,98]. This conventional mechanism (Scheme 12) involves the participation of Ti(III)–Alkyl species and is similar to the mechanism presented in Scheme 5, except that the Ti atom has zero charge and an oxidation state of +3.



Scheme 12. Cossee–Arman mechanism of α -olefin polymerization [97,98]; white square indicates the vacancy of the Ti(III) atom.

In approaching the topic of modern and efficient Ziegler–Natta (ZN) catalysts, tributes should be paid to the work of Rodriguez and van Looy, who formulated heterobimetallic concepts of the reaction mechanism to explain the impact of alkylating agents on stereospecificity of TiCl_3 catalyst. This concept was based on an assumption of the presence of Ti centers with two potential vacancies on the Ti atom at the surface of TiCl_3 (coordination number of the Ti atom CN_{Ti} is equal to 4) [99]. According to this concept (Scheme 13), after alkylation by R_3Al , a $\text{Ti}-(\mu\text{-Cl})\text{-Al}$ complex is formed ($\text{CN}_{\text{Ti}} = 5$). π -Coordination and subsequent insertion of the α -olefin molecule results in an alkyl complex, which further isomerizes with occupation of the position previously occupied by the R group, thus forming the isotactic polyolefin.



Scheme 13. Mechanistic concept of Rodriguez and van Looy [99].

It has been nearly 70 years since the pioneering works of Ziegler and Natta [100,101], and there have been several generations of ZN catalysts. At present, the polymerization of α -olefins with the use of heterogeneous Ti-based MgCl_2 -supported Ziegler–Natta catalysts (TMCs) is the most important industrial chemical process in the polyolefin industry [102–108]. However, despite the importance and impact of TMCs, these catalyst systems have not yet been completely explored. TMCs comprise the MgCl_2 support, the active Ti(III) [11,109,110], and Ti(II) [11,111] species; organoaluminum species formed from trialkylaluminum alkylating agent R_3Al , and Lewis base donors. Due to the practical importance of TMCs, thus far, thousands of articles and dozens of reviews have been published; in this section, we restrict ourselves to listing several examples of the possible or proven (very rarely) participation of R_2AlCl species in TMC-catalyzed polymerization.

Catalytic processes occur on the TMC surface. Pre-catalysts represent TiCl_4 adsorbed on MgCl_2 crystallites, and the binding strength and coordination environment of the Ti atom depend on the crystal structure of the MgCl_2 support. In their fundamental study [110], Cavallo et al. assumed the MgCl_2 bulk to be in the α -crystalline phase with the surface comprising (104) lateral cuts (Figure 6a) that have five-coordinate magnesium centers. The removal of one MgCl_2 unit results in a new (110) surface that can coordinate the titanium species (Figure 6b). Vanka et al. proposed the simpler model structure of the MgCl_2 support, close in meaning to Cavallo's model [102] (Figure 6c). In their subsequent publication, Cavallo et al. upgraded their MgCl_2 model by (104)-facets presenting low-energy step-defects as potential sites for the strong coordination of TiCl_4 [103].

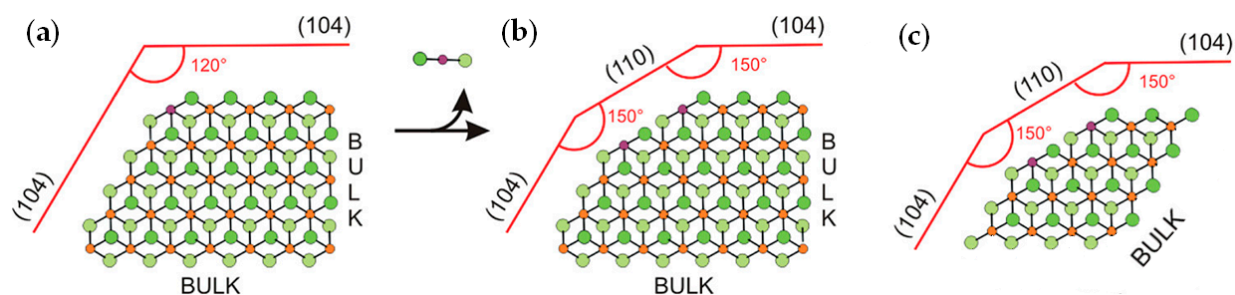


Figure 6. (a,b) The model for the MgCl_2 layers developed by Cavallo et al. [110]; (c) the modified MgCl_2 model with four layers instead of six employed in [102]. Reprinted with permission from [102]. Copyright (2014) Wiley-VCH Verlag GmbH & Co.

After the absorption of TiCl_4 , followed by the reaction with R_3Al , Ti(III)-Cl and Ti(III)-R species are formed [102]. Recent experimental DR UV/vis and NEXAFS data coupled with DFT simulation indicated that the majority of Ti sites in $\text{MgCl}_2/\text{TiCl}_4$ and MgCl_2 /ethyl benzoate/ TiCl_4 pre-catalysts are reduced by Et_3Al mostly to monomeric pentacoordinated Ti(III)Cl_5 species and, to a minor extent, to alkylated $\text{Ti(III)Cl}_4\text{Et}$ species. For MgCl_2 /dibutyl phthalate/ TiCl_4 pre-catalyst, Et_3Al additionally promoted the formation of small TiCl_3 clusters with low catalytic activity [112].

The above-mentioned articles considered two-component systems $\text{MgCl}_2/\text{TiCl}_3$, but their results are relevant to the subject of our review, determining Ti-containing species capable of $\text{Ti-(}\mu\text{-Cl)-Al}$ bonding. However, real TMCs may contain absorbed organoaluminum species. During the study of the activation of the $\text{TiCl}_4/\text{MgCl}_2$ pre-catalyst by Et_3Cl , Oct_3Al , and Et_2AlCl with the use of magic-angle spinning (MAS) ^{27}Al NMR [113], Potapov et al. detected three types of alkylaluminum chloride species. The changes in ^{27}Al NMR MAS spectra of the TMC before and after polymerization indicated that part of the Al compounds was removed from the catalyst surface or that the coordination environments of Al in these compounds became disordered. In the authors' view, the existence of Al compounds unremovable from the catalysts surface indicates the presence of inactive $\text{Ti-(}\mu\text{-Cl)-Al}$ species; in other words, R_2AlCl only acts as a catalyst inhibitor.

The same or a similar point of view received further development in a number of studies. In their theoretical study of the active sites in TMC [102], Vanka et al. used a simplified model of the MgCl_2 surface (Figure 6c) and optimized the geometries of different Ti(III)-Et catalytic species that are formed during the polymerization of ethylene, including the presence of the EtO^- ligand, ester donors, or Et_2AlCl . In the absence of additives, the calculated difference in free activation energies ΔG^\ddagger for the propagation and termination stages was only $1.2 \text{ kcal}\cdot\text{mol}^{-1}$. In the presence of esters, the difference increased to $12\text{--}13 \text{ kcal}\cdot\text{mol}^{-1}$ and was only $3 \text{ kcal}\cdot\text{mol}^{-1}$ when Et_2AlCl served as a donor. In the latter case, $\text{Ti-(}\mu\text{-Cl)-Al}$ coordination resulted in a substantial increase in the ΔG^\ddagger of ethylene insertion ($15.8 \text{ kcal}\cdot\text{mol}^{-1}$, see Figure 7). The results of this simulation explained how polymers can be successfully produced by TMCs without alkoxy groups and donor molecules [106]. In summary, the authors suggested that the possible role of organoaluminum activators is not limited by the reduction of Ti(IV) ; R_2AlCl can act as a donor due to its relatively weak $\text{Ti-(}\mu\text{-Cl)-Al}$ binding.

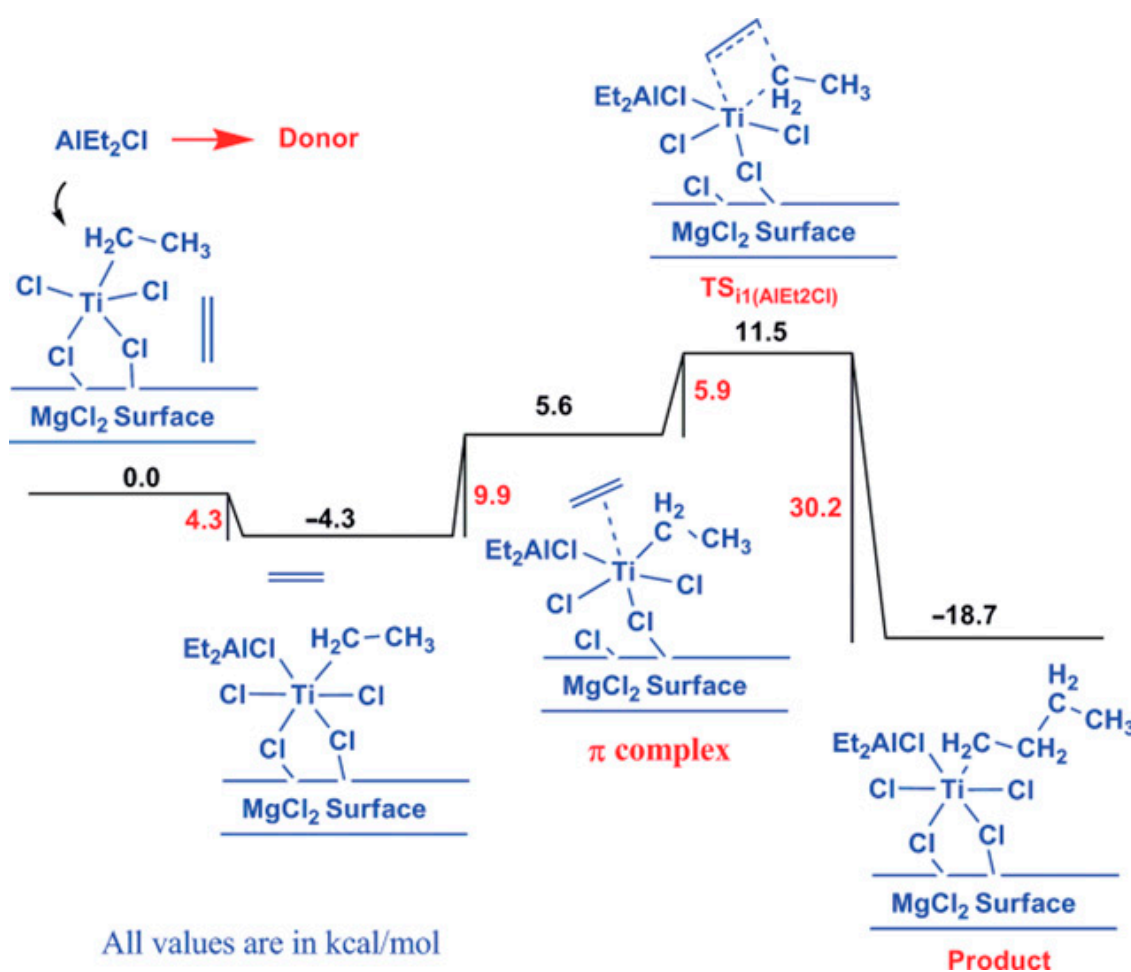


Figure 7. The free energy profile for the insertion of ethylene into the Ti-CH₂CH₃ chain with an AlClEt₂ group coordinated to the Ti center. Reprinted with permission from [102]. Copyright (2014) American Chemical Society.

In 2017, Linnolahti et al. reported the first quantum chemical description of the initial steps of olefin polymerization on TMCs involving all the relevant catalyst components—absorbed Ti chlorides, electron donor, and R₃Al [114]. They demonstrated that TiCl₄ is coordinated on the (104) surface of MgCl₂ as a binuclear Ti₂Cl₈ and on the (110) surface as a mononuclear TiCl₄ (CN_{Ti} = 6 for both binding modes). Et₃Al coordinates to the MgCl₂ surface via an unsaturated Cl atom to initiate Ti alkylation. After alkylation via the Ti-(μ-Cl)-Al transition state on the (104) surface, Et₂AlCl is released from the MgCl₂ surface and dimerizes (exergonic process). However, in the presence of dimethyl phthalate as a model donor molecule at the (110) surface, the formation of Ti-(μ-Cl)₂-Al and then Ti-(μ-Cl)(μ-Et)-Al species becomes energetically favorable (Figure 8). However, even in this case, the process is finished by Et₂AlCl desorption. However, DFT modeling, presented in [114], closes by examining alkylation stage with a formation of Ti(IV)-Et species, the further reduction with a formation of active Ti(III) centers, as well as ability of these centers to conduct Ti-(μ-Cl)-Al bonding, remains open.

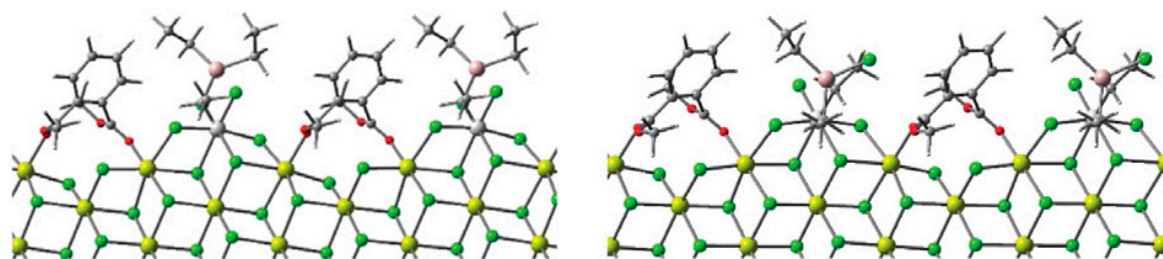


Figure 8. Optimized geometries of $\text{Ti}-(\mu\text{-Cl})_2\text{-Al}$ and $\text{Ti}-(\mu\text{-Cl})(\mu\text{-Et})\text{-Al}$ species formed during the alkylation of Ti chloride at the (110) surface of MgCl_2 . Reprinted with permission from [114]. Copyright (2017) Elsevier B.V.

A recent study by Boisson [115] provided answers to certain questions about the role of organoaluminum activators in TMC-catalyzed polymerization. Based on the results of the study of the microstructure and MWD of polyethylenes, the authors suggested that $\text{Ti}-(\mu\text{-Cl})\text{-Al}$ bonding may need to be considered in addressing the issue of the nature of ZN catalysts.

In [116], Busico's group reported the results of an extensive experimental and theoretical investigation of the latest-generation commercial TMC. During this study, the researchers proposed a new function of R_2AlCl species, namely, interactions with adsorbed internal donors that provide a higher degree of stereocontrol: for the insertion of prop-1-ene at the catalytic species formed by alkylation and reduction of the TiCl_4 precursors in panels (a) and (b) of Figure 9, the calculated $\Delta G_{\text{re/si}}$ values were ≈ 0 and $1.5 \text{ kcal}\cdot\text{mol}^{-1}$, respectively; the latter was in good agreement with the experimental data.

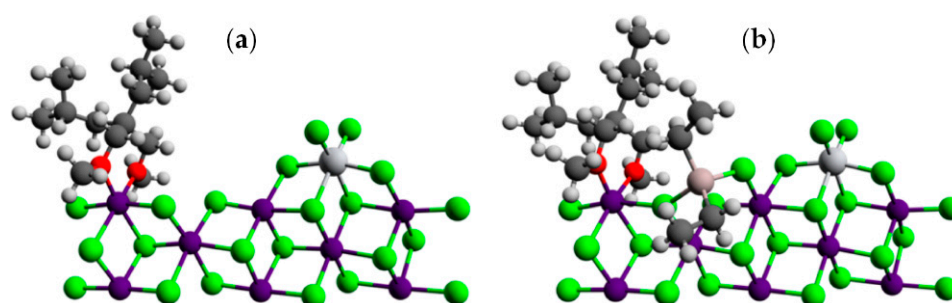


Figure 9. (a) DFT model of adjacent TiCl_4 and 2,2-diisobutyl-1,3-dimethoxypropane co-adsorption on a $\text{MgCl}_2(110)$ edge; (b) same as panel a after the adsorption of an AlEt_2Cl molecule. Reprinted with permission from [116]. Copyright (2017) American Chemical Society.

At the end of this section, it is appropriate to mention the most recent studies by Bahri-Laleh's group [117,118]. In [117], ethylene coordination/insertion at different TiEt and $\text{TiEt}-(\mu\text{-Cl})_2\text{-Al}$ sites (Figure 10a–d) was modeled. Ethylene coordination at the Ti center on the (110) surface was thermodynamically more favored in comparison with it on the (104) surface due to the more acidic nature of 4-coordinated surface Mg atoms in (110). π -complexation of the ethylene molecule was more exergonic in Al-doped catalysts. The activation energy values for the insertion of ethylene molecule were 8.3 (a), 11.6 (b), 6.1 (c), and 9.5 (d) $\text{kcal}\cdot\text{mol}^{-1}$. In this way, Al-doping increased the energy barrier needed for olefin insertion. In addition, the authors proposed that absorption of the Ti chloride at the (104) surface should not be ignored when analyzing distribution of the active sites, which is in contrast to the established paradigm. However, because TMCs represent a very striking example of the 'catalytic black box', any substantial expansions of the existing worldview can only be welcomed.

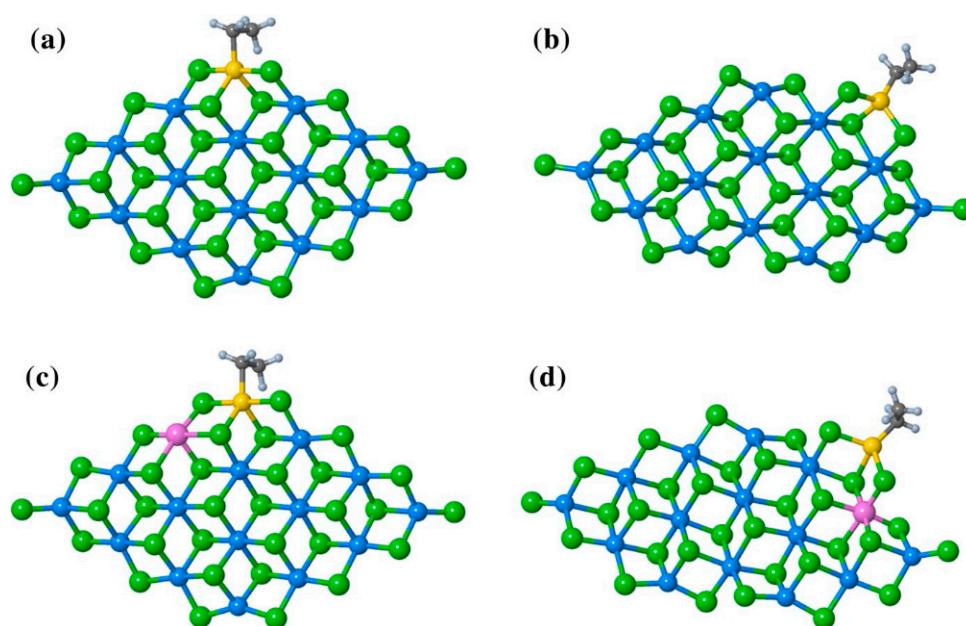


Figure 10. The structure of TiCl_2Et adsorbed on (a) undoped (110); (b) undoped (104); (c) Al-doped (110); and (d) Al-doped (104) surfaces. Reprinted with permission from [117]. Copyright (2022) Springer Nature.

In [118], the catalytic activity of TMCs when using different organoaluminum activators (Et_3Al , Et_2AlCl , EtAlCl_2 , and ${}^i\text{Bu}_3\text{Al}$) was studied experimentally, and the effect of $\text{Ti}-(\mu\text{-Cl})\text{-Al}$ bonding on catalytic activity was evaluated theoretically for Ti centers at the (110) MgCl_2 surface and these four organoaluminum compounds. From the results of the modeling, Et_2AlCl was the best Al component among others.

Concluding this section of the review, we have to note that, with the sole exception of complexes Ti09-Ti11 [82], the question of the participation of $\text{Ti}-(\mu\text{-Cl})\text{-Al}$ species in catalytic transformations of α -olefins still has no clear answer. Irrelevance of this question to Ti-based post-metallocenes (too high CN_{Ti}) and fundamental unknowability of the TMC (the most important Ti-based catalyst) leave room for speculations, not complete answers. However, in the field of Zr-based *polymerization* catalysts we are facing a slightly better situation.

3. Complexes of Zr

Zirconocenes have a special place among Zr-based catalysts used in α -olefin chemistry. The hydro- and carboalumination of α -olefins [18], single-site polymerization with the use of MAO and perfluoroborate activators [119], selective dimerization [37,41,42] and oligomerization [16,17] of higher α -olefins—this is not a complete list of the processes with relevance for laboratory and industry. Historically, two groups of zirconocene-based catalytic species stand apart by the criterion of the charge of the catalytic Zr center. The first, zero-charged, group is traditionally considered as catalysts of hydroalumination, carboalumination, and cyclocarboalumination of α -olefins and related reactions, limitedly used in the laboratory [18]. The second, ‘cationic’ species, represents highly efficient single-site α -olefin polymerization catalysts with a great potential of industrial applications [1,7,120,121]. Therefore, it is no surprise that the second group of the Zr catalysts attracted and continue to attract the most research attention; however, the participation of $\text{Zr}-(\mu\text{-Cl})\text{-Al}$ species in catalytic process has only been proven experimentally for ‘neutral’ zirconocene species.

3.1. Zirconocene Chemistry: Non-Charged Complexes

The mechanisms of zirconocene-catalyzed hydroalumination and carboalumination of α -olefin were discussed ten years ago in the review by Parfenova et al. [18]. In this section,

we consider only some key studies, published before 2010, and discuss the results of recent studies in more detail.

Before discussions of hydroalumination and carboalumination processes, it should be noted that the reaction of L_2ZrCl_2 with R_3Al until recently was considered as the natural and only possible pathway of the activation of metallocene dichlorides. When studying this reaction, it was found that the nature of the η^5 -ligand significantly affects the completion of the process. As shown by Beck and Brintzinger [122] for alkyl exchange reactions (Equation (1)), the values of apparent equilibrium constants K_{obs} were 0.005 ($L = \eta^5-C_5Me_5$), 0.016 ($L = \eta^5-C_5H_4^tBu$), 0.19 ($L = \eta^5-C_5H_4^tSiMe_3$), 0.49 ($L = Cp$) and 1.2 ($L_2 = rac-Me_2Si(Ind)_2$). Both steric and electronic factors affect this equilibrium, and in particular, decreased electron density at the Zr atom appears to favor uptake of the Me group.



The difference in equilibria constants for this reaction can be explained based on the results of DFT modeling, as shown by Linnolahti et al., who showed that catalyst alkylation step by $AlMe_3$ has two viable routes. $AlMe_3$ coordinates to the metallocene either from the side or from the front, leading to corresponding alkylation reaction pathways. The kinetically favorable route is dependent on the ligand structure of the catalyst: the front pathway is preferred for Cp_2ZrCl_2 (Figure 11) but is sterically hindered for $Me_2C(Cp)(Flu)ZrCl_2$, thereby preferring the side pathway [123]. Similar results have also been obtained in a more recent study by Kumawat and Gupta [124]. **Zr01** was also detected by IR spectroscopy during studies of the activation of Cp_2ZrCl_2 by MAO [125].

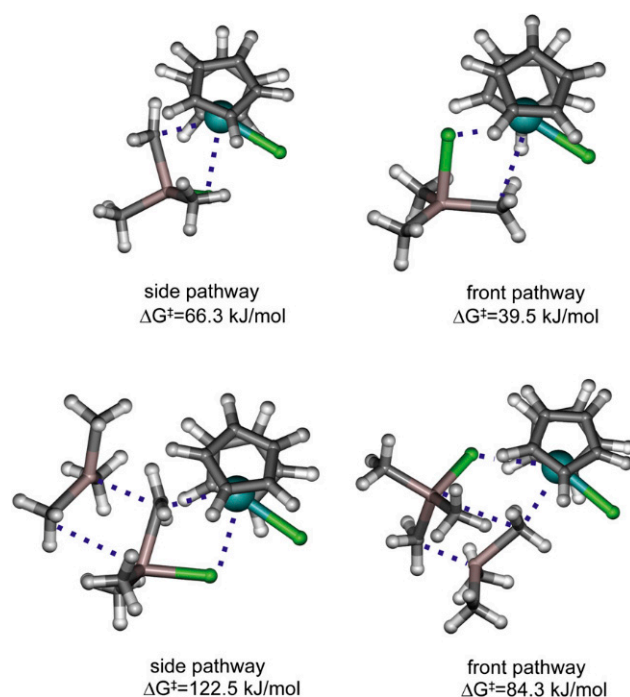


Figure 11. Illustration of transition states for the alkylation of Cp_2ZrCl_2 with Me_3Al (top) and Al_2Me_6 (bottom). Reprinted with permission from [123]. Copyright (2012) Elsevier B.V.

Dimethyl derivatives of zirconocenes are formed during the second stage of the process. The intermediate complex of the formula $Cp_2ZrMeCl \cdots AlMe_3$ (**Zr01**) was detected by 1H NMR at -85 °C; however, at -60 °C, the characteristic signal of Zr–Me group had already disappeared [126].

The presence of direct Zr–(μ -Cl)–Al bonding in $Cp_2ZrMeCl$ complexes with R_3Al has clearly been proven by Barron et al. [127]. They showed that even Me_2Al can coordinate

with Cl ($d(\text{Al}-\text{Cl}) = 2.46 \text{ \AA}$, $d(\text{Zr}-\text{Cl}) = 2.52 \text{ \AA}$, Figure 12) with the formation of a relatively stable complex $\text{Cp}_2\text{ZrMeCl} \cdots \text{AlMe}_3$ (**Zr01'**).

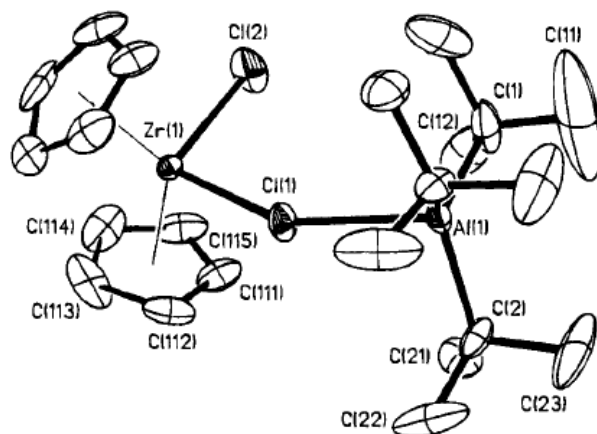
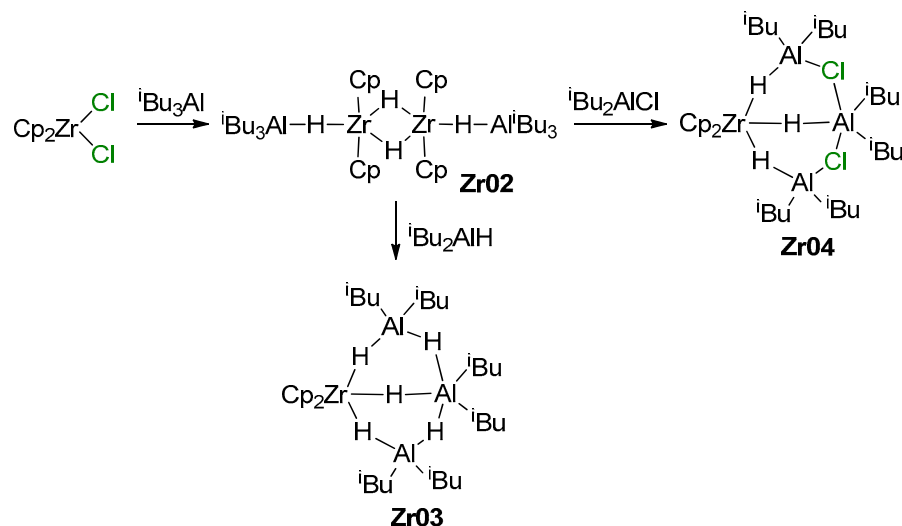


Figure 12. Molecular structure of one of the crystallographic independent molecules of $\text{Cp}_2\text{ZrMeCl} \cdots \text{AlMe}_3$ (**Zr01'**). Reprinted with permission from [127]. Copyright (1995) American Chemical Society.

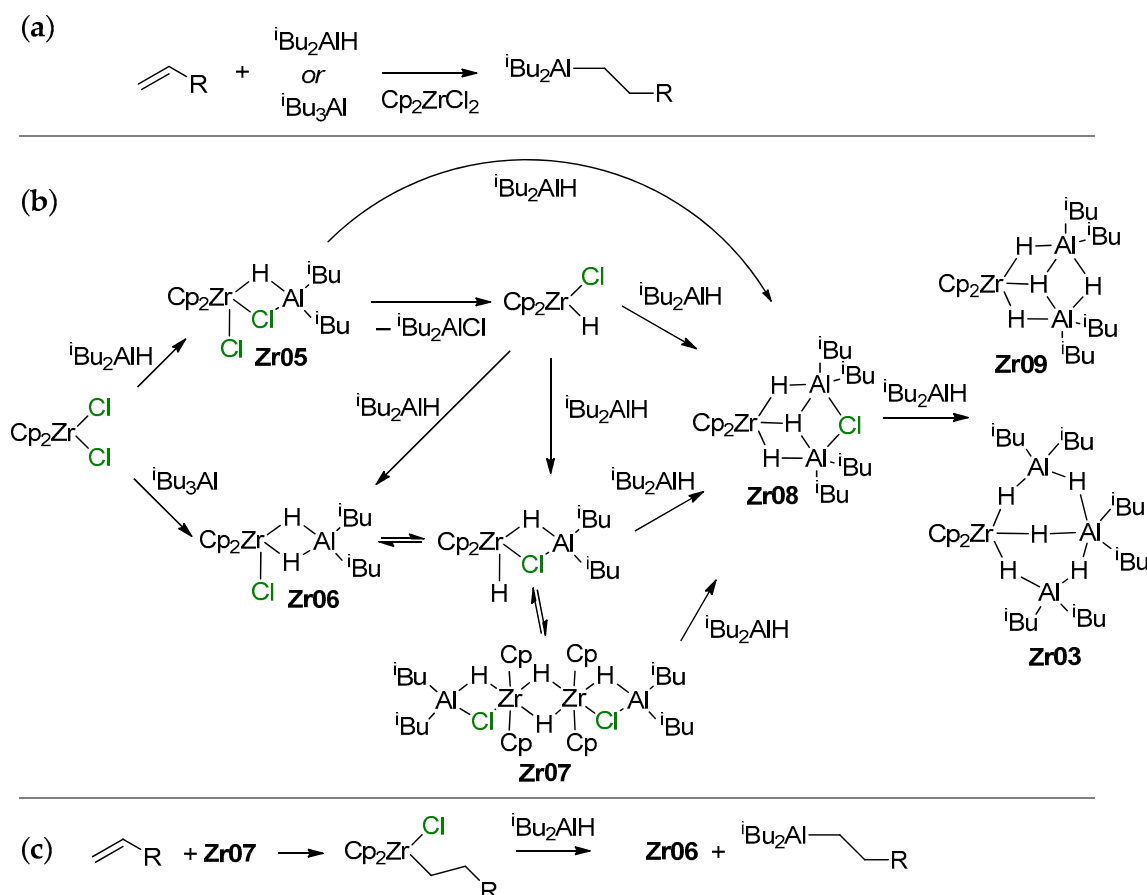
It is obvious that the reactions of L_2ZrCl_2 with ${}^i\text{Bu}_2\text{AlH}$ or ${}^i\text{Bu}_3\text{Al}$ may result in the formation of Zr–Al hydrides, which is accompanied by isobutylene elimination in the latter case [128]. The rate and equilibria of the reaction with ${}^i\text{Bu}_3\text{Al}$ also strongly depend on the nature of the η^5 -ligand fragment L_2 ; for instance, $\text{Ph}_2\text{C}(\text{Cp})(\text{Flu})\text{Zr}({}^i\text{Bu})\text{Cl}$ even with a 50-fold excess of ${}^i\text{Bu}_3\text{Al}$, whereas Cp_2ZrCl_2 reacts with an excess of ${}^i\text{Bu}_3\text{Al}$ with the formation of $[\text{Cp}_2\text{ZrH}_2 \cdot \text{Al}^i\text{Bu}_3]_2$ (**Zr02**) [128], and reaction with ${}^i\text{Bu}_2\text{AlH}$ results in **Zr03** [129] (Scheme 14). In the presence of ${}^i\text{Bu}_2\text{AlCl}$, **Zr02** forms the Zr–Al₃ complex **Zr04**; ring-substituted bis(cyclopentadienyl) L_2ZrCl_2 complexes demonstrate similar behavior [129]. For Zr *ansa*-complexes, the formation of $\text{L}_2\text{ZrCl}(\mu\text{-H})_2\text{Al}^i\text{Bu}_2$ species was detected.



Scheme 14. Reaction of Cp_2ZrCl_2 with ${}^i\text{Bu}_3\text{Al}$ or ${}^i\text{Bu}_2\text{AlH}$ [128,129].

Efficient Cp_2ZrCl_2 -catalyzed hydroalumination uses ${}^i\text{Bu}_2\text{AlH}$ or its equivalent ${}^i\text{Bu}_3\text{Al}$ as Al sources due to the ease of isobutylene elimination with the formation of Al–H bonds (Scheme 15a). A greatly simplified hypothetical mechanism of this reaction, proposed by Negishi [130], was substantially developed and supplemented by new experimental and theoretical results by Dzhemilev and Parfenova group. In [131], they proposed a hydroalumination mechanism involving the intermediate formation of $\text{Cp}_2\text{Zr}(\mu\text{-Cl})(\mu\text{-H})\text{Al}$ (**Zr05**) and $\text{Cp}_2\text{Zr}(\mu\text{-H})_2\text{Al}$ (**Zr06**) species that are able to perform π -coordination and insertion

of the α -olefin molecule. In the same study, a dimer of the Zr–Al complex (**Zr07**) was detected, and excess $i\text{Bu}_3\text{Al}$ or $i\text{Bu}_2\text{AlH}$ resulted in the formation of Zr–Al₂ and Zr–Al₃ complex hydrides (**Zr03**, **Zr08**, **Zr09**; the latter may contain $\mu\text{-Cl}$ fragments) (Scheme 15b). It was later discovered that in comparison with other Cp₂Zr-based complexes (including the Schwartz's reagent Cp₂ZrHCl), **Zr03** demonstrated the highest catalytic activity in hydroalumination (Scheme 15c) [132,133]. Probably, Cl-containing organoaluminum fragments in Zr–Al hydride complexes accelerate the intramolecular exchange between bridging and terminal H atoms and shift the equilibrium between the dimeric and active monomeric forms.



Scheme 15. (a) Hydroalumination of α -olefins; (b) Zr–Al species formed during the reaction of Cp₂ZrCl₂ with $i\text{Bu}_3\text{Al}$ or $i\text{Bu}_2\text{AlH}$; (c) the stages of Cp₂ZrCl₂-catalyzed hydroalumination [18,131–133].

The validity of Scheme 15 was confirmed in follow-up studies of the reaction of different L₂ZrCl₂ complexes with $i\text{Bu}_2\text{AlH}$ [134]; **Zr08**-type complexes were found to be active species of the hydroalumination process. **Zr08** species are formed via Zr–($\mu\text{-Cl}$)–Al intermediate **Zr06'**; therefore, the presence of Cl in the catalytic system is important for the hydroalumination process. These experimental results were in line with the results of a number of theoretical studies on the mechanism of L₂ZrCl₂-catalyzed hydroalumination performed by Parfenova et al. In [135], the formation of Cp₂ZrCl₂-based catalytic species was analyzed in detail. The main results of the modeling matched Scheme 15; in particular, by the optimization of the molecular structure of **Zr06** that was found to be relatively stable (Figure 13). In accordance with Scheme 15, the kinetic model for the reaction steps was developed [136,137].

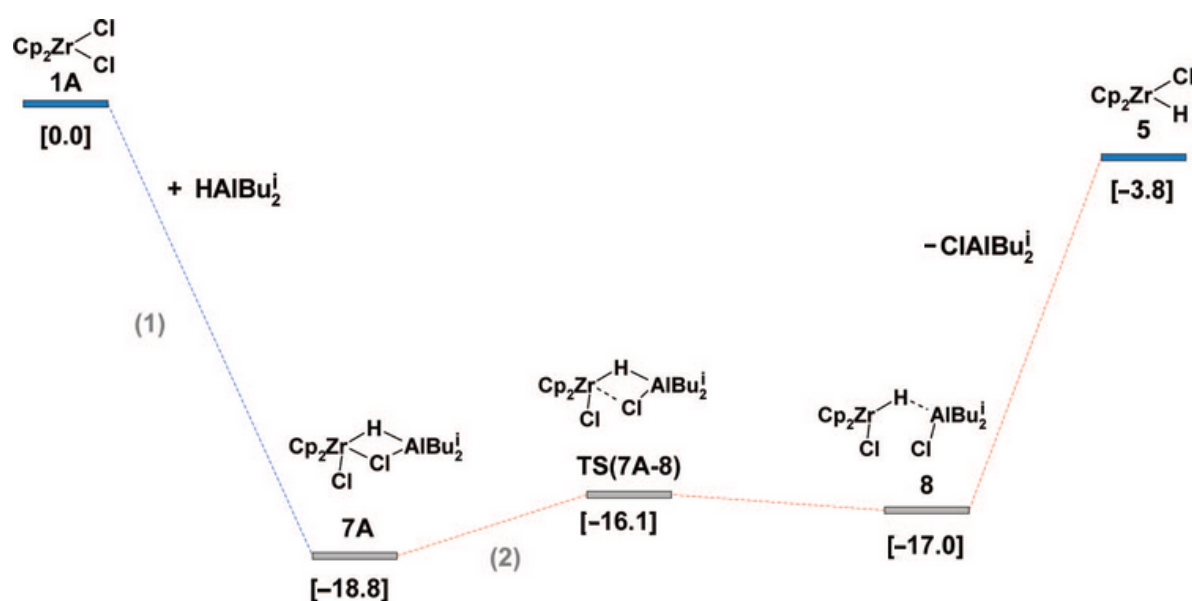
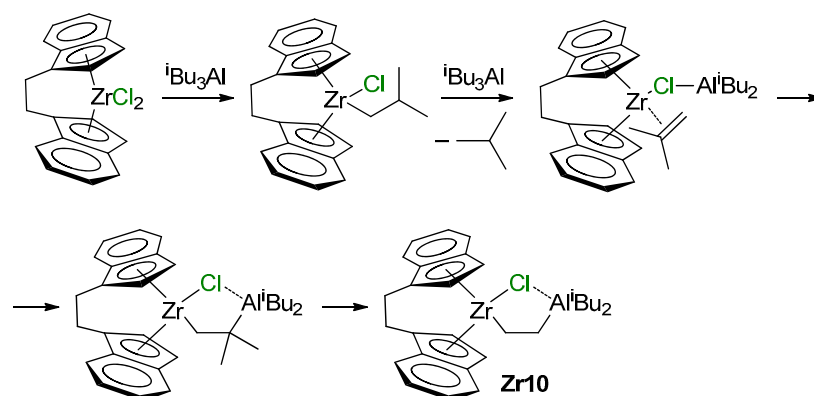


Figure 13. Energy profile of Cp_2ZrHCl formation (reaction enthalpies in $\text{kcal}\cdot\text{mol}^{-1}$ are shown in square brackets). Reprinted with permission from [135]. Copyright (2009) American Chemical Society.

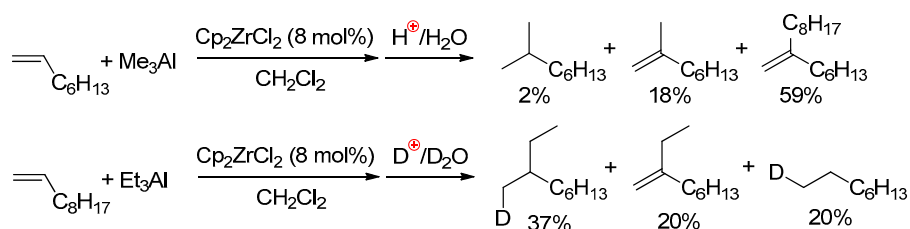
In [138], α -olefin interactions with catalytically active centers were studied by DFT and ab initio calculations. It was shown that Cp_2ZrHCl , **Zr06**, **Zr08**, and **Zr09** are able to perform coordination and insertion of the α -olefin molecule; the activity decreases in the order $\text{Cp}_2\text{ZrHCl} > \text{Zr06} > \text{Zr08} > \text{Zr09}$. The results of the modeling correlate with experimental data on Cp_2ZrCl_2 -catalyzed hydroalumination, considering the equilibria between **Zr07** (isolated active catalyst) and **Zr06** (highly reactive intermediate) and low solubility of Cp_2ZrHCl that slows down the reaction. DFT modeling of the final stage of hydroalumination ($\text{Zr} \rightarrow \text{Al}$ alkyl transfer) was conducted for $\text{Cp}_2\text{ZrCl}(\text{Pr})\text{Al}^i\text{Bu}_2\text{AlX}$ system ($\text{X} = \text{H}, \text{Cl}, \text{Bu}^i$) [139]. It was shown that the reaction of ${}^i\text{Bu}_2\text{AlH}$ needed no activation energy and proceeded through the coordination of ${}^i\text{Bu}_2\text{AlH}$ both outside and inside of the $\text{C}-\text{Zr}-\text{Cl}$ angle, and led to the $\text{Cp}_2\text{ZrHCl} \cdots \text{Al}^i\text{Bu}_2\text{Pr}$ association, which further dissociated into the $\text{Al}^i\text{Bu}_2\text{Pr}$ and $\text{Al}^i\text{Bu}_2\text{Pr}$. Transmetalation in $\text{Cp}_2\text{ZrCl}(\text{Pr}) \cdots \text{ClAl}^i\text{Bu}_2$ occurs via the coordination of ${}^i\text{Bu}_2\text{AlCl}$ to the inside of the $\text{C}-\text{Zr}-\text{Cl}$ angle with the formation of a bridging complex $\text{Cp}_2\text{ZrCl}(\mu\text{-Cl})(\mu\text{-Pr})\text{Al}^i\text{Bu}_2$, followed by intramolecular ligand exchange that results in $\text{Cp}_2\text{ZrCl}_2 \cdots \text{Al}^i\text{Bu}_2\text{Pr}$ association which further decomposes into $\text{Al}^i\text{Bu}_2\text{Pr}$ and Cp_2ZrCl_2 . It was also shown that the transmetalation of the propyl group in $\text{Cp}_2\text{ZrCl}(\text{Pr}) \cdots \text{Al}^i\text{Bu}_3$ is less probable due to the high activation barrier ($\Delta G^\ddagger = 31.9 \text{ kcal}\cdot\text{mol}^{-1}$). In this way, the transmetalation rates of $\text{Cp}_2\text{ZrCl}(\text{Pr})$ under the action of ${}^i\text{Bu}_2\text{AlX}$ decrease in the order ${}^i\text{Bu}_2\text{AlCl} > {}^i\text{Bu}_2\text{AlH} > {}^i\text{Bu}_3\text{Al}$ [139].

Current views on the mechanism of the reaction of L_2ZrCl_2 with ${}^i\text{Bu}_3\text{Al}$ were substantially expanded in the recent study by Conley et al. [140]. When studying reactions of $[\text{CH}_2\text{CH}_2(\eta^5\text{-C}_9\text{H}_6)_2]\text{ZrCl}_2$ with 12 eq. of organoaluminum compound, they detected the formation of $\text{Zr}-(\mu\text{-Cl})\text{-Al}$ complex **Zr10**, presumably through β -Me elimination/carboalumination stages (Scheme 16). Notably, the π -complex in this Scheme represents the Zr(II) complex.



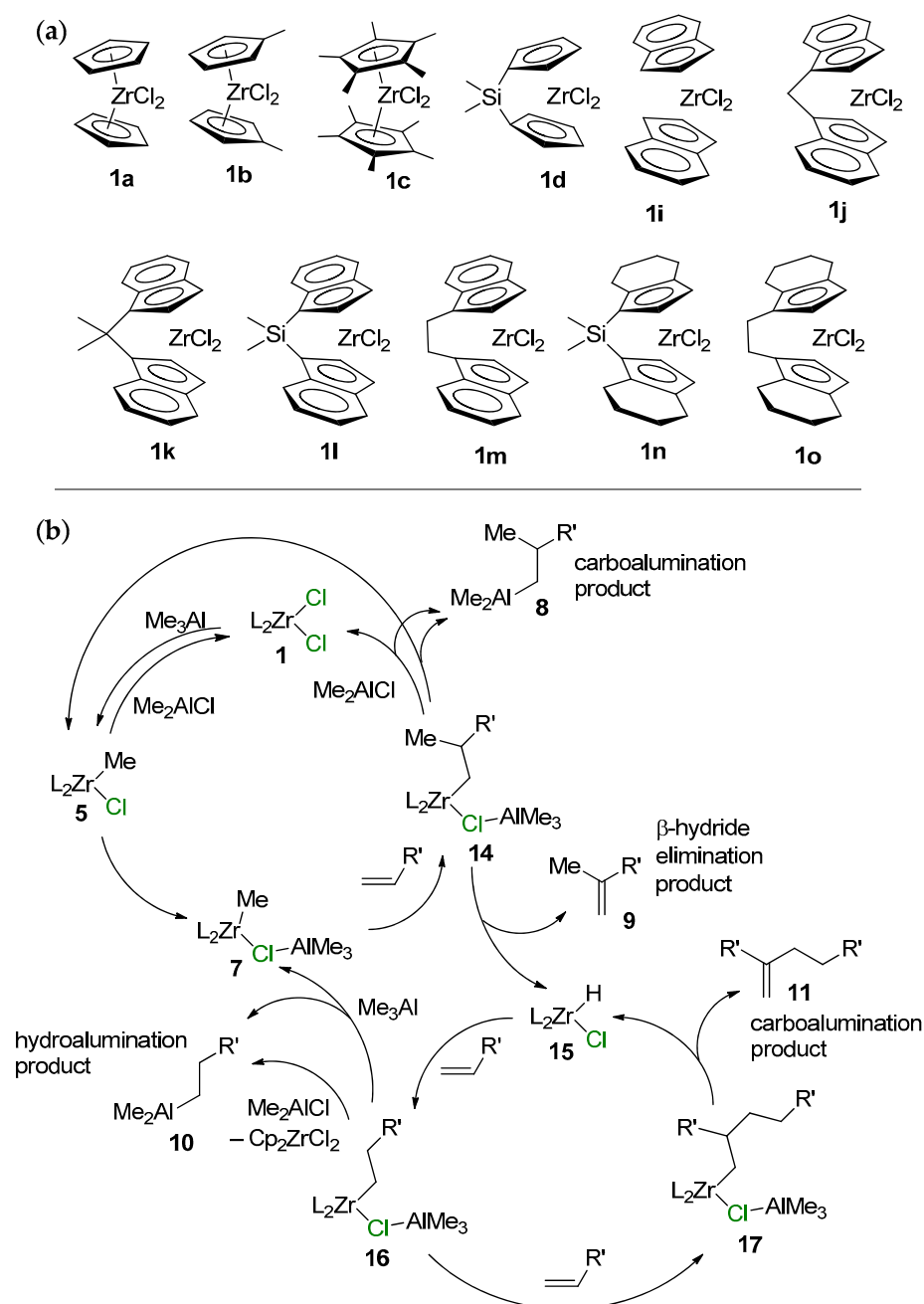
Scheme 16. The formation of Zr10 [140].

Cp_2ZrCl_2 -catalyzed carboalumination was discovered by Van Horn and Negishi [141]. This reaction was also considered in the review by Parfenova [18] and in the more recent review of Negishi [142]. In most studies on catalytic carboalumination, Me_3Al and (*n*-Alkyl) $_3\text{Al}$ have been used to avoid β -hydride elimination. Cp_2ZrCl_2 is not an efficient carboalumination catalyst (Scheme 17) [143,144]. As shown by Parfenova et al., the efficiency of carboalumination can be increased by the rational design of η^5 -ligands in the L_2ZrCl_2 pre-catalyst [145].



Scheme 17. Cp_2ZrCl_2 -catalyzed carboalumination [143,144].

When using Me_3Al as an activator, both carboalumination and hydroalumination processes can take place in the presence of other L_2ZrCl_2 complexes. In 2018, Parfenova et al. [126] studied the ligand exchange in 15 different zirconocenes, and the oct-1-ene reactivity of 11 of them (Scheme 18a) for L_2ZrCl_2 - Me_3Al systems. Based on the results of NMR spectral studies and catalytic experiments, a mechanism of the L_2ZrCl_2 -catalyzed reaction of alkenes with Me_3Al was proposed (Scheme 18b). In the first step, complex 1 reacted with Me_3Al to yield L_2ZrClMe (5). The subsequent reaction of complex 5 with Me_3Al yielded intermediate 7 (**Zr01**, see above), in which the Zr-Me bond is more polarized due to associations with electron-deficient Me_3Al . As shown above, complex **Zr01** exists in the associated state at temperatures below 230 K. At room temperature, it dissociates to Cp_2ZrMeCl and Me_3Al and its concentration becomes negligibly low; thus, the alkene does not react. Switching to the catalytic reaction shifts the equilibrium towards **Zr01**, and products 8–11 are formed in the system.



Scheme 18. (a) Structural formula of the L_2ZrCl_2 complexes studied in the catalytic reaction of oct-1-ene with Me_3Al ; (b) probable mechanism of the L_2ZrCl_2 -catalyzed reaction of alkenes with Me_3Al [126].

Notably, Cp_2ZrMe_2 demonstrated low catalytic activity in the reaction with oct-1-ene and Me_3Al . Complex **6** is not formed in the reaction of Cp_2ZrCl_2 with Me_3Al ; thus, a key role is played by **Zr01**-type intermediates. The degree of association of $L_2ZrMeCl$ with Me_3Al also depends on the π -ligand environment of Zr and the nature of the solvent. In this way, realization of the process presented in Scheme 18b requires the presence of Cl in the reaction mixture. In other words, the presence of the Zr-(μ -Cl)-Al structural fragment in key catalytic species and the alkene insertion would, most likely, be accelerated in the $L_2ZrMe(\mu-Cl)AlMe_3$ active complex.

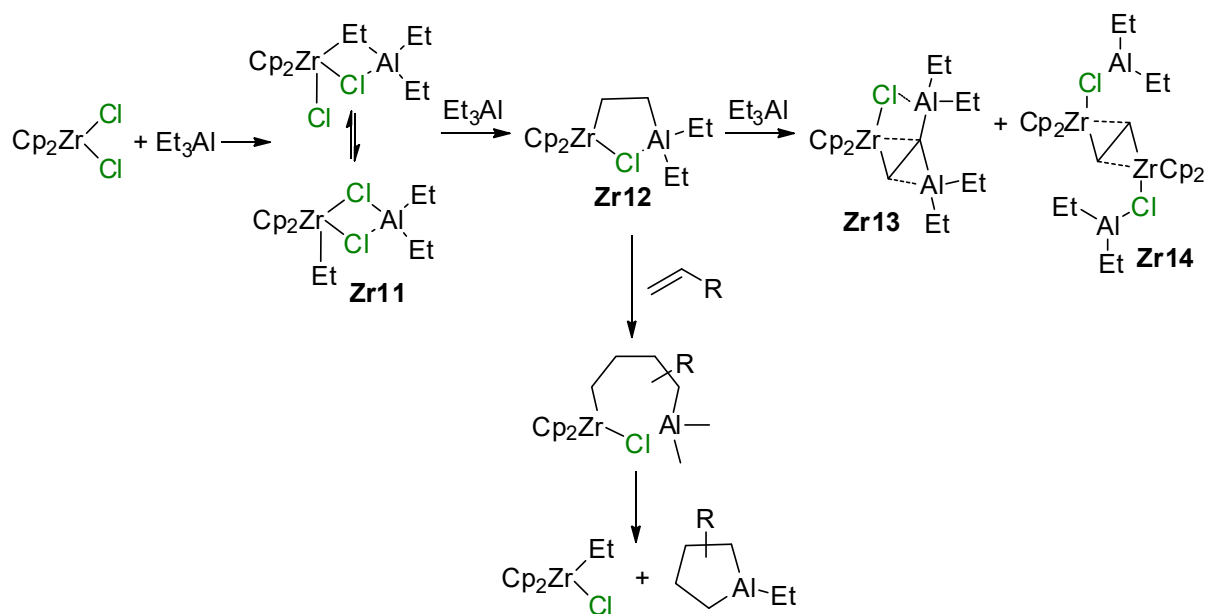
Catalytic reactions were conducted in two different solvents (CH_2Cl_2 and toluene) using a $\text{L}_2\text{ZrCl}_2/\text{alkene}/\text{AlMe}_3$ ratio of 1:50:60. The results of the experiments are presented in Table 1.

Table 1. Conversion and product yields in the reaction of the oct-1-ene with Me_3Al in the presence of 2 mol% L_2ZrCl_2 ($\text{L}_2\text{ZrCl}_2/\text{alkene}/\text{Me}_3\text{Al} = 1:50:60$, 20 °C, 24 h) [126].

L_2ZrCl_2	Solvent	Conversion, %	Product Yield, %			
			8	9	10	11
1a	CH_2Cl_2	92	3	14	7	68
	toluene	69	3	21	7	38
1b	CH_2Cl_2	84	11	14	7	52
	toluene	39	9	9	9	12
1c	CH_2Cl_2	68	53	8	7	-
	toluene	44	15	14	14	1
1d	CH_2Cl_2	24	<1	5	5	13
	toluene	13	<1	4	6	2
1i	CH_2Cl_2	89	31	19	-	39
	toluene	70	38	14	10	8
1j	CH_2Cl_2	0	-	-	-	-
	toluene	11	9	-	-	2
1k	CH_2Cl_2	2	0.6	0.3	0.7	-
	toluene	4	<1	1.6	1	1
1l	CH_2Cl_2	30	20	1	<1	9
	toluene	99	63	2	-	34
1m	CH_2Cl_2	16	15	-	<1	<1
	toluene	26	22	-	1	3
1n	CH_2Cl_2	3	1	-	-	-
	toluene	35 ¹	13	-	-	-
1o	CH_2Cl_2	17	16	<1	<1	-
	toluene	2	46	2	<1	4
Cp_2ZrMe_2	CH_2Cl_2	16	6	4	5	1
	toluene	9	3	3	<1	<1

¹ Dimers and oligomers formed.

The reaction between Et_3Al and Cp_2ZrCl_2 has a complex mechanism, which occurs in several elementary steps [146]. When using 1 eq. of Et_3Al , the $\text{Zr}-(\mu\text{-Cl})\text{-Al}$ complex **Zr11** is formed. With an excess of Et_3Al , C–H activation takes place to yield a relatively unstable species, **Zr12**, which is subsequently converted to a more stable **Zr13** via the secondary C–H activation along with a smaller amount of **Zr14** (Scheme 19). The molecular structure of **Zr13** was determined by XRD [147] (Figure 14). In the presence of α -olefin, the highly reactive species **Zr12** is further transformed into a cycloaluminum product [148]. The mechanism of this reaction was studied by DFT modeling, which confirmed the importance of $\text{Zr}-(\mu\text{-Cl})\text{-Al}$ bonding for all key reaction stages [149–152].



Scheme 19. Reaction of Cp_2ZrCl_2 with Et_3Al [146] and the cycloalumination process [148].

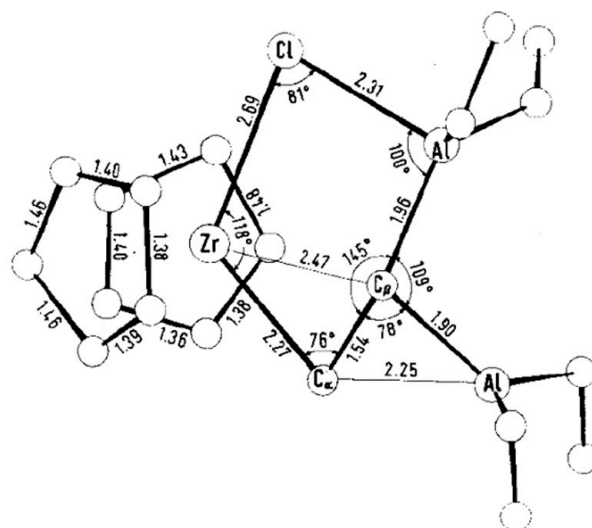
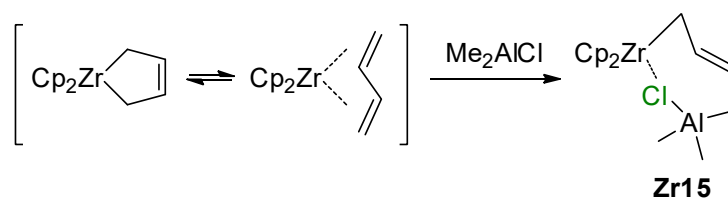


Figure 14. Molecular structure of **Zr13**. Reprinted with permission from [147]. Copyright (1974) Wiley-VCH Verlag GmbH & Co.

An interesting complex, **Zr15** with a $\text{Zr}-(\mu\text{-Cl})\text{-Al}$ fragment, was formed as a result of the reaction of the Cp_2Zr buta-1,3-diene complex with Me_2AlCl (Scheme 20) [153].



Scheme 20. Reaction of the $\text{Zr}(\text{IV})$ buta-1,3-diene complex with Me_2AlCl [153].

Zr analogs of the Tebbe reagent $\text{Cp}_2\text{Zr}(\mu\text{-CHR})(\mu\text{-Cl})\text{AlR}'_2$ were obtained (a) by the reaction of $\text{Cp}_2\text{Zr}(\text{Cl})\text{CH}=\text{CHR}$ with $\text{R}'_2\text{AlH}$ or (b) by the reaction of Cp_2ZrHCl with $\text{R}'_2\text{AlCH}=\text{CHR}$ [154,155]. The molecular structure of one of these complexes with

$R = \text{CH}_2^t\text{Bu}$ and $R' = ^i\text{Bu}$ (**Zr16**) was proven by XRD (Figure 15). Similar complexes have not demonstrated any synthetic or catalytic prospects.

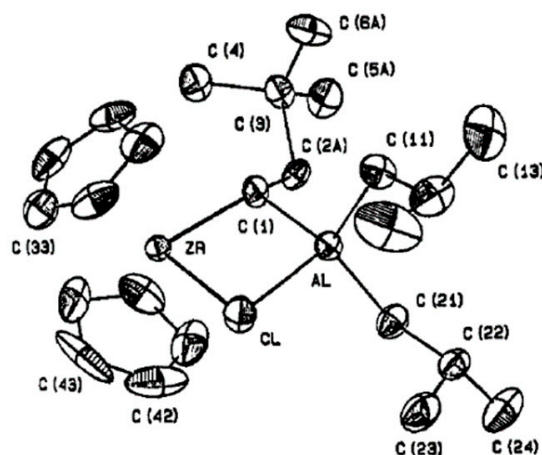
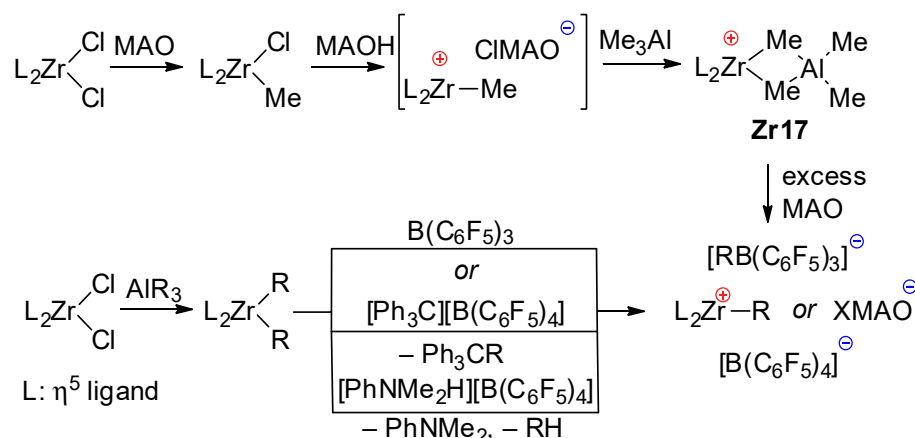


Figure 15. Molecular structure of complex **Zr16**. Reprinted with permission from [155]. Copyright (1987) American Chemical Society.

3.2. Zirconocene Cationic Complexes in Oligomerization and Polymerization of α -Olefins

Generally accepted mechanisms of the activation of zirconocene pre-catalysts L_2ZrCl_2 depend on the type of activator. When using MAO, methylation results in a L_2ZrMeCl complex, which eliminates Cl^- under the action of MAO. However, when using a slight excess of MAO, Me_3Al (inevitably present in MAO due to its dynamic nature), the intermediate active cation forms the inactive cationic complex **Zr17**, which can be reactivated when using a large excess of MAO. Notably, MAO has limited ability to activate L_2ZrCl_2 ; the nature of the primary η^5 -ligand environment (L_2Zr fragment) affects the rate and equilibria of the formation of the catalytic species [122,156]. In the presence of trialkylaluminum and perfluoroaryl borates, an alkylzirconocene cation is formed through the alkylation of L_2ZrCl_2 with AlR_3 , followed by the elimination of one Zr-alkyl under the action of $\text{B}(\text{C}_6\text{F}_5)_3$ or by the alkyl abstraction or protonation of Zr-alkyl by $[\text{Ph}_3\text{C}]^+$ or $[\text{PhNMe}_2\text{H}]^+$ counterions of $[\text{B}(\text{C}_6\text{F}_5)_4]^-$, respectively (Scheme 21).



Scheme 21. Conventional mechanism of L_2ZrCl_2 activation by MAO and perfluoroaryl borates.

The negative role of Cl^- in the zirconocene-catalyzed polymerization of α -olefins when using MAO as an activator was demonstrated by Cramail et al. in the framework of the simplified MAO model [157]; however, further studies have shown that not everything is so unambiguous, primarily because of the incompleteness of the early conceptions of the MAO structure. In recent years, this issue was clarified; essentially, the presence of

Cl-containing MAO species as counter-ions was confirmed experimentally [28,125,158,159]. In particular, the molecular ion with an m/z ratio of 1395 (Figure 16) was detected when analyzing the activation of Cp_2ZrCl_2 by MAO. Evidently, it is the Al–Cl fragment in this molecule that can coordinate at the Zr catalytic center. This model of ‘chlorinated’ MAO was developed on the basis of previous mass spectrometry studies [26].

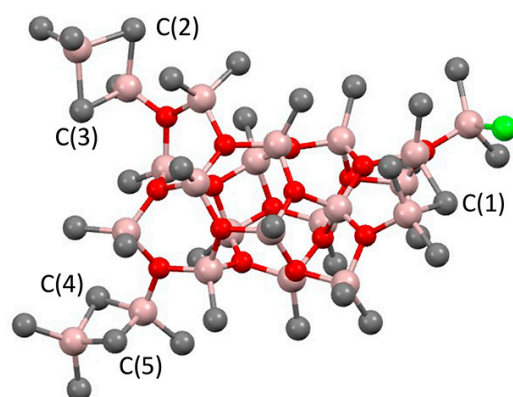


Figure 16. Model for anion with m/z 1395 featuring a terminal Me_2AlCl . Reprinted with permission from [28]. Copyright (2017) American Chemical Society.

In [23], Linnolahti et al. proposed a simple and visual model of the structure of an MAO cluster, suitable for DFT modeling. They demonstrated that the chlorination of MAO leads to the overall facilitation of catalyst activation processes.

There are no examples of cationic *catalytically active* zirconocene species with $\text{Zr}-(\mu\text{-Cl})\text{-Al}$ fragments whose molecular structures have been proven by XRD. It is worth pointing out here that cationic Zr complexes with $[\text{MeAl}(2\text{-C}_6\text{F}_5\text{C}_6\text{F}_4)_3]^-$ (**Zr18**) [160] and $[\text{FAl}(2\text{-C}_6\text{F}_5\text{C}_6\text{F}_4)_3]^-$ ions (**Zr19**) [22] have been separated and analyzed by XRD. As can be seen in Figure 17, the differences between $\text{Zr}-(\mu\text{-X})$ and $\text{Al}-(\mu\text{-X})$ are equal to 0.48 and 0.33 Å for $\text{X} = \text{C}$ and $\text{X} = \text{F}$, respectively. Whether $\text{Al}(\text{C}_6\text{F}_5)_3$ is capable of Cl abstraction from $\text{L}_2\text{CpCl}(\text{Alkyl})$ complexes is now an open question.

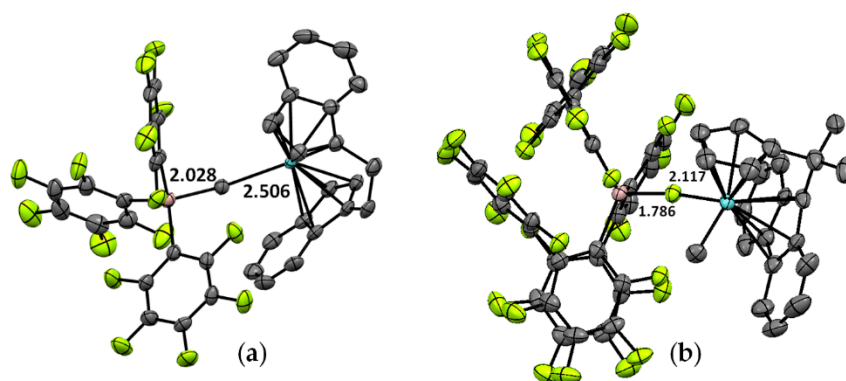


Figure 17. Molecular structures of the complexes (a) $\{[(\text{CH}_2\text{CH}_2)\text{Ind}_2]\text{ZrMe}\}^+[\text{MeAl}(\text{C}_6\text{F}_5)_3]^-$ (**Zr18**) [160] and (b) $[\text{Me}_2\text{C}(\text{Cp})(\text{Flu})]\text{ZrMe}\}^+[\text{FAl}(2\text{-C}_6\text{F}_5\text{C}_6\text{F}_4)_3]^-$ (**Zr19**) [22].

In recent publications [161,162], the mechanism of the activation of L_2ZrCl_2 pre-catalysts by MAO was significantly revised with new experimental data that point to the intermediate formation of $[\text{L}_2\text{Zr}(\mu\text{-Cl})_2\text{AlR}_2]^+$ cationic species via the generation of R_2Al^+ , followed by their reaction with L_2ZrCl_2 . At the same time, an alternative activation pathway was proposed for the reaction of L_2ZrCl_2 with $[\text{Bu}_2\text{Al}][\text{B}(\text{C}_6\text{F}_5)_4]$, namely, Cl^- abstraction with a formation of L_2ZrCl^+ species [33].

Notably, the cationic complex $\{rac\text{-}[\text{Me}_2\text{Si}(\eta^5\text{-C}_9\text{H}_6)_2]\text{Zr}(\mu\text{-Cl})_2\text{Al}^i\text{Bu}_2\}^+$ (**Zr20**) was formed by the reaction of $\{rac\text{-}[\text{Me}_2\text{Si}(\eta^5\text{-C}_9\text{H}_6)_2]\text{Zr}(\mu\text{-H})_3(\text{Al}^i\text{Bu}_2)_2\}^+$ and characterized by

NMR spectroscopy [163]. The complex $\{rac-[Me_2Si(\eta^5-C_9H_6)_2]Zr(\mu-Cl)_2AlMe_2\}^+$ (**Zr21**) was similarly obtained by the reaction of $\{rac-[Me_2Si(\eta^5-C_9H_6)_2]Zr(\mu-Cl)_2AlMe_2\}^+$ with Me_3AlCl [164]. XRD studies of type $[L_2Zr(\mu-Cl)_2AlR_2]^+$ complexes are mentioned in [33], referring to conference papers [165,166]; however, the Cambridge Crystallographic Data Centre (CCDC) has no information about these compounds. The structure of $\{rac-[Me_2Si(\eta^5-C_9H_6)_2]Zr(\mu-Cl)_2AlMe_2\}^+$ was proven by a combination of chemical modification and XRD analysis of the Zr(III) neutral complex $rac-[Me_2Si(\eta^5-C_9H_6)_2]Zr(\mu-Cl)_2AlMe_2$ (**Zr22**) obtained by the reduction of **Zr21** (Figure 18). The complexes **Zr20–Zr22** were inactive in α -olefin polymerization.

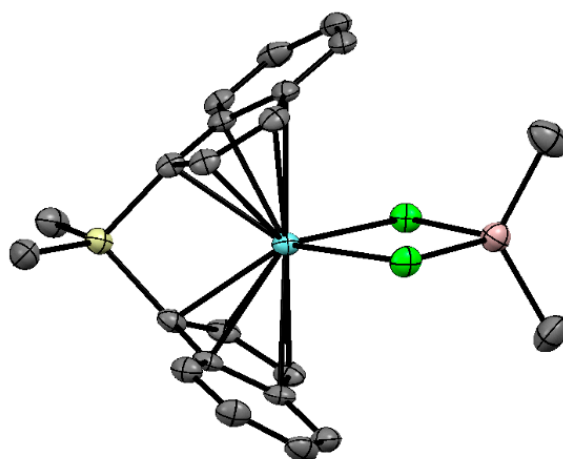
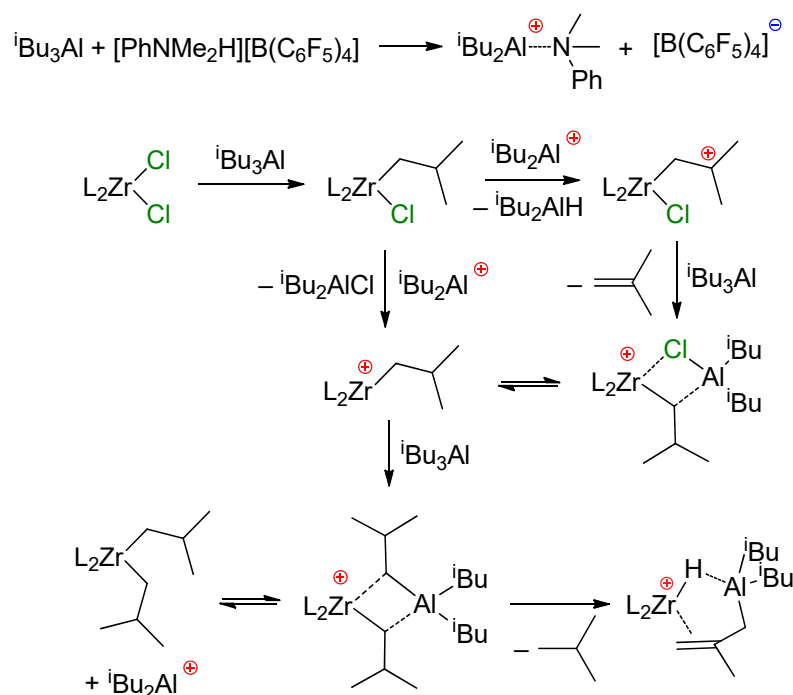


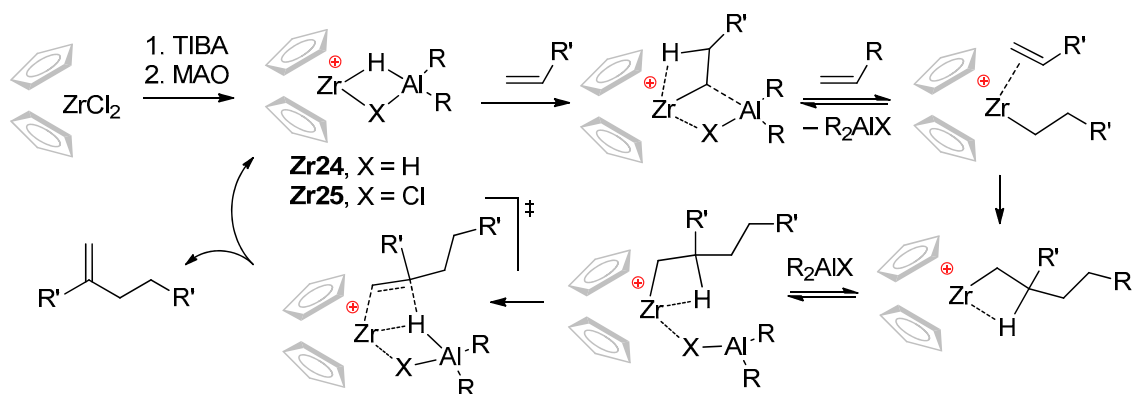
Figure 18. Molecular structure of $rac-[Me_2Si(\eta^5-C_9H_6)_2]Zr(\mu-Cl)_2AlMe_2$ (**Zr22**). Reprinted with permission from [164]. Copyright (2013) American Chemical Society.

In the presence of $[Ph_3C][B(C_6F_5)_4]$, the activation of L_2ZrCl_2 by iBu_2AlH results in the formation of complex cationic hydrides $L_2Zr(\mu-H)_3(Al^iBu_2)_2^+$ via a $L_2ZrCl(\mu-H)_2Al^iBu_2$ intermediate [163]. However, the reaction of L_2ZrCl_2 ($L_2 = Ph_2C(Cp)(Flu)$) with TIBA and a $[PhNM_e_2H][B(C_6F_5)_4]$ activator proceeds in a complex pathway, allegedly involving Zr–(μ -Cl)–Al species (Scheme 22) [128].



Scheme 22. Proposed formation of $[Ph_2C(Cp)(Flu)Zr(\mu-H)(\mu-C_4H_7)Al^iBu_2]^+$ [128].

of α -olefins [39,40]. This hypothesis implies the participation of Zr–Al catalytic species **Zr24** and **Zr25** capable of reversible insertion of the α -olefin molecule. After the second α -olefin insertion, the reversible coordination of R_2AlX fragment can facilitate irreversible β -hydride elimination with the formation of methylenealkanes that are inert towards **Zr24** and **Zr25** (Scheme 24). It was also supposed that R_2AlCl should demonstrate the best efficiency as a selective ‘limiter’ of the degree of polymerization (DP_n) to 2.



Scheme 24. Mechanistic concept explaining the selective formation of α -olefin dimers by Zr–(μ -Cl)–Al bonding (X = H, Cl) [39–42].

These hypotheses were supported by additional experiments and DFT calculations [41,42]. In [41], oligomerization of hex-1-ene with the use of Cp_2ZrCl_2 pre-catalyst was studied experimentally, and DFT optimizations for all possible reaction pathways of prop-1-ene oligomerization with and without the involvement of R_2AlX (R = Me, i Bu; X = H, Cl, Me) were performed. The key stage of the α -olefin formation was chain termination after insertion of the second α -olefin molecule. For the simple cationic model, this process is carried out on the mechanism of β -hydride transfer to monomer, whereas with the assistance of the R_2AlX β -hydride, elimination occurs. In the latter case, Al atom demonstrates a cooperative effect (Figure 19). For R = Me, the values of the activation barriers ΔG^\ddagger of β -hydride elimination stage were 17.7 (H), 13.6 (Cl), and 16.2 (Me) kcal/mol. Thus, β -hydride elimination is the most affected by Me_2AlCl coordination at the Zr atom.

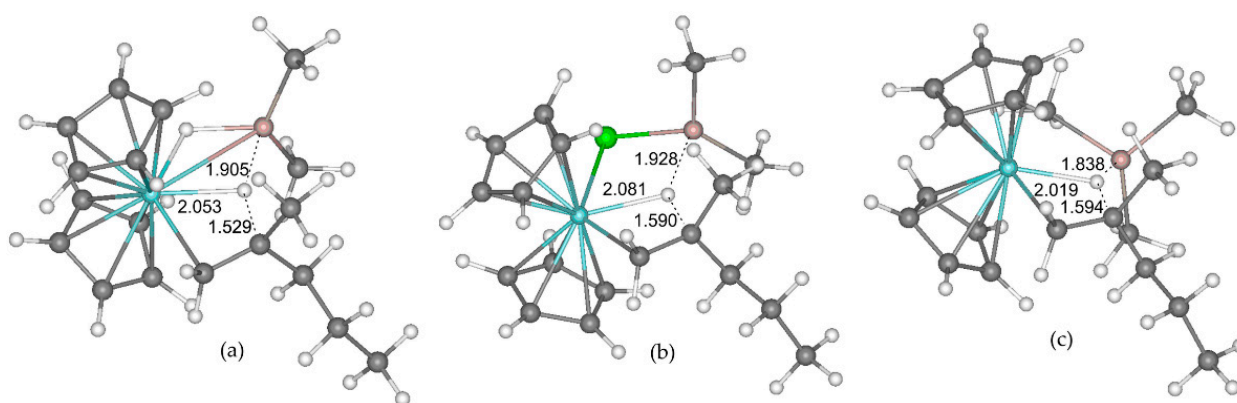


Figure 19. Calculated geometries of the transition states of β -hydride elimination in $Cp_2Zr(\mu-X)(CH_2CHMePr)AlMe_2$ model complexes. (a) X = H; (b) X = Cl; (c) X = Me. The distances Zr–H, Al–H and β C–H are specified (Å). Reprinted with permission from [41]. Copyright (2019) MDPI.

In the study by Nifant'ev et al. [42], oct-1-ene oligomerization with the use of pre-catalysts Cp_2ZrCl_2 , Cp_2ZrMe_2 , $O[SiMe_2(\eta^5-C_5H_4)]_2ZrCl_2$ (**Zr23**), and its dimethyl derivative **Zr23'** was studied, DFT modeling was conducted for both zirconocenes using but-1-ene as a model α -olefin. The main theoretical results with regard to Cp_2Zr -derived species

were in line with the results of prior research [41], whereas in the case of **Zr23**-based catalytic species, additional Zr–O and Al–O interactions played a significant role in the catalytic process, stabilizing the reaction intermediates and lowering the activation barriers (Figures 20 and 21).

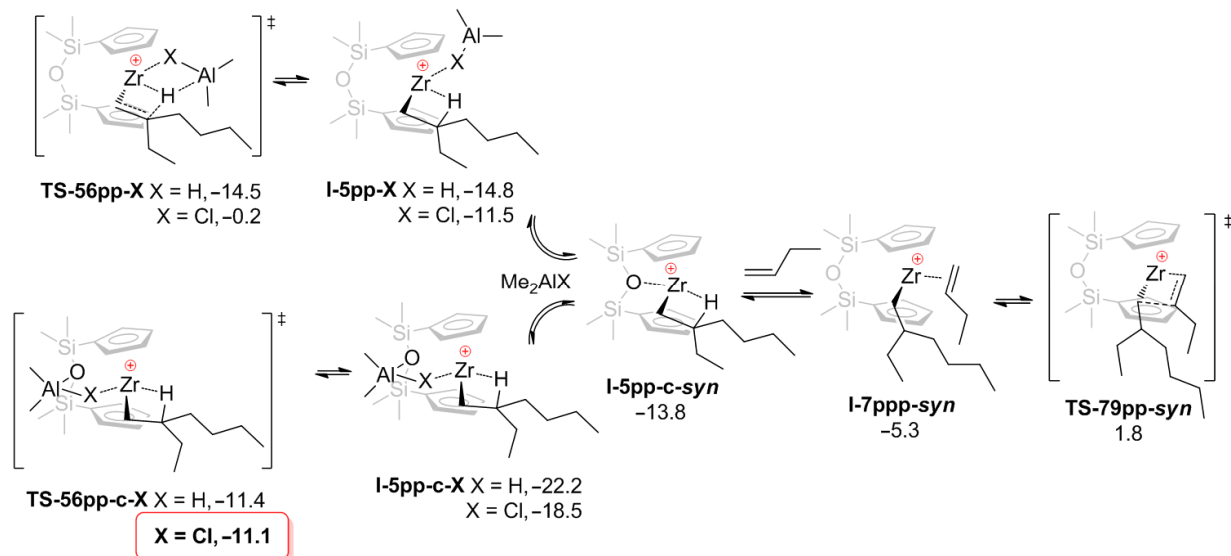


Figure 20. Transformations of $O[SiMe_2(\eta^5-C_5H_4)]_2Zr$ -derived β -agostic complex **I-5pp** with the participation of Me_2AlX species. The values of calculated free energies (kcal/mol) relative to **I-2p β -c** are given. Reprinted with permission from [42]. Copyright (2020) MDPI.

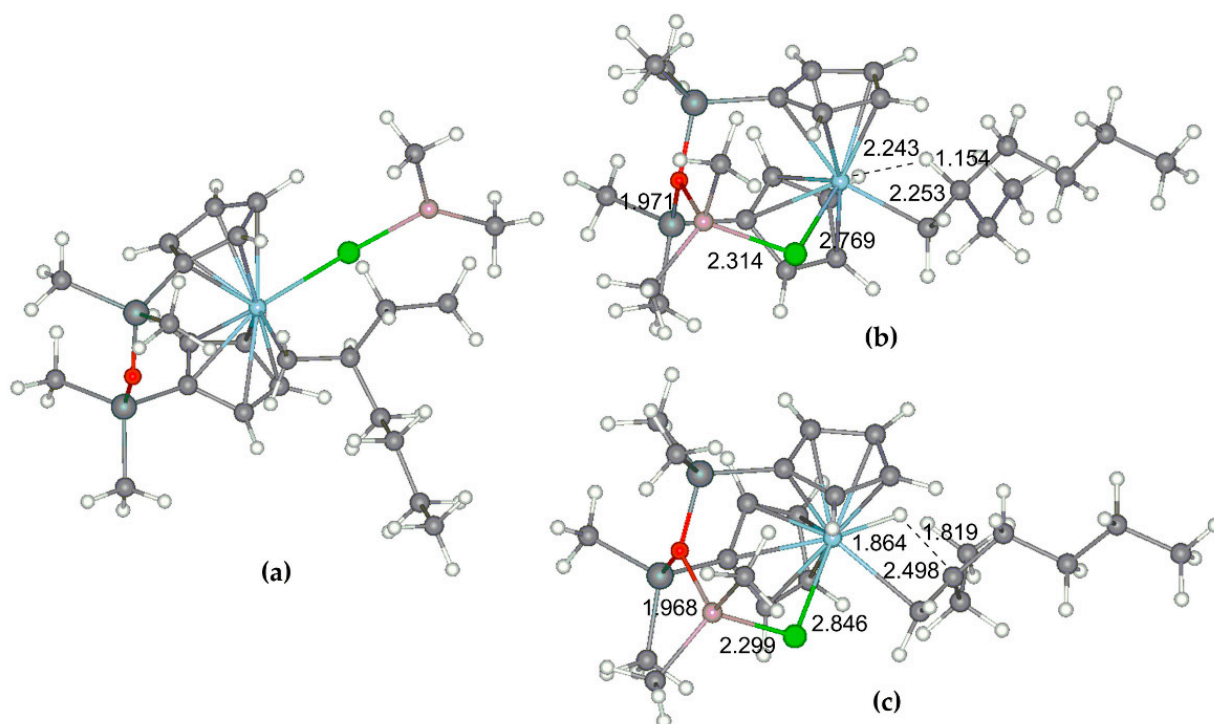
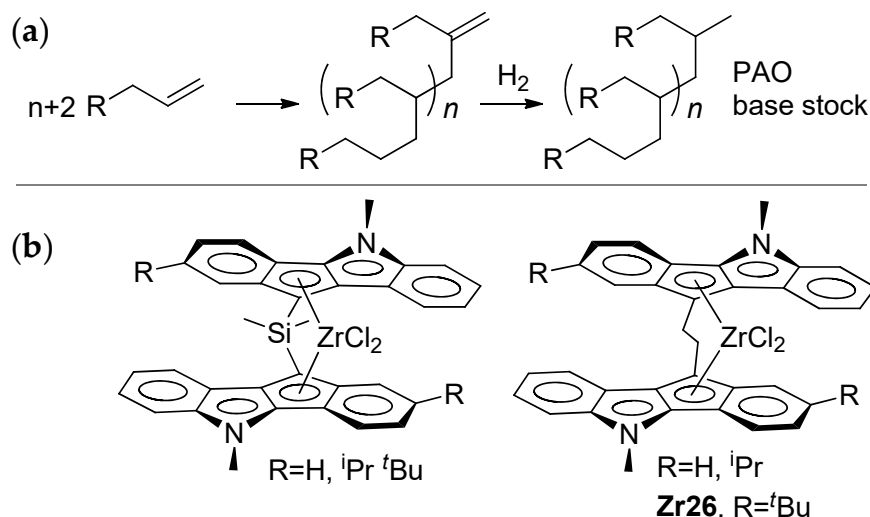


Figure 21. Optimized geometries of $O[SiMe_2(\eta^5-C_5H_4)]_2Zr$ -derived stationary points **I-5pp-Cl** (a), **I-5pp-c-Cl** (b), and transition state **TS-56pp-c-Cl** (c). Reprinted with permission from [42]. Copyright (2020) MDPI.

Thus, if zirconocene-catalyzed dimerization requires the a minimal excess of MAO (less than 10 eq.) and zirconocenes of the cyclopentadienyl type (Cp_2ZrCl_2 , **Zr23**), the cat-

alytic oligomerization of α -olefins (Scheme 25a) is usually conducted at higher $\text{Al}_{\text{MAO}}/\text{Zr}$ ratios. However, these ratios are hardly capable of the complete ‘fixation’ of R_2AlCl (MAO as a ‘sponge’ for organoaluminum compounds in the reaction mixture). On the other hand, the greater diversity of zirconocenes used in this reaction still attracts researchers’ attention [17,186–192]. The activation of L_2ZrCl_2 by R_3Al and perfluoroaryl borates was also found to be efficient in α -olefin oligomerization. This type of activation was used in the recent study by Nifant’ev et al., who reported that $-\text{CH}_2\text{CH}_2-$ bridged indeno[1,2-*b*]indole *ansa*-complexes (Scheme 25b) demonstrate high efficiency in the synthesis of lightweight oligomers of dec-1-ene ($\text{DP}_n = 3\text{--}5$) with uniquely homogeneous molecular structures [43].



Scheme 25. (a) Coordination oligomerization of α -olefins; the idealized uniform molecular structure of the oligomers was achieved when using ‘heterocene’ catalysts (b) [43].

Such catalytic behavior differs from both the activity and selectivity of conventional zirconocenes; therefore, additional research was carried out. Surprisingly, the addition of $\text{}^i\text{Bu}_3\text{Al}$ to the solution of **Zr26** did not result in $\text{Cl} \rightarrow \text{}^i\text{Bu}$ exchange at the Zr atom. One can assume that the dissolution of **Zr26** occurs through the formation of the **Zr26**- $\text{}^i\text{Bu}_3\text{Al}$ complex with weak Cl-Al coordination. Notably, a similar complexation of L_2ZrCl_2 with metal alkyls was recently discussed by Kumawat and Gupta in their study on the DFT modeling of zirconocene activation and chain transfer [124].

At the first stage of the activation, **Zr26** does not exhibit substantial conversion to Zr-Al hydrides under the action of TIBA. However, after the addition of $[\text{PhNHMe}_2][\text{B}(\text{C}_6\text{F}_5)_4]$, a rapid reaction proceeded with the sedimentation of oily low-soluble product. After the addition of dec-1-ene, no oligomerization was observed. Rapid oligomerization was detected when the activation of **Zr26** by TIBA and borate were conducted in the presence of molecular hydrogen, and light-brown crystals of **Zr27** were formed at the end of the reaction. After the addition of dec-1-ene to the reaction mixture, oligomerization started again. It turned out that **Zr27** alone was inactive in dec-1-ene oligomerization in the presence of H_2 ; however, when TIBA was added to the **Zr27** suspension in toluene, the rapid oligomerization of dec-1-ene occurred. The final product of the catalyst transformation of **Zr27** was separated and characterized by NMR (Figure 22) and XRD analysis (Figure 23). The spectral view of **Zr27** remained unchanged after 7 days, which indicates high stability of the cationic complex in the solvating solvent (THF).

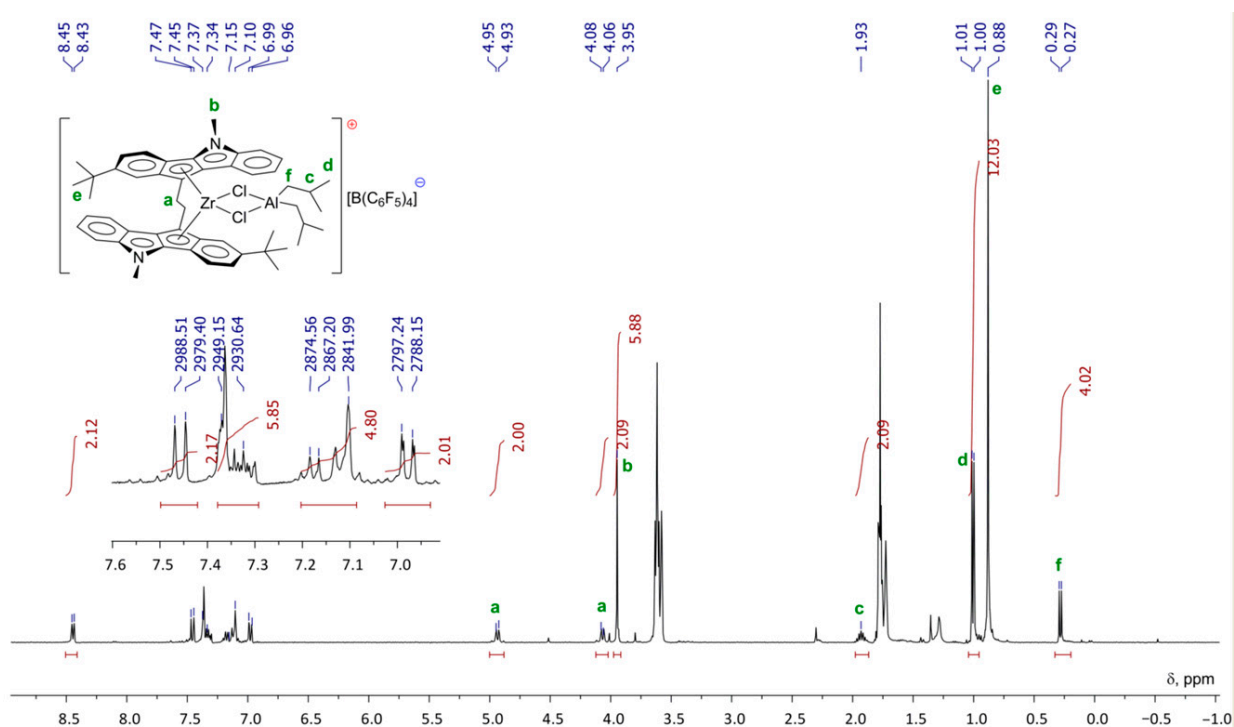


Figure 22. ^1H NMR spectra (400 MHz, THF-d_8 , 20°C) of **Zr27**. Reprinted with permission from [43]. Copyright (2022) Elsevier B.V.

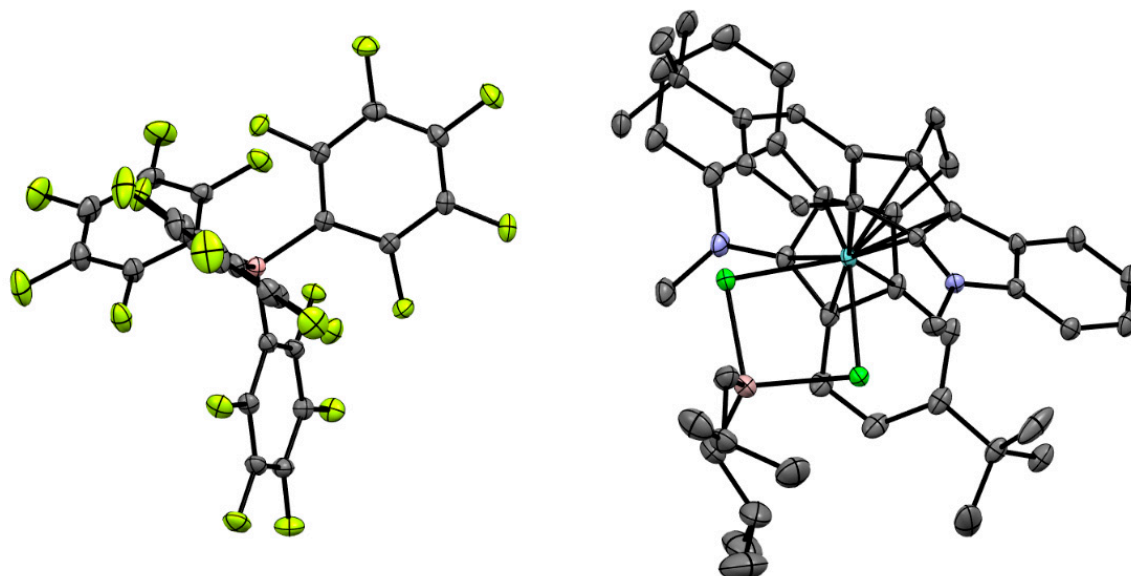


Figure 23. Schemes follow the same formatting. Reprinted with permission from [43]. Copyright (2022) Wiley-VCH Verlag GmbH & Co. Copyright (2016) Royal Society of Chemistry. Copyright (2012) American Chemical Society. Copyright (2015) Springer Nature. Copyright (2019) Elsevier B.V.

The experimental fact of the ‘recovery’ of $\text{Zr}-(\mu\text{-Cl})_2\text{-Al}$ complex **Zr27** clearly indicates that the mechanism of heterocene-catalyzed oligomerization went beyond the conventional cationic mechanism of the zirconocene-catalyzed polymerization of α -olefins. There is a very realistic chance that it is the retention of Zr-Cl-Al coordination that provides structural homogeneity of dec-1-ene oligomers when using heterocene catalysis.

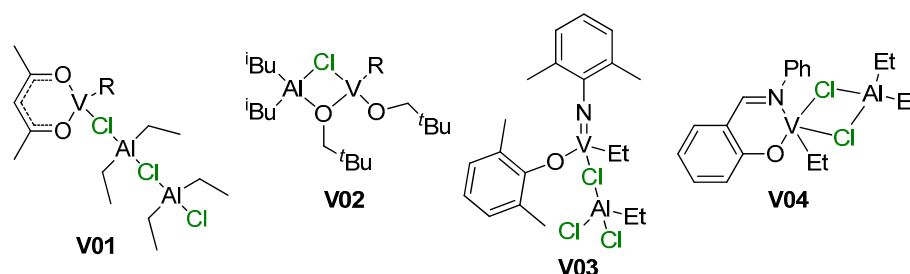
Comparison of the hydrogen response during ethylene polymerization, demonstrated by dichloro- and dimethyl *ansa*-complexes $[(\eta^5\text{-C}_9\text{Me}_6)\text{SiMe}_2(\eta^5\text{-C}_5\text{H}_4)]\text{ZrX}_2$ ($\text{X} = \text{Cl}$, **Zr28**; $\text{X} = \text{Me}$, **Zr29**), immobilized on solid MAO, may also be seen as indirect evidence of $\text{Zr}-(\mu\text{-Cl})_2\text{-Al}$ complex **Zr27**.

Cl)–Al bonding in catalytic species: **Zr28**-based catalysts turned out to be inert to molecular hydrogen [193]. The relative stability of Zr–(μ -Cl)–Al bonding in catalyst precursor, $L_2Zr(R)$ –(μ -Cl)– AlR'_3 complexes, essentially depends on the electrophilicity of the Al atom. With the introduction of the electron acceptor fragments, e.g., when using $^iBu_2Al(OC_6F_5)$ [194], an ion pair is easily formed, as evidenced by polymerization experiments.

On the basis of the latest investigations [33,43,161,162], it can be concluded that the difference in the mechanisms of the $L_2ZrCl_2 + AlR_3$ reactions in the absence and presence of MAO (or perfluoroaryl borates) consists of various degrees of ‘chlorination’ for the first-stage products. In the absence of MAO or borate, alkyl transfer from Al to Zr occurs with the formation of $LZrR_2 \cdots ClAlR_2$ complexes with weak $Zr \cdots Cl$ bonds (if $R = ^iBu$, the transformation to Zr–Al hydrides results in heterometallic complexes with stronger Zr–(μ -H)–Al bonds). When using MAO or perfluoroaryl borates, resulting R_2Al^+ species rapidly react with $LZrCl_2$ to form cationic $[LZr(\mu-Cl)_2AlR_2]^+$, thus creating certain preconditions for the involvement of R_2AlCl in further reactions with α -olefins.

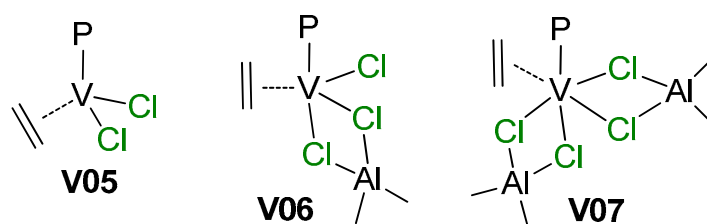
4. Complexes of V

Vanadium-catalyzed α -olefin polymerization was previously reviewed by van Koten et al. in 2002 [195]; by Gambarotta in 2003 [196]; by Redshaw in 2010 [197]; by Wu and Li in 2011 [198]; by Nomura and Zhang in the same year [199]; and by Phillips et al. in 2020 [44]. In these reviews, the focus was on different types of the coordination compounds of V, pre-catalysts of α -olefin polymerization. The mechanisms of polymerization in these reviews were fragmented; however, in contrast to reviews on group 4 metal Ziegler–Natta and single-site catalysts, the importance of V–(μ -Cl)–Al bonding in pre-catalysts and in catalytic species was not ignored (Scheme 26). Here, in strong contrast to Ti- and Zr-based pre-catalysts, a large number of V-based catalysts are effectively activated by R_2AlCl or $AlCl_2$, as opposed to ineffective R_3Al and MAO. In this section, we discuss several examples of V–(μ -Cl)–Al complexes that have been missed in previous reviews, or that had been served poorly, as well as new examples of these complexes.



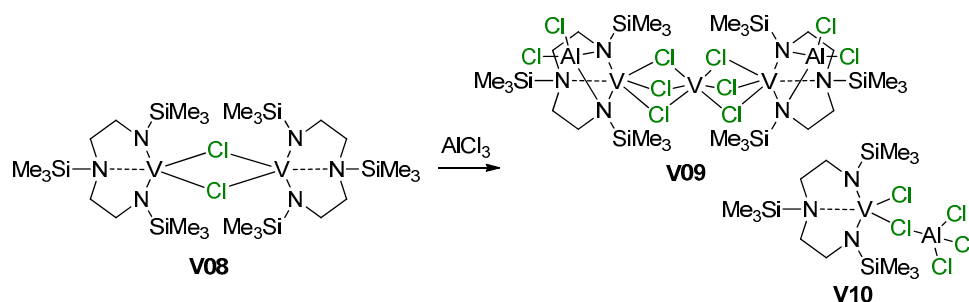
Scheme 26. Examples of V–(μ -Cl)–Al active species mentioned in previous reviews [44,195,199].

Among older publications on the subject of V-catalyzed polymerizations of α -olefins, the feature article of Zambelli et al. [200] merits special attention. The authors reinvestigated three models of catalytic complexes **V05**–**V07** proposed in the literature for VCl_3/R_2AlCl catalyst systems (Scheme 27). DFT modeling of the insertion of ethylene molecule was conducted for $P = Me$ according to the conventional Cossee–Arlman scheme. Thermodynamic data for ethylene insertion were close for all three complexes, but significant differences were observed for values of the activation barrier of insertion that were 16, 16, and only $1.7 \text{ kcal}\cdot\text{mol}^{-1}$ for **V05**, **V06**, and **V07**, respectively. DFT modeling of prop-1-ene insertion explained the observed syndiotacticity of prop-1-ene polymerization.



Scheme 27. The hypothetical active species for V catalysts (P = polymer chain) [200].

As can be seen in Schemes 26 and 27, V(III) species are active in polymerization. Obviously, the mechanisms of the deactivation of V centers are important for the development of efficient catalysts. It is thought that the most likely route for deactivation would be reactions with the organoaluminum compound. However, in 2002, Gambarotta et al. demonstrated an alternative pathway of such deactivation via disproportionation of the V(III) complex **V08** with the formation of V(II)/V(III) (**V09**) and V(IV) (**V10**) species [201] (Scheme 28, Figure 24); AlCl_3 in this process acts as Lewis acid and it cannot be ruled out that organoaluminum co-catalysts can promote catalyst deactivation in a similar way.



Scheme 28. Disproportionation of V(III) complex **V08** [201].

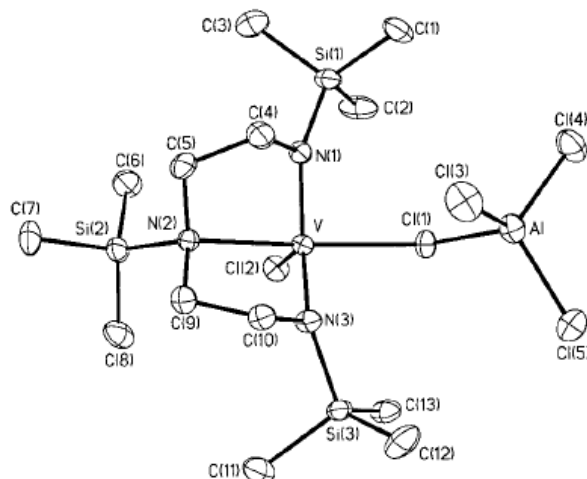
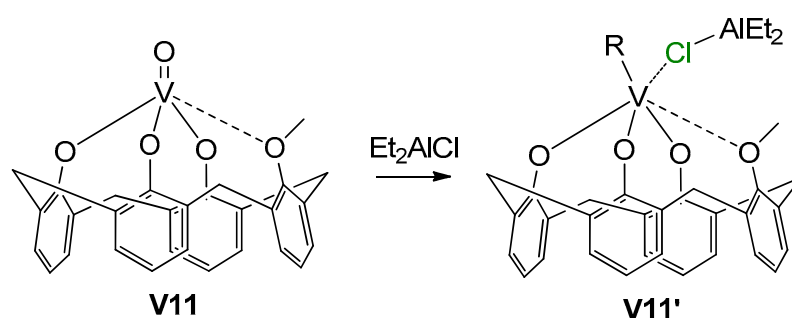


Figure 24. ORTEP plot of **V10**. Thermal ellipsoids are drawn at the 30% probability level. Reprinted with permission from [201]. Copyright (2002) American Chemical Society.

Another important aspect of V catalysis in α -olefin and diene polymerization was demonstrated by Centore et al. [202], who studied the catalytic activity of the pre-catalyst $[(\kappa^1\text{-}i\text{PrN}=\text{C}(\text{Ph})\text{N}^i\text{Pr})\text{V}(\text{O})\text{Cl}(\mu\text{-Cl})_2]$ using different organoaluminum activators. They showed that the amidinate ligand can easily be removed from the vanadium in the reaction with organometallic cocatalysts, and the active species are closely related to those obtained from other vanadium precatalysts such as VCl_4 (for example, **V07**). This result imposes certain restrictions on the ligand-oriented design of V-based polymerization

catalysts. Stronger V–ligand bonding, such as in **V03** [203], provides a retention of the base ligand environment. Polyphenolate ligands can also provide stability of the catalytic species [204]; in particular, activation of the pre-catalyst **V11** (Scheme 29) resulted in the formation of V(IV) complex **V11'**, which is active in ethylene polymerization. V(III) complexes with bidentate *N,N*-chelating iminopyrrolyl ligands also demonstrated stability in the base ligand environment and relatively high catalytic activity in the polymerization of ethylene when using Et_2AlCl as an activator; in the presence of Et_3Al or MAO, PE was formed in trace amounts [205]. The complexes with tridentate iminopyrrolyl and tetradentate bis(iminopyrrolyl) ligands [206], well as with bidentate phenoxy-phosphine ligands [207] and with tridentate 2,6-bis(diphenylhydroxymethyl)pyridyl ligand [208], have demonstrated similar behavior. However, in the last case, when comparing V(III) and V(V) derivatives in Et_2AlCl -activated polymerization, the V(V) complex demonstrated higher activity. Apparently, even when using the same Cl-containing activator, the nature of the active site essentially depends on the nature of the polydentate ligand.



Scheme 29. Formation of active V(IV) phenolate complex **V11'** [204].

V(III) complexes bearing salicylaldiminato ligands (similar to **V04**), synthesized by Lee et al. [209,210], also showed high activity when using Et_2AlCl as an activator. In their later work [211], these same authors reported the results of theoretical studies of the mechanism of ethylene polymerization with **V04**-type complexes. Actually, **V04** was chosen for DFT calculations, together with the consideration of Et_2AlCl -free species, in the modeling of ethylene insertion in the framework of the Cossee–Arlman mechanism (Figure 25). In the first step, the ethylene molecule coordinates to the vacant site in **V04**, forming a π -complex ($-18.1 \text{ kcal}\cdot\text{mol}^{-1}$). Subsequently, ethylene inserts into the vanadium–carbon bond via the four-membered cyclic transition state which has an activation energy barrier of $14.7 \text{ kcal}\cdot\text{mol}^{-1}$ relative to the π -complex. The overall ethylene insertion was found to be highly exothermic (-27.1 kcal/mol), and insertion product resembled the starting structure of **V04**. For hypothetical cationic active species $[(\text{PhN}=\text{CHC}_6\text{H}_4\text{O})\text{V}(\text{THF})]^+$, ethylene complexation was less exothermic and the insertion barrier was higher by 5.7 kcal/mol . An additional argument in favor of the $\text{V}-(\mu\text{-Cl})_2\text{-Al}$ model was a clear correlation between the results of modeling and polymerization experiments for V(III) complexes with substituted salicylaldiminato ligands.

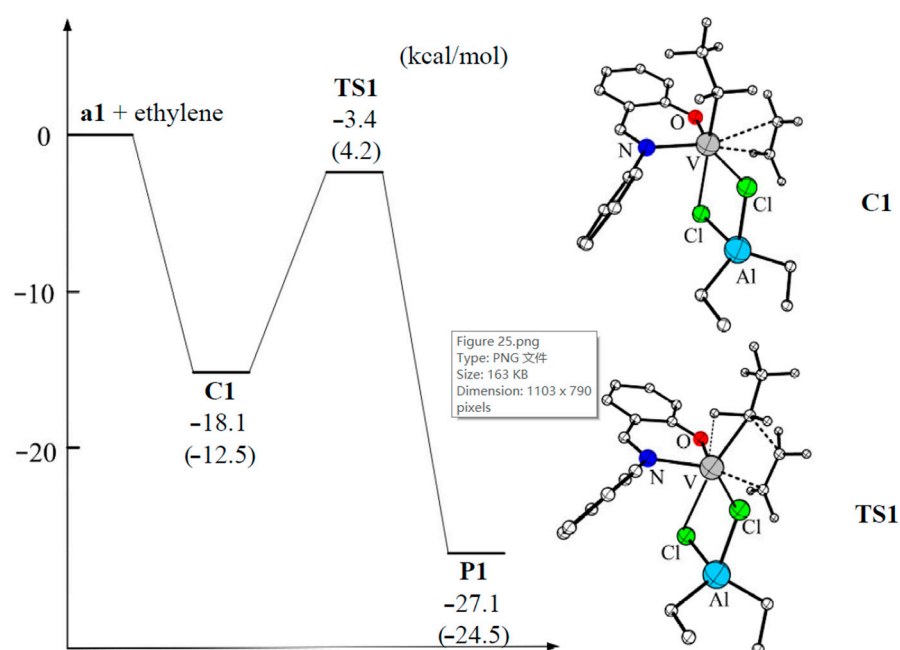
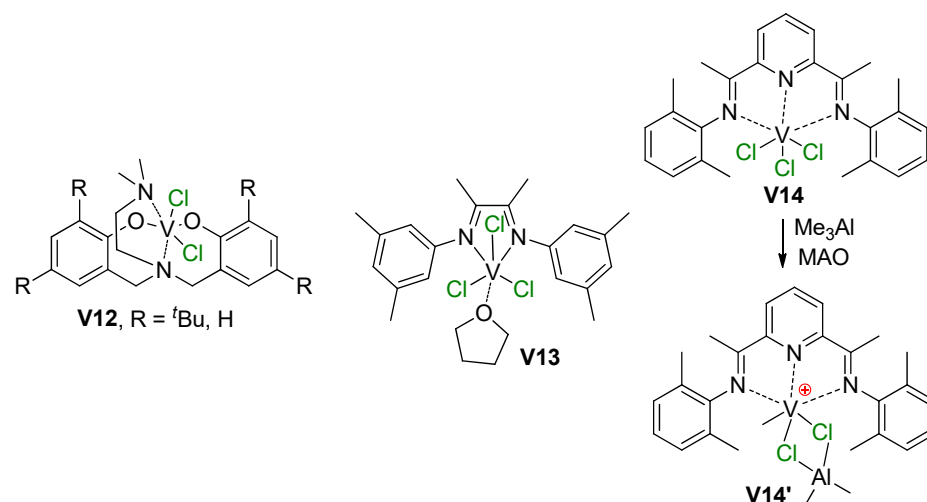


Figure 25. Potential energy surface and optimized geometries of the π -complex and transition state of the ethylene insertion catalyzed by the active species **V04**. The energy was calculated at the M06-L functional level, with energy changes calculated at the B3LYP-D3 functional level given in parentheses. Reprinted with permission from [211]. Copyright (2015) Elsevier B.V.

The results of relatively recent studies on V-catalyzed polymerization also confirm a distinct ‘chlorine effect’. In this regard, the study by Białek and Bisz [212] deserves a separate mention. In the polymerization of ethylene, ONNO-type bis(phenolates) **V12** (Scheme 30) were manifold more active in the presence of Et_2AlCl in comparison with MAO and perfluoroaryl borates. In ethylene/oct-1-ene copolymerization, the difference in activities decreased when using Et_2AlCl and ${}^3\text{Bu}_3\text{Al}/[\text{Ph}_3\text{C}][\text{B}(\text{C}_6\text{F}_5)_4]$, but higher comonomer incorporation was observed in the first case.



Scheme 30. V(III) pre-catalysts **V12–V14** studied recently [212,213] and the formation of V-(μ -Cl)–Al cationic active species, confirmed by NMR experiments [213].

In 2018 [213], Talsi et al. reported the results of the study of α -diimine (**V13**) and bis(imino)pyridine (**V14**) trichloro complexes of V(III) (Scheme 30) with the use of MAO, Me_2AlCl , $\text{Me}_2\text{AlCl}/[\text{Ph}_3\text{C}][\text{B}(\text{C}_6\text{F}_5)_4]$, and $\text{Me}_3\text{Al}/[\text{Ph}_3\text{C}][\text{B}(\text{C}_6\text{F}_5)_4]$ activators. Through careful NMR experimentation, they demonstrated the formation of **V13**-based cationic

complexes without V-(μ -Cl)-Al bonding, whereas **V14** formed V(Me)-(μ -Cl)₂-Al species **V14'**. Notably, when Me₂AlCl alone was used, an inactive V(Cl)-(μ -Cl)₂-Al complex was the main reaction product.

In a series of recent publications [214–216], Nomura et al. presented the results of the study of the activation of V complexes with the use of V K-edge X-ray absorption near-edge structure analysis (XANES) and extended X-ray absorption fine structure (EXAFS) analysis. Regarding V(V) pre-catalysts of (imido)VCl₂(OAr), (imido)VCl₃, and similar types, as well as VOCl₃, these studies clearly indicated the presence of V(III) species in the reaction mixture after activation by the organoaluminum compounds Me₂AlCl, Et₂AlCl, and EtAlCl₂. In this way, the attribution of **V03** (Scheme 26) to active species should be corrected. However, no significant changes in either the oxidation state or the basic geometry were observed when (imido)vanadium(V) complexes were treated with MAO. In this way, the role of R₂AlCl is in both the formation and stabilization of catalytic species.

In conclusion, it should be noted that the chemistry of V-based single-site catalysts of α -olefin and diene polymerization primarily focuses on post-metallocene-type complexes. V-based catalysts exhibit some similarities to Ti(III) Ziegler–Natta catalysts (see **V07** in Scheme 27); however, half-sandwich and sandwich complexes of V have not found wide application. What is more interesting is the possible role of V-(μ -Cl)-Al bonding in the catalytic behavior of Cp-ligated complexes of vanadium. Recent qualitative research of the catalytic activity of *supported* Cp₂V, carried out by Liu et al. [217], sheds some light on the issue. The authors suggested the formation of cationic CpV–O–Si(μ -O)₃(silica) species under the action of Et₂AlCl, and proposed a non-trivial mechanism of ethylene coordination/insertion with a marked V–Al cooperative effect (Figure 26). The stages of chain initiation and release were also studied. The activation barrier of the chain propagation was found to be ~ 16 kcal·mol⁻¹.

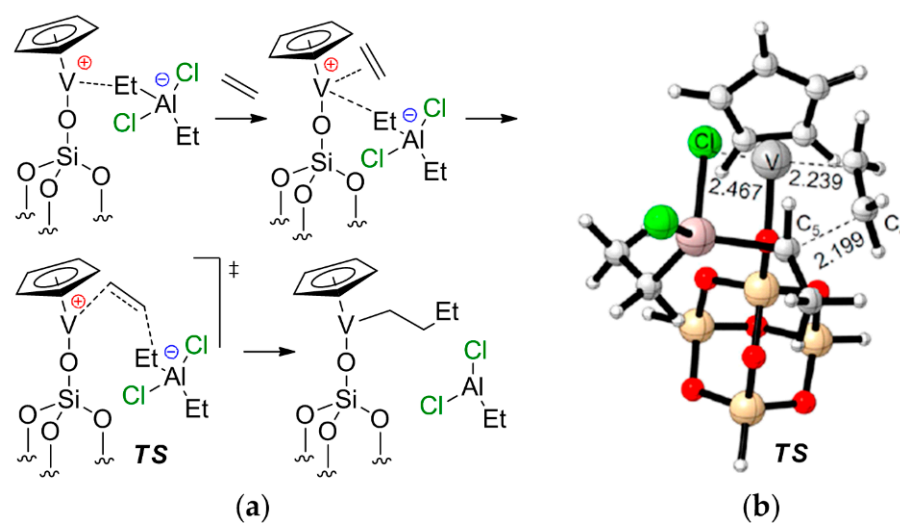


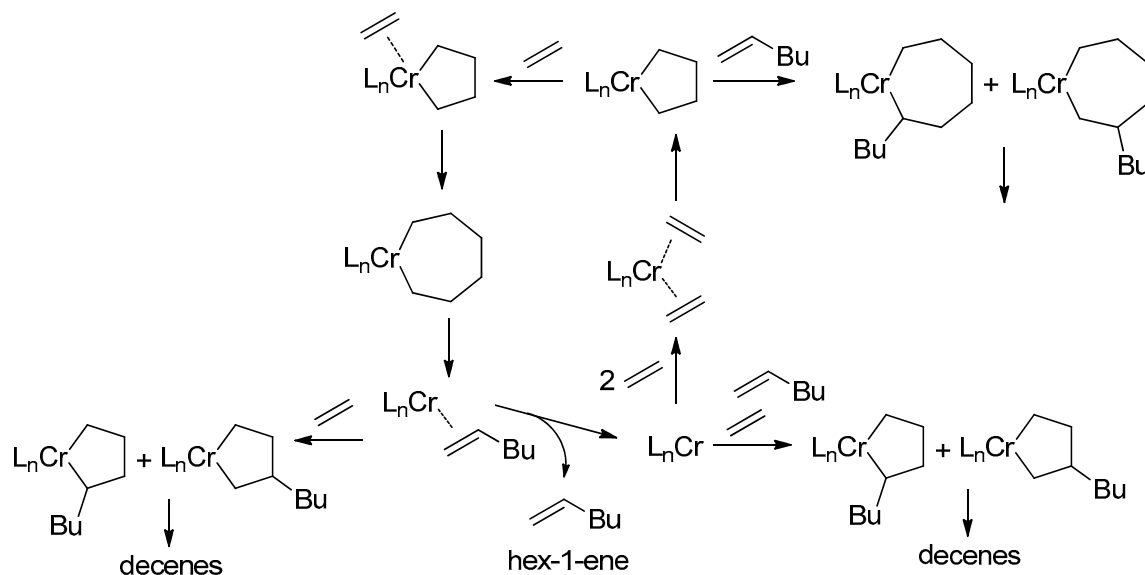
Figure 26. (a) Proposed mechanism of ethylene coordination/insertion on the supported CpV–Et₂AlCl complex; (b) optimized geometry of the key transition state. Reprinted with permission from [217]. Copyright (2020) Elsevier B.V.

5. Complexes of Cr

5.1. Selective Oligomerization of Ethylene Catalyzed by Cr Complexes

The selective oligomerization of ethylene with the use of Cr catalysts, resulting in the formation of hex-1-ene and oct-1-ene, is becoming an important contemporary industrial process [14]. The mechanism of the selective trimerization of ethylene [13,47,48,218] qualitatively differs from the Cossee–Arlman mechanism of polymerization and non-selective oligomerization of α -olefins by the coordination of two olefin molecules and the intermediate formation of metallacyclic species. As a result, when using selective trimerization catalysts, isomeric decenes are formed [219,220] (Scheme 31). The reaction intermediates

and products, presented in this scheme, only provide a general idea of the Cr-catalyzed trimerization. Cr catalysts, unlike half-sandwich Ti complexes (Scheme 10), are of a more complex nature, selective tetramerization is possible, and the oxidation numbers of Cr reaction intermediates still are subject of discussion.



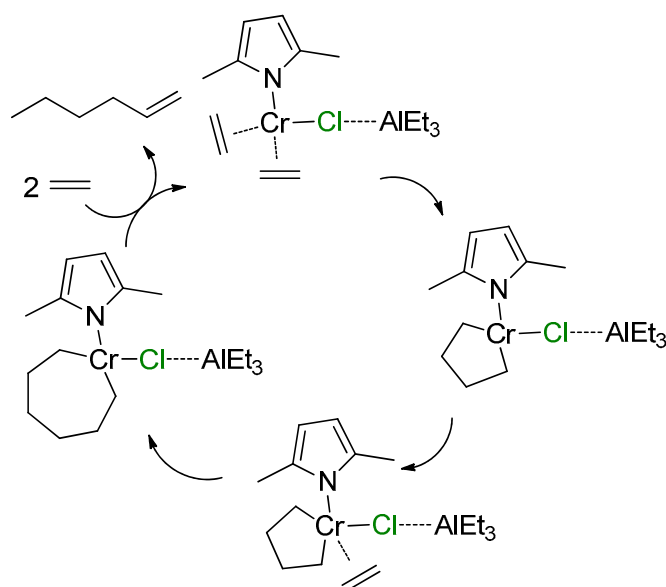
Scheme 31. The main idea of metallacyclic mechanism of selective trimerization of ethylene, catalyzed by Cr complexes [219].

The Cr-catalyzed selective tri- and tetramerization of ethylene has been the subject of numerous reviews which have discussed both the practical and theoretical aspects of the reaction [13,14,47,48,84,221–227]. Pyrrole-based Cr catalysts were historically the first system for the synthesis of hex-1-ene [228], which is widely used in the petrochemical industry. Other groups of homogeneous Cr catalysts of tri-/tetramerization often outperform Cr/pyrrole systems on catalytic activity, but research is still ongoing.

At the very beginning of the study of Cr oligomerization catalysts, a substantial ‘chlorine effect’ was detected: Cr/pyrrole systems only demonstrated high activity in the presence of $\text{Et}_2\text{AlCl}/\text{Et}_3\text{Al}$ mixtures of the activators. This fact was explained successfully from a mechanistic point of view (see Section 5.2 below), and the possible importance of Cr-($\mu\text{-Cl}$)-Al bonding in Cr-based catalytic species was not completely ignored during the ligand-oriented design of new single-site oligomerization catalysts, accompanied by oligomerization experiments.

5.2. Cr Complexes with Pyrrole and Similar Ligands

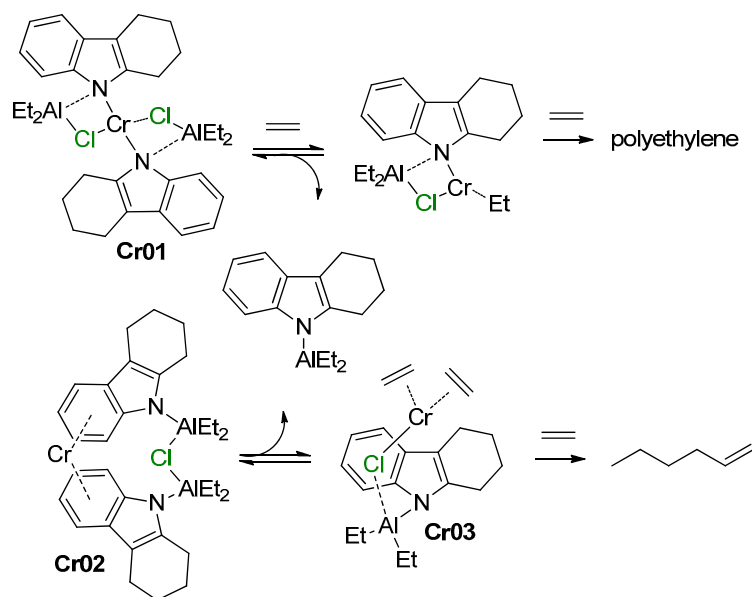
Discovered in the late 1980s by Reagan [228], catalytic systems containing Cr(III) 2-ethylhexanoate, 2,5-dimethyl-1*H*-pyrrole, Et_2AlCl , and Et_3Al were optimized to a 1:3:8:11 ratio during the further research by Phillips Petroleum and Mitsubishi [229–233]. This catalyst is commonly known as the Chevron–Phillips ethylene trimerization system. In augmenting the main idea of the metallacyclic mechanism, the scientists of Sasol Technology proposed a novel mechanistic concept, which included the formation of Cr-($\mu\text{-Cl}$)-Al catalytic species [234]. They suggested that the Cr(II) center coordinates two ethylene molecules. Then, a Cr(IV) metallacycle is formed, subsequent π -coordination/insertion of the ethylene molecule results in a seven-membered metallacycle which is further subjected to reductive eliminative intramolecular β -hydrogen migration to the ζ -carbon followed by the coordination of two ethylene molecules with hex-1-ene release (Scheme 32).



Scheme 32. Proposed metallacycle mechanism for the Cr/pyrrolyl-catalyzed trimerization of ethylene involving Cr-(μ -Cl)-Al species [234].

During DFT modeling, unsubstituted pyrrole was used as a ligand, with the consideration of possible η^5 - and κ^1 -coordination. In addition, optimizations were performed for catalytic species with and without Me_3Al coordination ('Cl' and ' Me_3AlCl ' models, respectively). Based on the results of the modeling, the triplet spin states for both Cr(II) and Cr(IV) were predicted to be the ground state. When comparing Cl and Me_3AlCl models, significant lowering of the activation energy of the rate-limiting step by $11.3 \text{ kcal}\cdot\text{mol}^{-1}$ was found for the catalytic species with Cr-(μ -Cl)-Al bonding.

In follow-up studies of pyrrole-based catalytic systems, Gambarotta, Duchateau et al., after failed attempts to isolate single crystals of 2,5-dimethyl-1*H*-pyrrole derivatives, obtained characterizable complexes of 2,3,4,5-tetrahydro-1*H*-carbazole [235]. In particular, by the treatment of $[\text{CrCl}_3(\text{THF})_3]$ or $[\text{CrCl}_2(\text{THF})_2]$ with a mixture of the ligand and Et_3Al , the square-planar Cr(II) complex **Cr01** was obtained as a blue paramagnetic crystals. When chromium(III) 2-ethylhexanoate was used, the presence of AlEt_2Cl was crucial, and the reaction afforded the new paramagnetic Cr(I) complex **Cr02**. Complex **Cr02** was also obtained by the reduction of **Cr01** using potassium (Scheme 33). The molecular structures of **Cr01** and **Cr02** are presented in Figure 27.



Scheme 33. Structural formula and catalytic activity of 2,3,4,5-tetrahydro-1*H*-carbazole complexes **Cr01** and **Cr02** [235].

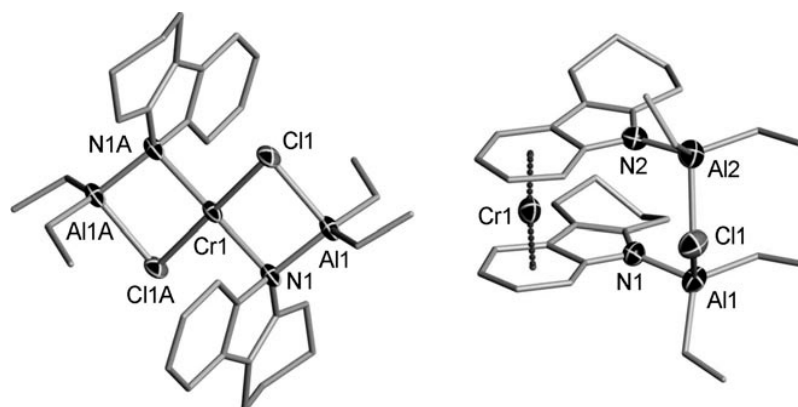
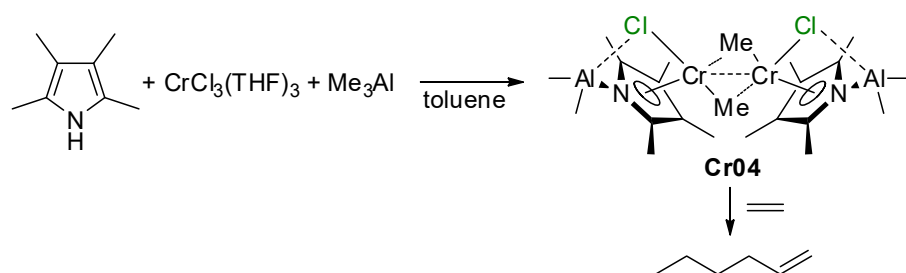


Figure 27. Molecular structures of the complexes **Cr01** and **Cr02**. Reprinted with permission from [235]. Copyright (2008) Wiley-VCH Verlag GmbH & Co.

Complex **Cr01** catalyzed the polymerization of ethylene. In methylocyclohexane, complex **Cr02** was an unprecedented single-component trimerization catalyst, producing hex-1-ene with only trace amounts of higher oligomers. The structure of the possible active complex **Cr03** is also presented in Scheme 33. The role of Cr-(μ -Cl)-Al bonds in the formation of the ligand environment of the catalytic center in **Cr03** seems clear.

One year later, the same research team reported the synthesis of the 2,3,4,5-tetramethyl-1*H*-pyrrole-based Cr-(μ -Cl)-Al complex **Cr04** [236] (Scheme 34). Similarly to complex **Cr02**, in methylocyclohexane, complex **Cr04** turned out to be the highly active ethylene trimerization catalyst without any activators. Apparently, the dimer of **Cr04** (Figure 28) dissociates in the solution with the retention of Cr-(μ -Cl)-Al coordination in the monomeric complex with an easily recognizable ‘constrained geometry’ structural motif.



Scheme 34. Synthesis and catalytic behavior of complex **Cr04** [236].

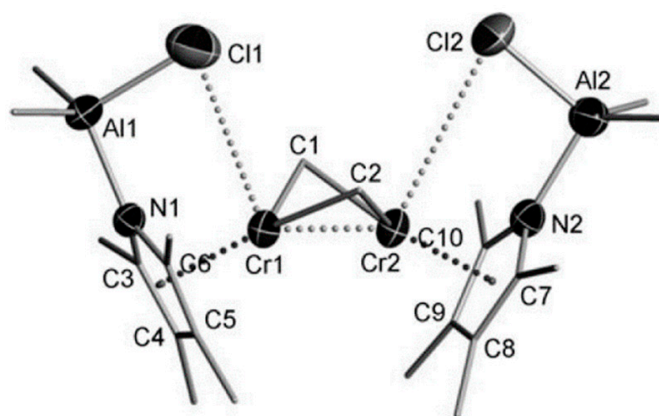


Figure 28. Molecular structures of complex **Cr04**. Reprinted with permission from [236]. Copyright (2009) Wiley-VCH Verlag GmbH & Co.

Taking into account the results of theoretical [234] and experimental [235,236] studies of Cr/pyrrole systems, Budzelaar offered his own mechanistic concept, based on the DFT modeling of Cr/*1H*-indole catalytic systems [237]. The modeling results indicated that, in addition to the Cr(II)/Cr(IV) cycle (Scheme 33), Cr(I)/Cr(III) cycle, based on [(Indol-1-yl) ··· AlMe₂(μ-Cl)Cr] species (**Cr05**), the role of the Cl atom was to stabilize metallacyclic intermediates and to block additional coordination of the ethylene molecule at the stage of hex-1-ene formation.

Finally, to determine the problem of the oxidation states of the Cr catalytic center in the Chevron–Phillips ethylene trimerization system, Liu et al. carried out a detailed theoretical study of the model catalyst species **Cr06** and **Cr07** (Figure 29) based on 2,5-dimethyl-1*H*-pyrrole [238]. Optimizations showed that the retention of Cr–(μ-Cl)–Al bonding (strong or weak, *d*(Cr–Cl)) was changed in the interval of 2.5–4.0 Å in all key reaction intermediates and transition states. Calculated free energy profiles (Figure 29) clearly showed the preference of the choice of **Cr06** as a model catalytic species—free activation energies were 19.0 and 31.4 kcal·mol^{−1} for **Cr06** and **Cr07**-based reaction pathways, respectively. In this way, the mechanistic concept of Cr(I)/Cr(III) catalytic cycle received additional confirmation.

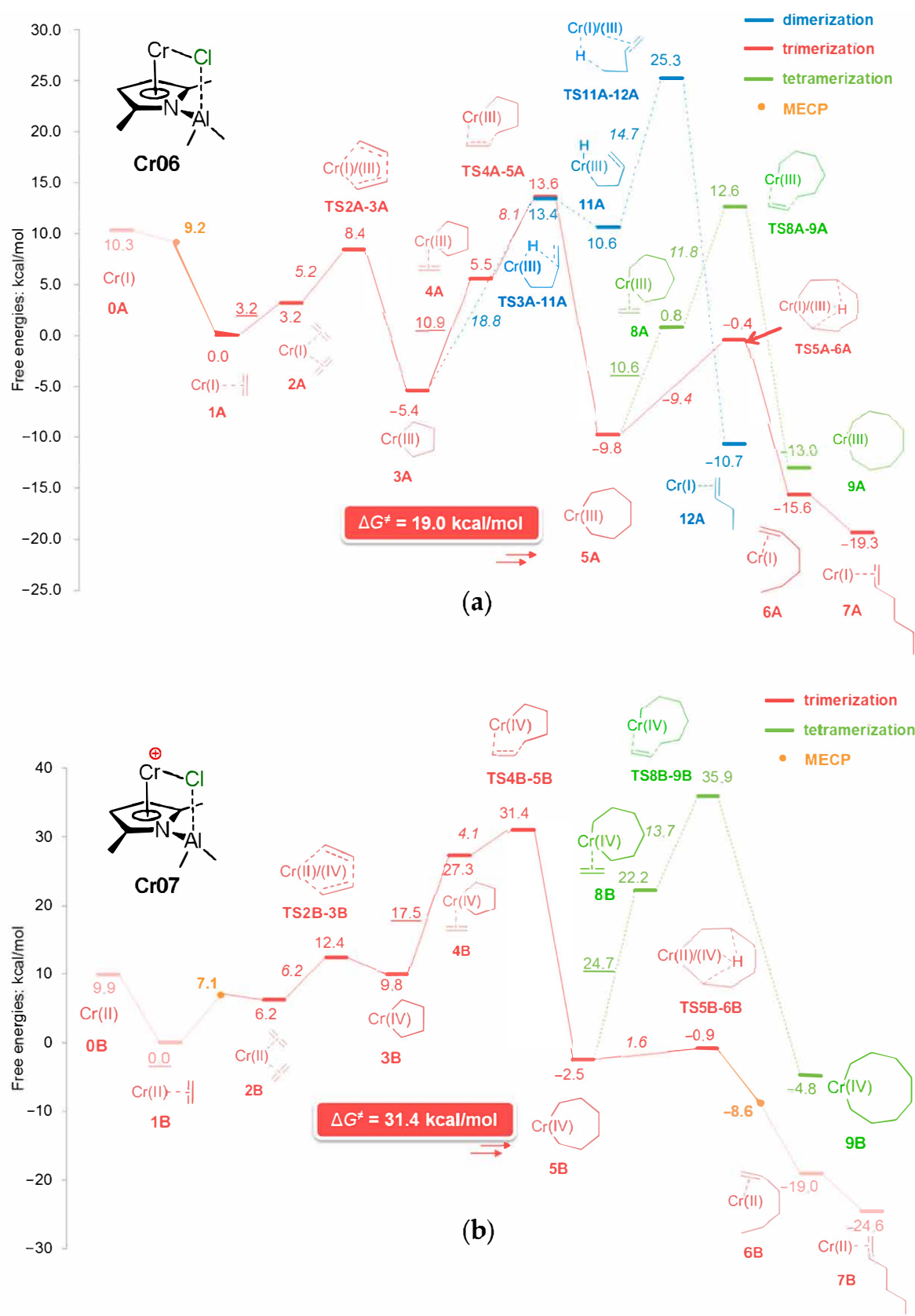


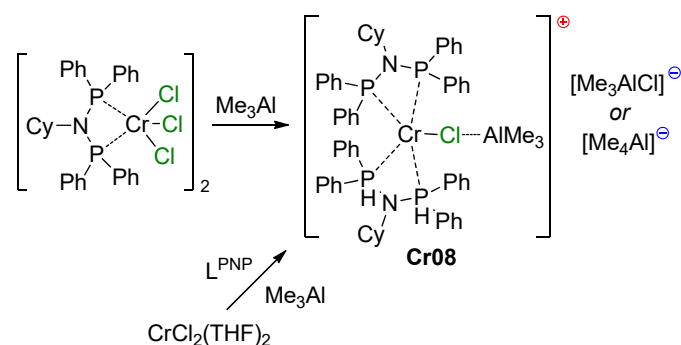
Figure 29. Calculated free energy diagram for model catalytic species Cr06 (a) and Cr07 (b). Me₂Al fragments are omitted. Reprinted with permission from [238]. Copyright (2014) American Chemical Society.

Recently, the activation of the Chevron–Phillips ethylene trimerization system was studied by Tromp et al. using catalytic and spectroscopic (XAS, EPR, UV–vis) experiments under industrial conditions [239]. It was found that 2,5-dimethyl-1*H*-pyrrole reacts with Et_2AlCl or Et_3Al with the formation of $[\text{2,5-dimethyl-2*H*-pyrrole}] \cdots \text{AlEt}_3$ and $[\mu\text{-2,5-dimethyl-1*H*-pyrrole}](\mu\text{-Cl})(\text{AlEt}_2)_2$ complexes, and their reaction with Cr(III) 2-ethylhexanoate results in polymeric Cr(II) pyrrolyl species containing Et_2AlCl fragments. However, the structure of real catalytic species remains unknown.

5.3. Cr Aminodiphosphine Complexes

Among others, Cr(III) derivatives of chelating ligands of the formula $\text{R}^1\text{R}^2\text{P-N}(\text{R}^3)\text{-PR}^4\text{R}^5$ (PNP–Cr complexes) represent pre-catalysts of the selective tri-/tetramerization of ethylene which are characterized by high catalytic activity and stability over time [14,47,84,221–225,240]. Usually, the activation of PNP–Cr pre-catalysts is performed by the reaction of $\text{L}^{\text{PNP}}\text{CrCl}_3$ complexes (L^{PNP} —PNP ligand) or mixtures of L^{PNP} with Cr(III) salts by MAO. The use of R_3Al /perfluoroaryl borate systems is rarely used [241] despite its undoubted merits. Evidently, the presence of R_2AlCl species, arising as a result of the reaction between $\text{L}^{\text{PNP}}\text{ZrCl}_3$ and organoaluminum activators, implies the possible formation of Cr–($\mu\text{-Cl}$)–Al species. The results of studies of PNP–Cr catalysts in view of this possibility are summarized and discussed below in chronological order.

When studying the activation of $[\text{CyN}(\text{PPh}_2)_2]\text{CrCl}_3$ by Me_3Al in toluene (Cy—cyclohexyl, Scheme 35), Gambarotta, Duchateau et al. separated and characterized a cationic complex of Cr(II), **Cr08** [242]. L^{PNP} does not react with $\text{CrCl}_2(\text{THF})_2$; nevertheless, in the presence of excess of Me_3Al , **Cr08** was obtained in a high yield. XRD studies confirmed the molecular structure of **Cr08** (Figure 30). Being activated by MAO, this complex was highly active in the oligomerization of ethylene with the formation of oct-1-ene as the main reaction product.



Scheme 35. Formation of cationic complex **Cr08** [242].

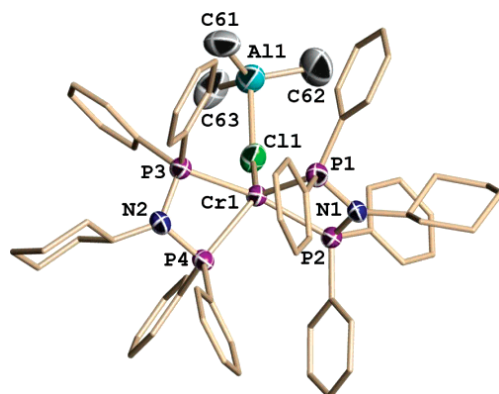
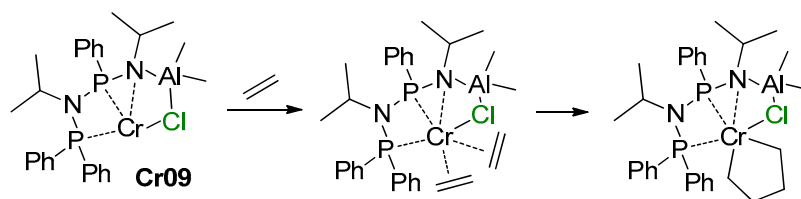


Figure 30. Plot of the Cr-containing cationic moiety of **Cr08** with thermal ellipsoids of the non-carbon atoms drawn at the 30% probability level. Reprinted with permission from [242]. Copyright (2006) American Chemical Society.

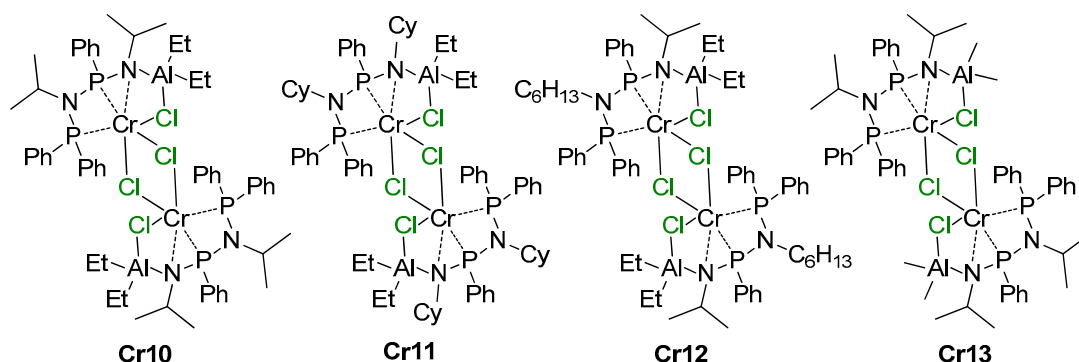
The authors also proposed that the catalytic behavior of **Cr08** and the failure of L^{PNP} to ligate to a CrCl_2 moiety in the absence of Me_3Al suggest that the acquisition of a second ligand and cationization are central to the stabilization of a $\text{Cr}(\text{II})$ catalyst precursor. Considering that excess MAO is necessary for the activation, they also speculated that the dicationic $[\text{L}^{\text{PNP}}_2\text{Cr}]^{2+}$ complex may be the actual catalytically active species. However, other hypotheses, involving the possibility of further abstraction of the [PNP] ligand from the ‘dormant’ catalyst precursor **Cr08**, cannot be ruled out [242]. For our part, we will merely add that in the latter case, the $\text{Cr}(\text{II})$ cation becomes open for both the π -coordination of ethylene and for $\text{Cr}-(\mu\text{-Cl})\text{-Al}$ bonding with organoaluminum components of the catalytic system.

PNP–Cr complexes containing diphosphine ligands with two amine groups at one of the phosphorus atoms (L^{PNPN}) are of interest to researchers due to the ability of similar pre-catalysts to be activated by Et_3Al , without the use of MAO [243]. Evidently, such unconventional reactivity forces the assumption that L^{PNPN} can form catalytic species which differ from L^{PNP} -based species. In [244], Müller et al. reported a study of the interaction of Et_3Al and Me_3Al with the $\text{Ph}_2\text{PN}(\text{iPr})\text{P}(\text{Ph})\text{NH}^{\text{iPr}}$ ligand. During this reaction, rearrangement to the $[\text{iPrNP}(\text{Ph})\text{P}(\text{Ph})_2=\text{N}^{\text{iPr}}$ ligand occurred. The complex of this ligand with CrCl_3 was inactive in oligomerization. After preparation of the active model pre-catalyst $[\text{Ph}_2\text{PN}(\text{iPr})\text{P}(\text{Ph})\text{N}^{\text{iPr}}]\text{Cr}(\text{Cp})\text{Cl}$, it was concluded that the active catalytic species **Cr09** exhibits a binuclear nature (Scheme 36). During further research [245], it was shown that the PNP–Cr system, generated by the reaction of $\text{Cr}(\text{III})$ acetylacetonate ($\text{Cr}(\text{acac})_3$) with L^{PNP} and Et_3Al , is inactive in oligomerization. At the same time, the addition of Cl-containing compounds of various nature resulted in the selective trimerization of ethylene.



Scheme 36. Supposed structure of the active PNP–Cr catalyst **Cr09** [244]. Copyright (20XX) Wiley-VCH Verlag GmbH & Co. Copyright (2016) Royal Society of Chemistry. Copyright (2012) American Chemical Society. Copyright (2015) Springer Nature. Copyright (2019) Elsevier B.V.

Attempts to isolate PNP–Cr–Al species have been successful; Cr_2Al_2 complexes **Cr10–Cr13** (Scheme 37) were obtained by the reaction of $L^{\text{PNPN}}\text{CrCl}_3$ with Et_3Al , or by the interaction of Al derivatives of L^{PNPN} with $\text{CrCl}_2(\text{THF})_2$ [246]. Molecular structures of all complexes were determined by XRD (see Figure 31 for an example). It was found that **Cr10** is inactive in ethylene oligomerization, indicating that **Cr10** is not a self-activating complex and that the oxidation state of $\text{Cr}(\text{II})$ is not sufficiently low to form hex-1-ene. Hence, the formation of **Cr09**-type catalytic species needs dissociation and further reduction.



Scheme 37. Cr_2Al_2 complexes **Cr10–Cr13** [246].

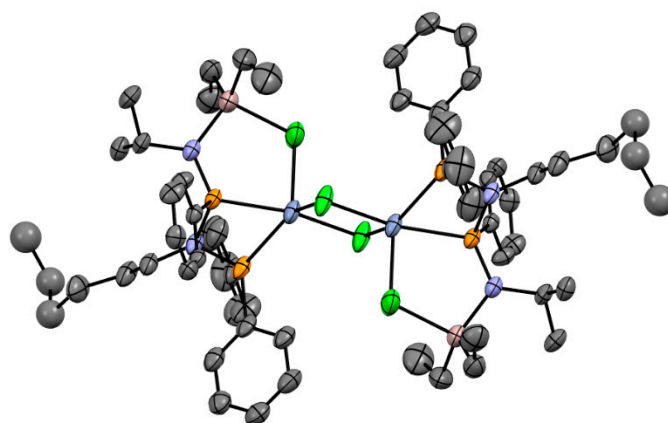
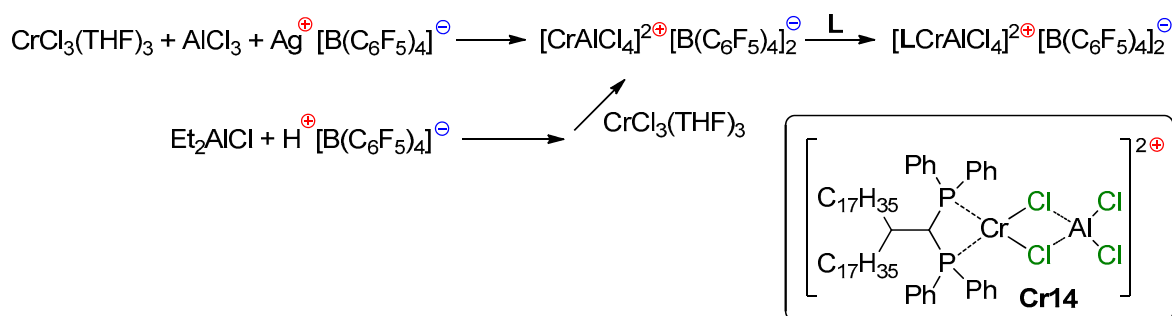


Figure 31. Molecular structure of complex Cr12 [246].

However, the studies listed above only contain suggestions about the nature of catalytic species in the systems containing PNP–Cr complexes and R_2AlCl . In 2016, Evans et al. reported the results of a study of $[^iPrN(PPh_2)_2]CrCl_3$ activation by Me_3Al [247]. The Cr K-edge XAFS spectrum after 1 min indicated the formation of $[^iPrN(PPh_2)_2]CrClMe(\mu-Cl)AlMe_3(THF)$ and then $[^iPrN(PPh_2)_2]CrMe(\mu-Cl)AlMe_3$. Such species are evidently able to form Cr(II) cations under the action of MAO; however, given that PNP–Cr catalysts usually operate under relatively low Al_{MAO}/Cr ratios (~ 100), in our view, the possibility of the intermediate coordination of R_2AlCl at the Cr center seems possible.

When studying the use of perfluoroaryl borates for the activation of PNP–Cr pre-catalysts, Lee et al. proposed an original method for the synthesis of Zr–Al dicationic complex Cr14 [241] (Scheme 38). This complex was found to be highly active in the selective tetramerization of ethylene, but a fairly large amount of PE (1.7 wt.%) was concomitantly generated. Further ligand design (introduction of SiR_3 substituents in *p*-positions of the Ph rings in L^{PNP}) resulted in an increase in the activity and suppression of the PE formation.



Scheme 38. Formation of dicationic complex Cr14 [241].

Summarizing the above-mentioned research, in view of the huge number of the articles on the PNP–Cr-catalyzed tri/tetramerization of ethylene, the role of $R_2AlCl \cdots Cr$ bonding was not examined in most studies. In many cases, this was due to the methodology of the experiment on pre-catalyst preparation and activation, based on the mixing of a soluble Cr source (for example, $Cr(acac)_3$) and L^{PNP} , followed by treatment with MAO. This, among other things, may be due to the low solubility and varied composition of the commonly used starting complex $CrCl_3(THF)_3$, which complicates the separation and purification of $L^{PNP}CrCl_3$ pre-catalysts (for instance, we have been unable to solve another similar problem, presented in [248]). The complex $[CrCl_2(\mu-Cl)(THF)_2]_2$, recently synthesized by Lee et al. [249], seems to be a more convenient and reliable starting compound for the synthesis of $L^{PNP}CrCl_3$. We can assume that more studies on the effect of the use of $[CrCl_2(\mu-Cl)(THF)_2]_2$, or additional amounts of R_2AlCl , on catalytic activity of known

'chlorine-free' PNP–Cr systems, may lead to further improvements in the PNP-based catalysts of ethylene tri- and tetramerization.

5.4. Other Cr Complexes in the Single-Site Catalysis of Oligomerization and Polymerization

The range of chelating ligands for the synthesis of Cr-based oligomerization and polymerization of single-site catalysts is not limited by PNP-type compounds. Thus, for example, complex **Cr15** was synthesized by the reaction of the $t\text{BuNPN}t\text{Bu}$ dianion with Cr chlorides, followed by treatment with $i\text{Bu}_3\text{Al}$ [250] (Figure 32). This complex was found to be a single-component catalyst of ethylene polymerization.

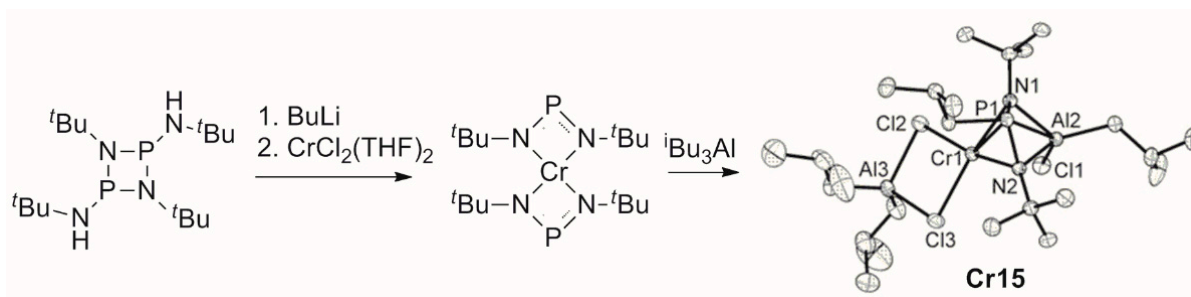


Figure 32. Preparation and molecular structure of complex **Cr15**. Reprinted with permission from [250]. Copyright (2008) Wiley-VCH Verlag GmbH & Co.

$\text{HN}(\text{CH}_2\text{CH}_2\text{PPh}_2)$ - and $\text{HN}(\text{CH}_2\text{CH}_2\text{SR})_2$ -based Cr(II) and Cr(III) chloro complexes were synthesized by McGuinness et al. [251]: the treatment of $[\text{HN}(\text{CH}_2\text{CH}_2\text{PPh}_2)]\text{CrCl}_2$ by 1,4-diazabicyclo[2.2.2]octane (DABCO) resulted in dimer $\{[\text{N}(\text{CH}_2\text{CH}_2\text{PPh}_2)]\text{Cr}(\mu\text{-Cl})_2\}_2$ and its $-\text{SR}$ analogs. Further studies of the activation of these complexes by MAO and $\text{Et}_3\text{Al}/\text{B}(\text{C}_6\text{F}_5)_3$ indicated that the Cr(II)/Cr(IV) cycle is preferable for this type of catalyst. When $\text{HN}(\text{CH}_2\text{CH}_2\text{SCy})_2$ was treated with $\text{CrCl}_2(\text{THF})_2$ and EtAlCl_2 , complex **Cr16** was obtained (Figure 33) [252]. This Cr(II) complex, after activation by MAO, was inferior to SNS Cr(III) complexes in catalytic activity in the trimerization of ethylene.

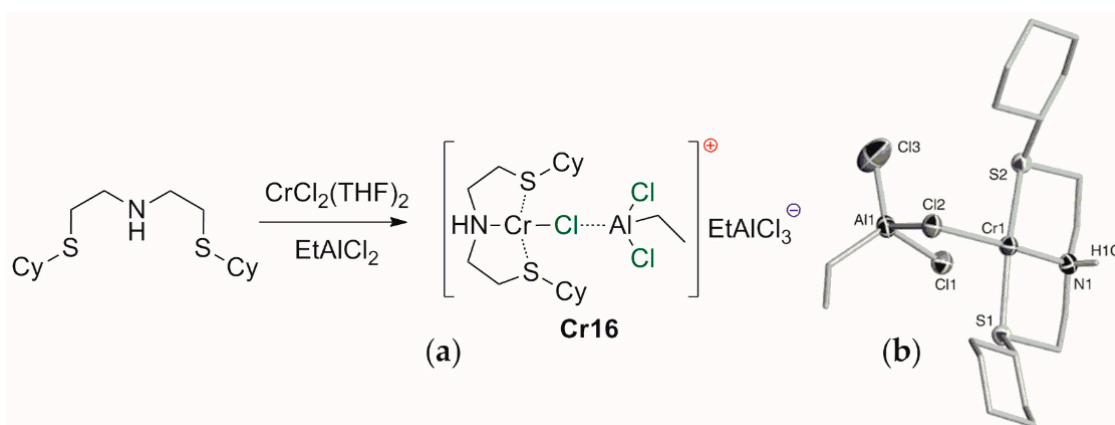


Figure 33. (a) Synthesis of complex **Cr16**; (b) ORTEP view of **Cr16** (thermal ellipsoids set at 30%), with the Al-containing counterion omitted for clarity. Reprinted with permission from [252]. Copyright (2006) Wiley-VCH Verlag GmbH & Co.

In 2011, the SNS ligand was modified by replacing CH_2 fragments near the N atom with SiMe_2 groups ($\text{HN}(\text{CH}_2\text{CH}_2\text{SR})_2$, $\text{R} = \text{Cy}, t\text{Bu}, \text{Ph}$). The reaction of $\text{HN}(\text{CH}_2\text{CH}_2\text{SCy})_2$ with Et_2AlCl and Cr(III) or Cr(II) chlorides afforded the Cr(II) complex **Cr17** (Figure 34) [253]. In the presence of MAO (500–1000 eq.), this complex catalyzed the oligomerization of ethylene (mainly trimerization). After abstraction of the N–H proton during the synthesis of the AlMe_2 analog of **Cr17**, complex **Cr18** was obtained (Figure 35): its selectivity in the oligomerization of ethylene was even lower.

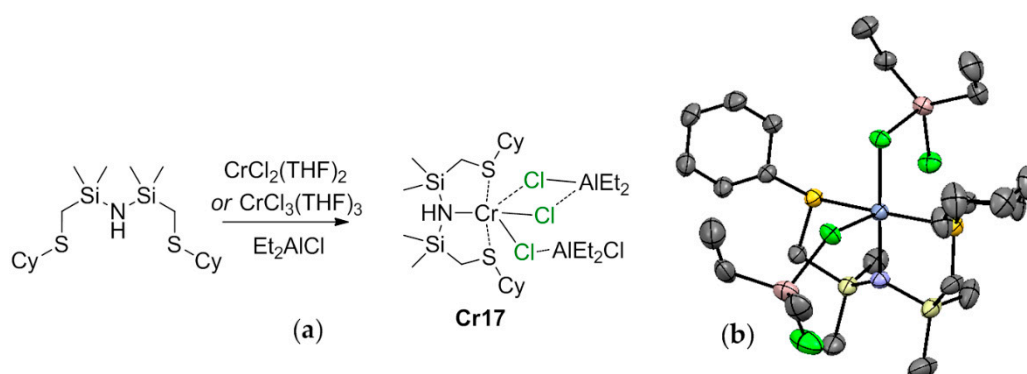


Figure 34. (a) Synthesis of complex **Cr17**; (b) ORTEP view of **Cr17** (hydrogen atoms are omitted) [253]. Copyright (20XX) Wiley-VCH Verlag GmbH & Co. Copyright (2016) Royal Society of Chemistry. Copyright (2012) American Chemical Society. Copyright (2015) Springer Nature. Copyright (2019) Elsevier B.V.

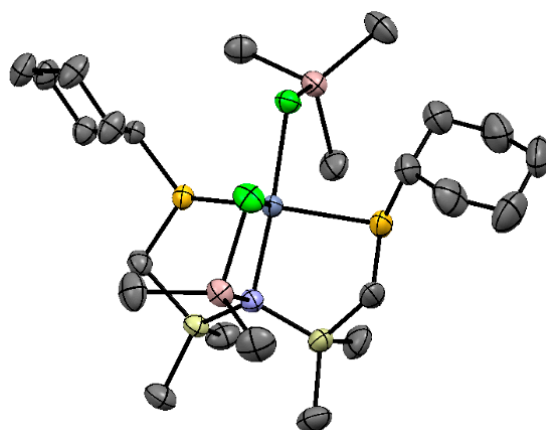
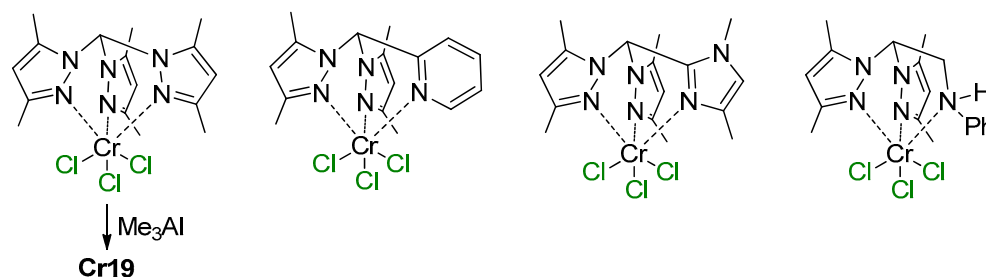


Figure 35. Molecular structure of complex **Cr18** [253].

A similar pattern was observed when studying Cr complexes with tris- and bis-pyrazolyl ligands [254] (Scheme 39). Depending on the absence or the presence of the -NH- fragment in the bridging ligand, the reaction of LCrCl_3 with Me_3Al resulted in the formation of $\text{Cr}(\mu\text{-Cl})\text{-Al}$ complexes with different types of Al-N bonding. After treatment with 200 eq. MAO, the activities of LCrCl_3 and $\text{Cr}(\mu\text{-Cl})\text{-Al}$ complexes (for example, **Cr19**, Figure 36) in the oligomerization of ethylene were close, with the same oligomer distributions. In this way, under the action of MAO, organoaluminum chloride is eliminated finally and irreversibly.



Scheme 39. CrCl_3 complexes with tris- and bis-pyrazolyl ligands [254].

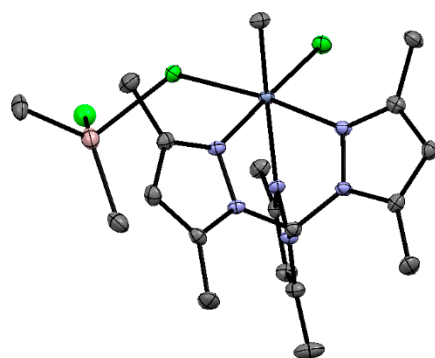


Figure 36. Molecular structure of complex Cr19 [254].

In the early 2010s, a number of articles were devoted to the preparation and catalytic studies of Cr complexes with bi- and polydentate ligands of different nature, including the synthesis and characterization of Cr-(μ -Cl)-Al complexes: in particular, Cr derivatives of $\text{Ph}_2\text{PN}^t\text{Bu}$ [255], $(\text{Ph}_2\text{P})_2\text{CHCO}_2^-$ and $(\text{Ph}_2\text{P})_2\text{C}=\text{C}(\text{NHR})\text{O}^-$ [256], 2,6-bis(CH_2PPh_2)pyridine [257], 2,6-bis($\text{NH}=\text{PPh}_2$)pyridine [258], 2-($\text{NHCH}_2\text{PPh}_2$)pyridine [259], and $\text{Ph}_2\text{C}(1H\text{-pyrrol-2-yl})$ [260]. In several studies, an explicit ‘chlorine effect’ was detected, although most of them included XRD data for isolated Cr-(μ -Cl)-Al molecules (Figure 37). However, as opposed to the relatively well-studied Chevron–Phillips ethylene trimerization system and its analogs, we are not even close to understanding the role of Cr-(μ -Cl)-Al bonding in the catalytic chemistry of Cr-based post-metallocenes.

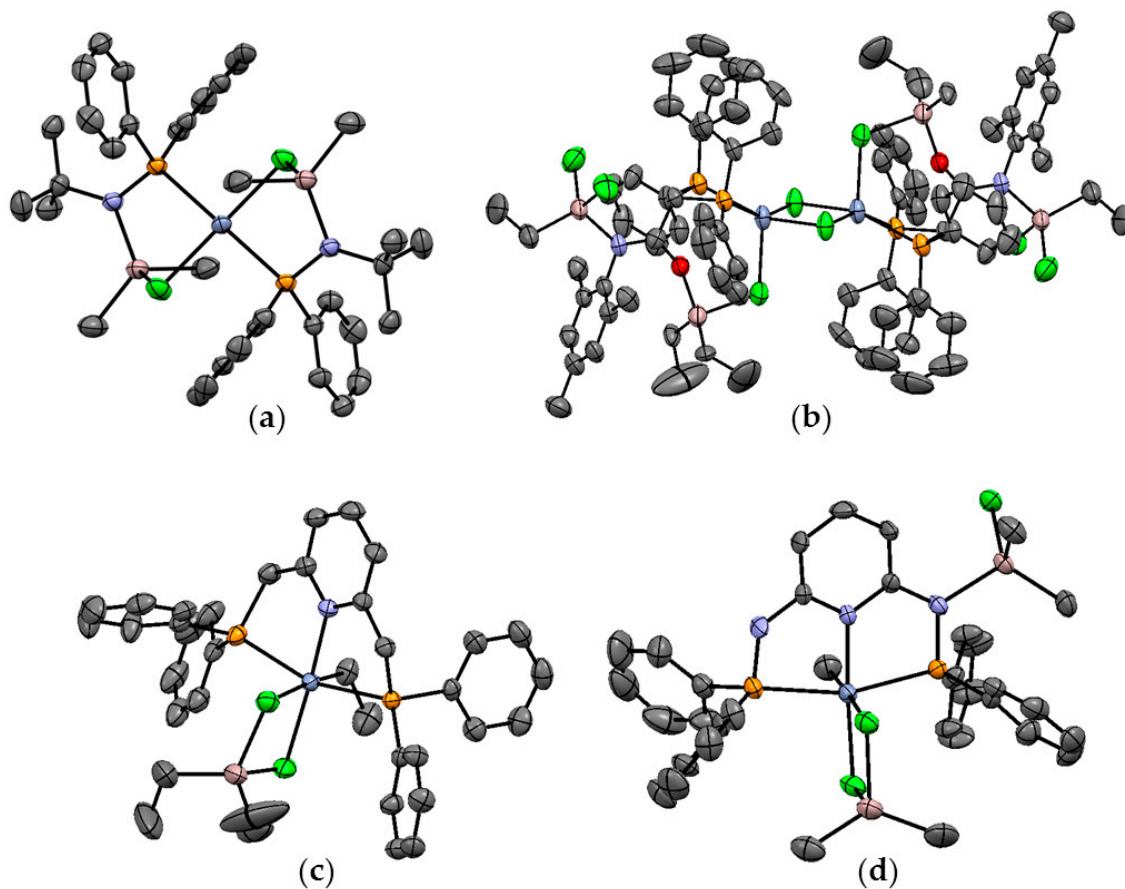


Figure 37. Examples of the molecular structures of the complexes containing Cr-(μ -Cl)-Al fragment (XRD analysis data), (a) Cr20 [255]; (b) Cr21 [256]; (c) Cr22 [257]; (d) Cr23 [257].

6. Complexes of Ni

Complexes of Ni are intensively being studied as efficient catalysts for the coordination oligomerization (SHOP process and beyond [46,261,262]) and polymerization [5,263–265] of α -olefins. Ni-based polymerization catalysts are very different from early transition metal (Ti, Zr, and V) complexes due to the lower sensitivity of Ni centers to electron-donor fragments, thus providing the copolymerization of α -olefins with polar vinyl monomers [266,267]. Another attractive property of Ni-based catalysts is their chain walking capability [268], which enables them to obtain branched polyolefins of different architectures. The direct participation of Ni-(μ -Cl)-Al species in catalytic processes at the Ni center is a matter of discussion; however, in the case of Ni, similar additional interactions are of dubious value. We have restricted the discussion in this section to a few examples of Ni-(μ -Cl)-Al bonding suspected of being associated with α -olefin polymerization.

The mere presence of Ni-(μ -Cl)-Al bonding in coordination compounds formed during the activation of Ni(II) chloro complexes by organoaluminum has been known for a fairly long time. Thus, for example, the formation of $\text{Cy}_3\text{P}(\eta^3\text{-allyl})\text{Ni}(\mu\text{-Cl})\text{AlMeCl}_2$ (**Ni01**) was clearly proven by XRD analysis [269] (Figure 38).

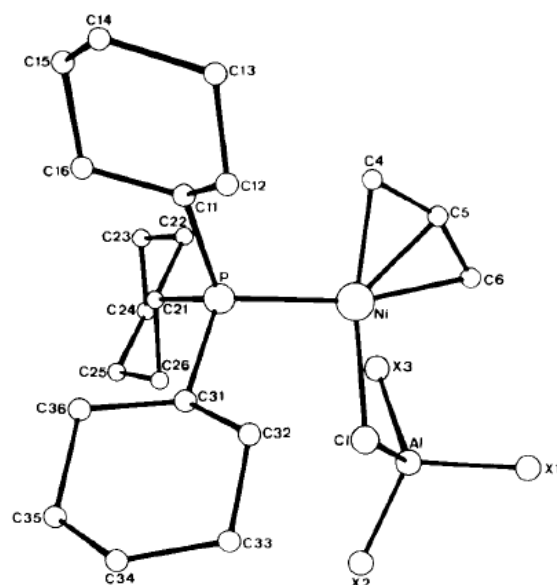
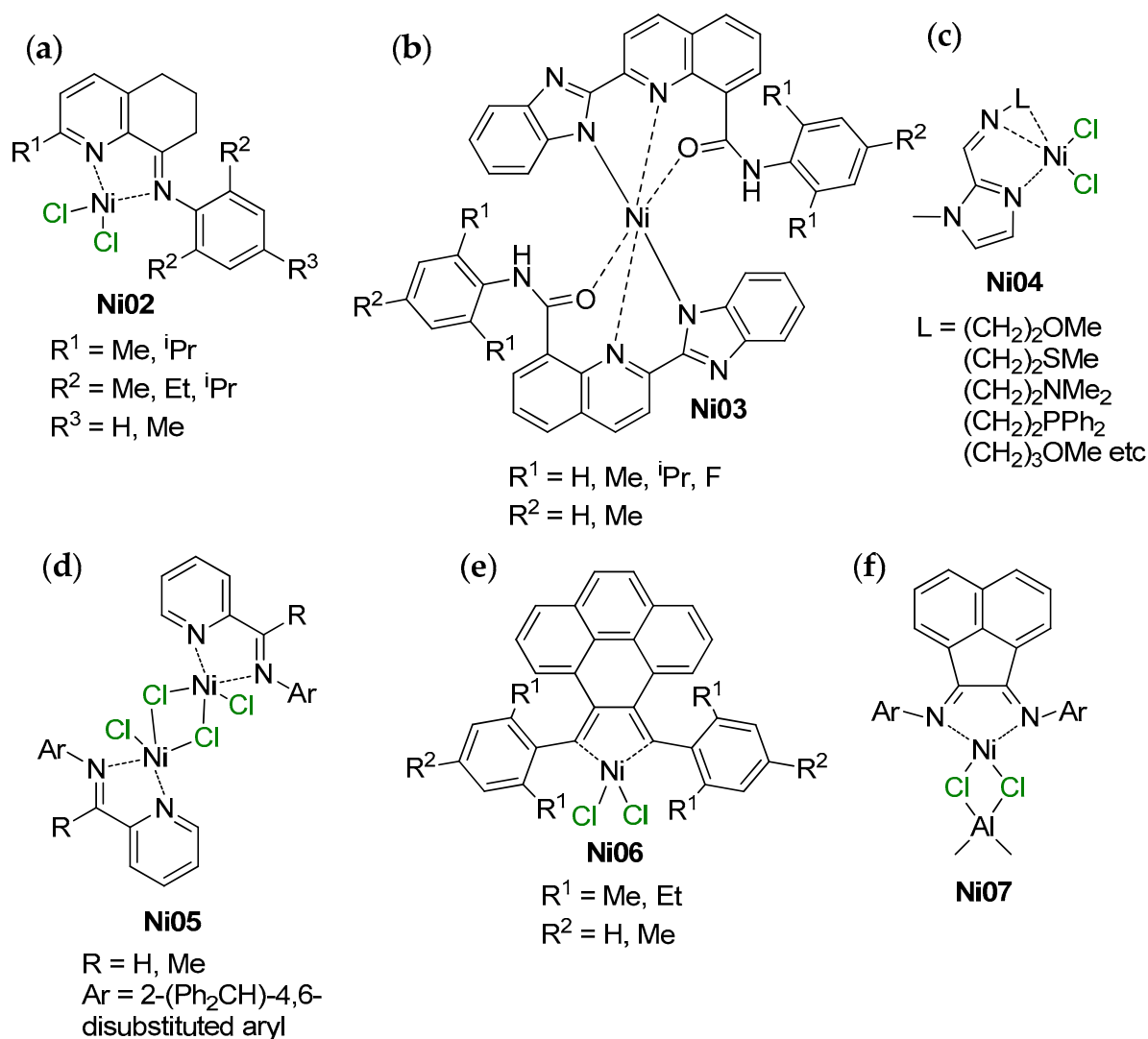


Figure 38. The molecular structure of complex **Ni01** comprising η^3 -allylnickel chloride, PCy_3 , and MeAlCl_2 ($X = \text{Cl}, \text{Me}$). Reprinted with permission from [269]. Copyright (1979) Elsevier B.V.

However, EXAFS studies of the reaction mixture formed from $\text{NiCl}_2(\text{PET}_3)_2$ and $\text{Me}_3\text{Al}_2\text{Cl}_3$ [270] showed the presence of C and P atoms in the first coordination shell of Ni; more distant shells included Al ($d = 3.0 \text{ \AA}$) and Cl ($d = 4.4 \text{ \AA}$), thus excluding Ni-(μ -Cl)-Al bonding. Similar spectral studies were continued by de Souza et al. [271], for example, with MAO-activated $\text{Ni}(\alpha\text{-diimine})\text{Cl}_2$. They showed that in the active catalyst species, the Ni(II) atom is surrounded by C and N atoms in the first shell and Cl atoms at a higher distance ($\sim 3.5 \text{ \AA}$), and proposed that the $\text{Ni} \cdots \text{Cl}$ interaction plays an important, previously underestimated, role in the polymerization of olefins.

In a number of later studies, the catalytic activity of different complexes was studied with the use of $\text{R}_x\text{AlCl}_{3-x}$ activators. Thus, for example, a number of N-(5,6,7-trihydroquinolin-8-ylidene)arylamino complexes of Ni(II) (**Ni02** in Scheme 40) have demonstrated high activity in the oligomerization of ethylene with the formation of but-1-ene (100% C4, 79–98% α -C4 selectivity) [272]. Higher activities were achieved when using $\text{Me}_3\text{Al}_2\text{Cl}_3$ instead of MAO. The authors have limited themselves to descriptions of the experimental results, without adding mechanistic interpretations. Complex **Ni03** with the 2-benzimidazolyl-N-arylquinoline-8-carboxamide ligand demonstrated lower activity and but-1-ene selectivity [273]; Et_2AlCl was the best activator. (Iminoalkyl)imidazole complex **Ni04** showed similar behavior [274].

Et_2AlCl and MAO equally successfully activated 2-iminopyridyl complex **Ni05** [275] and 4,5-bis(arylimino)pyrenylidene derivative **Ni06** [276] (Scheme 40).



Scheme 40. Structural formula of Ni pre-catalysts studied in α -olefin oligomerization and polymerization: (a) **Ni02** [272]; (b) **Ni03** [273]; (c) **Ni04** [274]; (d) **Ni05** [275]; (e) **Ni06** [276]; and (f) **Ni07** [277].

As shown in [278], when using EtAlCl_2 as an activator, ethylene oligomerization is complicated by Friedel–Crafts alkylation when using toluene as a reaction medium. Another side process with the participation of alkylaluminum chlorides is interaction with the polydentate ligand with the emergence of Ni coordination vacancies [279].

Recently, Soshnikov et al. have shown that α -diimine Ni(II) complexes under the action of R_2AlCl form the Ni(I) complex **Ni07** with Ni–(μ -Cl)–Al fragments, representing the catalyst's resting states [277]. It is quite possible that derivatives of similar species are essential to ensuring 'living' ethylene/ α -olefin copolymerization with the formation of *block*-polyolefins [280].

7. Conclusions

In the present review, we have summarized and commented on the data pertaining to the participation of M–(μ -Cl)–Al bonding in the formation of transition metal complexes which are active in α -olefin (and diene) chemistry. Of particular interest were the polymerization and oligomerization of α -olefins. We hypothesize that the theory and practice of single-site polymerization and oligomerization, catalyzed by Ti, Zr, and Cr complexes,

have suffered from the use of 10^2 – 10^4 equivalents of MAO for the activation of group 4 and 6 metal complexes in laboratory practice. In such conditions, consideration of the possibility of relatively weak M–(μ -Cl)–Al bonding makes no sense because MAO operates as an organoaluminum ‘sponge’. However, in recent years, with the growing interest in ‘low-MAO’ and ‘MAO-free’ catalytic processes, interest has re-focused on reversible M–(μ -Cl)–Al coordination on catalytic centers, as an additional factor affecting the chain propagation/chain termination balance, which appears to be reasonable.

The complex understanding of the nature of M–(μ -Cl)–Al bonds in metal complexes and reaction intermediates is significantly complicated by small amounts of fragmented data. For complexes with one bridging fragment, the (μ -Cl)–Al distance is not much different from the d(Al–Cl) value in R_2AlCl (and the M–(μ -Cl) distance is lengthened in comparison with d(M–Cl) in mononuclear chloro complexes). However, when forming two bridging fragments, the values of d((μ -Cl)–Al) and d(M–(μ -Cl)) converge in magnitude. Apparently, the former M–(μ -Cl)–Al species can be considered as reactive intermediates, whereas the latter M–(μ -Cl)(μ -X)–Al species represent dormant sites that can be separated and characterized. Obviously, lower stability of the M–(μ -Cl)–Al species complicates their identification.

Additionally, in contrast to alkyl, H and F fragments that have been established in the formation of M–X–Al catalytic species, M–Cl–Al bonding in the reaction intermediates cannot be detected by the only convenient and reliable method of analysis of diamagnetic species, i.e., NMR spectroscopy. Other spectral methods leave space for interpretation; XRD analysis has limited use. In this context, it is reasonable that quantum-chemical modeling has been used extensively in the studies of M–Cl–Al-containing molecules and processes which utilize them. Additionally, during studies of the catalytic processes, the possibility of the formation of the M–(μ -Cl)–Al species should not be ignored, at least in order to separate and characterize metal complexes exhibiting a non-trivial structure or, in the end, to formulate more efficient catalytic systems.

Author Contributions: Conceptualization, I.E.N., I.I.S. and P.V.I.; methodology, P.V.I.; resources, P.V.I.; writing—original draft preparation, I.E.N., I.I.S. and P.V.I.; writing—review and editing, I.E.N. and P.V.I.; visualization, P.V.I.; project administration, I.E.N.; funding acquisition, I.E.N. All authors have read and agreed to the published version of the manuscript.

Funding: This research was funded by Russian Science Foundation, grant number 21-73-30010.

Institutional Review Board Statement: Not applicable.

Informed Consent Statement: Not applicable.

Data Availability Statement: Not applicable.

Conflicts of Interest: The authors declare no conflict of interest.

Sample Availability: Not applicable.

References

1. Sauter, D.W.; Taoufik, M.; Boisson, C. Polyolefins, a Success Story. *Polymers* **2017**, *9*, 185. [[CrossRef](#)] [[PubMed](#)]
2. Jubinville, D.; Esmizadeh, E.; Saikrishnan, S.; Tzoganakis, C.; Mekonnen, T. A comprehensive review of global production and recycling methods of polyolefin (PO) based products and their post-recycling applications. *Sustain. Mater. Technol.* **2020**, *25*, e00188. [[CrossRef](#)]
3. Ricci, G.; Leone, G. Recent advances in the polymerization of butadiene over the last decade. *Polyolefins J.* **2014**, *1*, 43–60. [[CrossRef](#)]
4. Ricci, G.; Pampaloni, G.; Sommazzi, A.; Masi, F. Dienes Polymerization: Where We Are and What Lies Ahead. *Macromolecules* **2021**, *54*, 5879–5914. [[CrossRef](#)]
5. Baier, M.C.; Zuideveld, M.A.; Mecking, S. Post-Metallocenes in the Industrial Production of Polyolefins. *Angew. Chem. Int. Ed.* **2014**, *53*, 9722–9744. [[CrossRef](#)]
6. Franssen, N.M.G.; Reek, J.N.H.; de Bruin, B. Synthesis of functional ‘polyolefins’: State of the art and remaining challenges. *Chem. Soc. Rev.* **2013**, *42*, 5809–5832. [[CrossRef](#)]
7. Stürzel, M.; Mihan, S.; Mülhaupt, R. From Multisite Polymerization Catalysis to Sustainable Materials and All-Polyolefin Composites. *Chem. Rev.* **2016**, *116*, 1398–1433. [[CrossRef](#)]

8. Stalzer, M.M.; Delferro, M.; Marks, T.J. Supported Single-Site Organometallic Catalysts for the Synthesis of High-Performance Polyolefins. *Catal. Lett.* **2015**, *145*, 3–14. [[CrossRef](#)]
9. Mohite, A.S.; Rajpurkar, Y.D.; More, A.P. Bridging the gap between rubbers and plastics: A review on thermoplastic polyolefin elastomers. *Polym. Bull.* **2021**, *79*, 1309–1343. [[CrossRef](#)]
10. Zanchin, G.; Leone, G. Polyolefin thermoplastic elastomers from polymerization catalysis: Advantages, pitfalls and future challenges. *Prog. Polym. Sci.* **2021**, *113*, 101342. [[CrossRef](#)]
11. Kumawat, J.; Gupta, V.K. Fundamental aspects of heterogeneous Ziegler–Natta olefin polymerization catalysis: An experimental and computational overview. *Polym. Chem.* **2020**, *11*, 6107–6128. [[CrossRef](#)]
12. Al-Jarallah, A.M.; Anabtawi, J.A.; Siddiqui, M.A.B.; Aitani, A.M.; Al-Sa’doun, A.W. Ethylene dimerization and oligomerization to butene-1 and linear α -olefins: A review of catalytic systems and processes. *Catal. Today* **1992**, *14*, 1–121. [[CrossRef](#)]
13. Bariashir, C.; Huang, C.; Solan, G.A.; Sun, W.-H. Recent advances in homogeneous chromium catalyst design for ethylene tri-, tetra-, oligo- and polymerization. *Coord. Chem. Rev.* **2019**, *385*, 208–229. [[CrossRef](#)]
14. Salian, S.M.; Bagui, M.; Jasra, R.V. Industrially relevant ethylene trimerization catalysts and processes. *Appl. Petrochem. Res.* **2021**, *11*, 267–279. [[CrossRef](#)]
15. Tembe, G. Catalytic tri- and tetramerization of ethylene: A mechanistic overview. *Catal. Rev.* **2022**, 1–56. [[CrossRef](#)]
16. Breuil, P.-A.R.; Magna, L.; Olivier-Bourbigou, H. Role of Homogeneous Catalysis in Oligomerization of Olefins: Focus on Selected Examples Based on Group 4 to Group 10 Transition Metal Complexes. *Catal. Lett.* **2015**, *145*, 173–192. [[CrossRef](#)]
17. Nifant’ev, I.; Ivchenko, P. Fair Look at Coordination Oligomerization of Higher α -Olefins. *Polymers* **2020**, *12*, 1082. [[CrossRef](#)]
18. Parfenova, L.V.; Khalilov, L.M.; Dzhemilev, U.M. Mechanisms of reactions of organoaluminium compounds with alkenes and alkynes catalyzed by Zr complexes. *Russ. Chem. Rev.* **2012**, *81*, 524–548. [[CrossRef](#)]
19. Lamberti, M.; Mazzeo, M.; Pappalardo, D.; Pellicchia, C. Mechanism of stereospecific polymerization of α -olefins by late-transition metal and octahedral group 4 metal catalysts. *Coord. Chem. Rev.* **2009**, *253*, 2082–2097. [[CrossRef](#)]
20. Bryliakov, K.P.; Talsi, E.P. Frontiers of mechanistic studies of coordination polymerization and oligomerization of α -olefins. *Coord. Chem. Rev.* **2012**, *256*, 2994–3007. [[CrossRef](#)]
21. Parveen, R.; Cundari, T.R.; Younker, J.M.; Rodriguez, G.; McCullough, L. DFT and QSAR Studies of Ethylene Polymerization by Zirconocene Catalysts. *ACS Catal.* **2019**, *9*, 9339–9349. [[CrossRef](#)]
22. Chen, M.-C.; Roberts, J.A.S.; Marks, T.J. Marked Counteranion Effects on Single-Site Olefin Polymerization Processes. Correlations of Ion Pair Structure and Dynamics with Polymerization Activity, Chain Transfer, and Syndioselectivity. *J. Am. Chem. Soc.* **2004**, *126*, 4605–4625. [[CrossRef](#)] [[PubMed](#)]
23. Kuklin, M.S.; Hirvi, J.T.; Bochmann, M.; Linnolahti, M. Toward Controlling the Metallocene/Methylaluminoxane-Catalyzed Olefin Polymerization Process by a Computational Approach. *Organometallics* **2015**, *34*, 3586–3597. [[CrossRef](#)]
24. Tymiąska, N.; Zurek, E. DFT-D Investigation of Active and Dormant Methylaluminoxane (MAO) Species Grafted onto a Magnesium Dichloride Cluster: A Model Study of Supported MAO. *ACS Catal.* **2015**, *5*, 6989–6998. [[CrossRef](#)]
25. Laine, A.; Coussens, B.B.; Hirvi, J.T.; Berthoud, A.; Friederichs, N.; Severn, J.R.; Linnolahti, M. Effect of Ligand Structure on Olefin Polymerization by a Metallocene/Borate Catalyst: A Computational Study. *Organometallics* **2015**, *34*, 2415–2421. [[CrossRef](#)]
26. Trefz, T.K.; Henderson, M.A.; Linnolahti, M.; Collins, S.; McIndoe, J.S. Mass Spectrometric Characterization of Methylaluminoxane-Activated Metallocene Complexes. *Chem. Eur. J.* **2015**, *21*, 2980–2991. [[CrossRef](#)]
27. Theurkauff, G.; Bondon, A.; Dorcet, V.; Carpentier, J.-F.; Kirillov, E. Heterobi- and -trimetallic Ion Pairs of Zirconocene-Based Isoselective Olefin Polymerization Catalysts with AlMe₃. *Angew. Chem. Int. Ed.* **2015**, *54*, 6343–6346. [[CrossRef](#)]
28. Collins, S.; Linnolahti, M.; Garcia Zamora, M.; Zijlstra, H.S.; Rodriguez Hernández, M.T.; Perez-Camacho, O. Activation of Cp₂ZrX₂ (X = Me, Cl) by Methylaluminoxane As Studied by Electrospray Ionization Mass Spectrometry: Relationship to Polymerization Catalysis. *Macromolecules* **2017**, *50*, 8871–8884. [[CrossRef](#)]
29. Oliva, L.; Oliva, P.; Galdi, N.; Pellicchia, C.; Sian, L.; Macchioni, A.; Zuccaccia, C. Solution Structure and Reactivity with Metallocenes of AlMe₂F: Mimicking Cation–Anion Interactions in Metallocenium–Methylalumoxane Inner-Sphere Ion Pairs. *Angew. Chem. Int. Ed.* **2017**, *56*, 14227–14231. [[CrossRef](#)]
30. Desert, X.; Proutiere, F.; Welle, A.; Den Dauw, K.; Vantomme, A.; Miserque, O.; Brusson, J.-M.; Carpentier, J.-F.; Kirillov, E. Zirconocene-Catalyzed Polymerization of α -Olefins: When Intrinsic Higher Activity Is Flawed by Rapid Deactivation. *Organometallics* **2019**, *38*, 2664–2673. [[CrossRef](#)]
31. Sian, L.; Macchioni, A.; Zuccaccia, C. Understanding the Role of Metallocenium Ion-Pair Aggregates on the Rate of Olefin Insertion into the Metal–Carbon Bond. *ACS Catal.* **2020**, *10*, 1591–1606. [[CrossRef](#)]
32. Parveen, R.; Cundari, T.R.; Younker, J.M.; Rodriguez, G. Computational Assessment of Counterion Effect of Borate Anions on Ethylene Polymerization by Zirconocene and Hafnocene Catalysts. *Organometallics* **2020**, *39*, 2068–2079. [[CrossRef](#)]
33. Zaccaria, F.; Zuccaccia, C.; Cipullo, R.; Budzelaar, P.H.M.; Vittoria, A.; Macchioni, A.; Busico, V.; Ehm, C. Methylaluminoxane’s Molecular Cousin: A Well-defined and “Complete” Al-Activator for Molecular Olefin Polymerization Catalysts. *ACS Catal.* **2021**, *11*, 4464–4475. [[CrossRef](#)]
34. Collins, S.; Linnolahti, M. Activation of Substituted Metallocene Catalysts Using Methylaluminoxane. *ChemCatChem* **2022**, *14*, e202101918. [[CrossRef](#)]
35. Culver, D.B.; Dorn, R.W.; Venkatesh, A.; Meeprasert, J.; Rossini, A.J.; Pidko, E.A.; Lipton, A.S.; Lief, G.R.; Conley, M.P. Active Sites in a Heterogeneous Organometallic Catalyst for the Polymerization of Ethylene. *ACS Central Sci.* **2021**, *7*, 1225–1231. [[CrossRef](#)]

36. Parfenova, L.V.; Kovyazin, P.V.; Bikmeeva, A.K.; Palatov, E.R. Catalytic Systems Based on Cp_2ZrX_2 ($X = Cl, H$), Organoaluminum Compounds and Perfluorophenylboranes: Role of Zr,Zr- and Zr,Al-Hydride Intermediates in Alkene Dimerization and Oligomerization. *Catalysts* **2021**, *11*, 39. [CrossRef]
37. Christoffers, J.; Bergman, R.G. Catalytic Dimerization Reactions of α -Olefins and α,ω -Dienes with Cp_2ZrCl_2 /Poly(methylalumoxane): Formation of Dimers, Carbocycles, and Oligomers. *J. Am. Chem. Soc.* **1996**, *118*, 4715–4716. [CrossRef]
38. Christoffers, J.; Bergman, R.G. Zirconocene-alumoxane (1:1)—A catalyst for the selective dimerization of α -olefins. *Inorg. Chim. Acta* **1998**, *270*, 20–27. [CrossRef]
39. Nifant'ev, I.E.; Vinogradov, A.A.; Vinogradov, A.A.; Ivchenko, P.V. Zirconocene-catalyzed dimerization of 1-hexene: Two-stage activation and structure–catalytic performance relationship. *Catal. Commun.* **2016**, *79*, 6–10. [CrossRef]
40. Nifant'ev, I.; Ivchenko, P.; Tavtorkin, A.; Vinogradov, A.; Vinogradov, A. Non-traditional Ziegler-Natta catalysis in α -olefin transformations: Reaction mechanisms and product design. *Pure Appl. Chem.* **2017**, *89*, 1017–1032. [CrossRef]
41. Nifant'ev, I.; Vinogradov, A.; Vinogradov, A.; Karchevsky, S.; Ivchenko, P. Zirconocene-Catalyzed Dimerization of α -Olefins: DFT Modeling of the Zr-Al Binuclear Reaction Mechanism. *Molecules* **2019**, *24*, 3565. [CrossRef] [PubMed]
42. Nifant'ev, I.; Vinogradov, A.; Vinogradov, A.; Karchevsky, S.; Ivchenko, P. Experimental and Theoretical Study of Zirconocene-Catalyzed Oligomerization of 1-Octene. *Polymers* **2020**, *12*, 1590. [CrossRef] [PubMed]
43. Nifant'ev, I.E.; Vinogradov, A.A.; Vinogradov, A.A.; Bagrov, V.V.; Churakov, A.V.; Minyaev, M.E.; Kiselev, A.V.; Salakhov, I.I.; Ivchenko, P.V. A competitive way to low-viscosity PAO base stocks via heterocene-catalyzed oligomerization of dec-1-ene. *Mol. Catal.* **2022**, *529*, 112542. [CrossRef]
44. Phillips, A.M.F.; Suo, H.; Guedes da Silva, M.F.C.; Pombeiro, A.J.L.; Sun, W.-H. Recent developments in vanadium-catalyzed olefin coordination polymerization. *Coord. Chem. Rev.* **2020**, *416*, 213332. [CrossRef]
45. Olivier-Bourbigou, H.; Breuil, P.A.R.; Magna, L.; Michel, T.; Pastor, M.F.E.; Delcroix, D. Nickel Catalyzed Olefin Oligomerization and Dimerization. *Chem. Rev.* **2020**, *120*, 7919–7983. [CrossRef]
46. Bekmukhamedov, G.E.; Sukhov, A.V.; Kuchkaev, A.M.; Yakhvarov, D.G. Ni-Based Complexes in Selective Ethylene Oligomerization Processes. *Catalysts* **2020**, *10*, 498. [CrossRef]
47. Alferov, K.A.; Belov, G.P.; Meng, Y. Chromium catalysts for selective ethylene oligomerization to 1-hexene and 1-octene: Recent results. *Appl. Catal. A Gen.* **2017**, *542*, 71–124. [CrossRef]
48. Petit, J.; Magna, L.; Mézailles, N. Alkene oligomerization via metallacycles: Recent advances and mechanistic insights. *Coord. Chem. Rev.* **2022**, *450*, 214227. [CrossRef]
49. Tebbe, F.N.; Parshall, G.W.; Reddy, G.S. Olefin homologation with titanium methylene compounds. *J. Am. Chem. Soc.* **1978**, *100*, 3611–3613. [CrossRef]
50. Thompson, R.; Nakamaru-Ogiso, E.; Chen, C.-H.; Pink, M.; Mindiola, D.J. Structural Elucidation of the Illustrious Tebbe Reagent. *Organometallics* **2014**, *33*, 429–432. [CrossRef]
51. Kurogi, T.; Kuroki, K.; Moritani, S.; Takai, K. Structural elucidation of a methylenation reagent of esters: Synthesis and reactivity of a dinuclear titanium(III) methylene complex. *Chem. Sci.* **2021**, *12*, 3509–3515. [CrossRef] [PubMed]
52. Scott, J.; Mindiola, D.J. A tribute to Frederick Nye Tebbe. Lewis acid stabilized alkylidyne, alkylidene, and imides of 3D early transition metals. *Dalton Trans.* **2009**, *40*, 8463–8472. [CrossRef] [PubMed]
53. Finch, W.C.; Anslyn, E.V.; Grubbs, R.H. Substituent effects on the cleavage rates of titanocene metallacyclobutanes. *J. Am. Chem. Soc.* **1988**, *110*, 2406–2413. [CrossRef]
54. Hartner, F.W., Jr.; Schwartz, J. Synthesis and Characterization of “Long-Chain” Alkylidene-Bridged Hetero Bimetallic Complexes. *J. Am. Chem. Soc.* **1981**, *103*, 4979–4981. [CrossRef]
55. Halterman, R.L.; Ramsey, T.M. Conversion of *meso*-alkenes to chiral alkenes via titanocene-catalyzed ring-opening/ring-closing olefin metathesis. *J. Organomet. Chem.* **1997**, *547*, 41–48. [CrossRef]
56. Pine, S.H.; Pettit, R.J.; Geib, G.D.; Cruz, S.G.; Gallego, C.H.; Tijerina, T.; Pine, R.D. Carbonyl Methylenation Using a Titanium-Aluminum (Tebbe) Complex. *J. Org. Chem.* **1985**, *50*, 1212–1216. [CrossRef]
57. Nasrallah, D.J.; Zehnder, T.E.; Ludwig, J.R.; Steigerwald, D.C.; Kiernicki, J.J.; Szymczak, N.K.; Schindler, C.S. Hydrazone and Oxime Olefination via Ruthenium Alkylidenes. *Angew. Chem. Int. Ed.* **2022**, *61*, e202112101. [CrossRef]
58. Howard, T.R.; Lee, J.B.; Grubbs, R.H. Titanium metallacarbene-metallacyclobutane reactions: Stepwise metathesis. *J. Am. Chem. Soc.* **1980**, *102*, 6876–6878. [CrossRef]
59. Brown-Wensley, K.A.; Buchwald, S.L.; Cannizzo, L.; Clawson, L.; Ho, S.; Meinhardt, D.; Stille, J.R.; Straus, D.; Grubbs, R.H. Cp_2TiCH_2 complexes in synthetic applications. *Pure Appl. Chem.* **1983**, *55*, 1733–1744. [CrossRef]
60. Ikariya, T.; Ho, S.C.H.; Grubbs, R.H. Mechanism of rearrangement of titanacyclobutanes. *Organometallics* **1985**, *4*, 199–200. [CrossRef]
61. Lee, J.B.; Ott, K.C.; Grubbs, R.H. Kinetics and stereochemistry of the titanacyclobutane-titanaethylene interconversion. Investigation of a degenerate olefin metathesis reaction. *J. Am. Chem. Soc.* **1982**, *104*, 7491–7496. [CrossRef]
62. Law, J.A.; Bartfield, N.M.; Frederich, J.H. Site-Specific Alkene Hydromethylation via Protonolysis of Titanacyclobutanes. *Angew. Chem. Int. Ed.* **2021**, *60*, 14360–14364. [CrossRef] [PubMed]
63. Zefirova, A.K.; Shilov, A.E. The kinetics and mechanism of the interaction of aluminium alkyls with titanium halides. *Dokl. Akad. Nauk SSSR* **1961**, *136*, 599–602.
64. Dyachkovskii, F.S.; Shilova, A.K.; Shilov, A.E. The role of free ions in reactions of olefins with soluble complex catalysts. *J. Polym. Sci. Part C Polym. Symp.* **1967**, *16*, 2333–2339. [CrossRef]

65. Bryliakov, K.P.; Babushkin, D.E.; Talsi, E.P.; Voskoboynikov, A.Z.; Gritzko, H.; Schroder, L.; Damrau, H.-R.H.; Wieser, U.; Schaper, F.; Brintzinger, H.H. *ansa*-Titanocene Catalysts for α -Olefin Polymerization. Syntheses, Structures, and Reactions with Methylaluminoxane and Boron-Based Activators. *Organometallics* **2005**, *24*, 894–904. [[CrossRef](#)]
66. Machat, M.R.; Jandl, C.; Rieger, B. Titanocenes in Olefin Polymerization: Sustainable Catalyst System or an Extinct Species? *Organometallics* **2017**, *36*, 1408–1418. [[CrossRef](#)]
67. Williams, T.J.; Smith, A.D.H.; Buffet, J.-C.; Turner, Z.R.; O'Hare, D. Group 4 constrained geometry complexes for olefin (co)polymerisation. *Mol. Catal.* **2020**, *486*, 110872. [[CrossRef](#)]
68. Klosin, J.; Fontaine, P.P.; Figueroa, R. Development of Group IV Molecular Catalysts for High Temperature Ethylene- α -Olefin Copolymerization Reactions. *Acc. Chem. Res.* **2015**, *48*, 2004–2016. [[CrossRef](#)]
69. Yuan, S.-F.; Yan, Y.; Solan, G.A.; Ma, Y.; Sun, W.-H. Recent advancements in N-ligated group 4 molecular catalysts for the (co)polymerization of ethylene. *Coord. Chem. Rev.* **2020**, *411*, 213254. [[CrossRef](#)]
70. Nifant'ev, I.E.; Ivchenko, P.V.; Vinogradov, A.A. Heterocycle-fused cyclopentadienyl metal complexes: Heterocene synthesis, structure and catalytic applications. *Coord. Chem. Rev.* **2021**, *426*, 213515. [[CrossRef](#)]
71. Walsh, D.J.; Hyatt, M.G.; Miller, S.A.; Guironnet, D. Recent Trends in Catalytic Polymerizations. *ACS Catal.* **2019**, *9*, 11153–11188. [[CrossRef](#)]
72. Mach, K.; Antropiusová, H.; Poláček, J. Ethyl-substituted (π^5 -cyclopentadienyl)-bis(dihaloalane- μ -halo)titanium(III) and (η^6 -benzene)bis(dihaloalane- μ -halo)titanium(II) chloro and bromo complexes. *J. Organomet. Chem.* **1980**, *194*, 285–295. [[CrossRef](#)]
73. Mach, K.; Varga, V.; Antropiusová, H.; Poláček, J. Effects of methyl substituents at the cyclopentadienyl ligand on the properties of $C_5H_5TiCl_3$ and $C_5H_5TiAl_2Cl_{8-x}(C_2H_5)_x$ ($x = 0-4$) complexes. *J. Organomet. Chem.* **1987**, *333*, 205–215. [[CrossRef](#)]
74. Bonoldi, L.; Abis, L.; Fiocca, L.; Fusco, R.; Longo, L.; Simone, F.; Spera, S. Monotitanocene catalysts: An ESR study of Ti(III) derivatives formed in presence of MAO and other organoaluminium compounds. *J. Mol. Catal. A Chem.* **2004**, *219*, 47–56. [[CrossRef](#)]
75. Jensen, V.R.; Ystenes, M.; Waernmark, K.; Aakermark, B.; Svennson, M.; Siegbahn, P.E.M.; Blomberg, M.R.A. Strength of the metal-olefin bond in titanium complexes related to Ziegler-Natta catalysis. A theoretical model study of a square-pyramidal active center postulated to be found in titanium halide-based catalysts. *Organometallics* **1994**, *13*, 282–288. [[CrossRef](#)]
76. Jensen, V.R.; Borve, K.J.; Westberg, N.; Ystenes, M. Titanium-Ethylene Complexes Proposed To Be Intermediates in Ziegler-Natta Catalysis. Can They Be Detected through Vibrational Spectroscopy? *Organometallics* **1995**, *14*, 4349–4358. [[CrossRef](#)]
77. Jensen, V.R.; Borve, K.J.; Ystenes, M. Ziegler-Natta Ethylene Insertion Reaction for a Five-Coordinate Titanium Chloride Complex Bridged to an Aluminum Hydride Cocatalyst. *J. Am. Chem. Soc.* **1995**, *117*, 4109–4117. [[CrossRef](#)]
78. Sakai, S. Ab Initio Studies on the Ziegler-Natta Polymerization Reaction Mechanisms. The Role of Cocatalysis. *J. Phys. Chem.* **1994**, *98*, 12053–12058. [[CrossRef](#)]
79. Huang, Q.; Chen, L.; Ma, L.; Fu, Z.; Yang, W. Synthesis and characterization of oligomer from 1-decene catalyzed by supported Ziegler-Natta catalysts. *Eur. Polym. J.* **2005**, *41*, 2909–2915. [[CrossRef](#)]
80. Huang, Q.; Chen, L.; Sheng, Y.; Ma, L.; Fu, Z.; Yang, W. Synthesis and characterization of oligomer from 1-decene catalyzed by $AlCl_3/TiCl_4/SiO_2/Et_2AlCl$. *J. Appl. Polym. Sci.* **2006**, *101*, 584–590. [[CrossRef](#)]
81. Gagieva, S.C.; Kurmaev, D.A.; Tuskaev, V.A.; Khrustalev, V.N.; Churakov, A.V.; Golubev, E.K.; Sizov, A.I.; Zvukova, T.M.; Buzin, M.I.; Nikiforova, G.G.; et al. First example of cationic titanium (III) complexes with crown ether as catalysts for ethylene polymerization. *Eur. Polym. J.* **2022**, *170*, 111166. [[CrossRef](#)]
82. Kulangara, S.V.; Jabri, A.; Yang, Y.; Korobkov, I.; Gambarotta, S.; Duchateau, R. Synthesis, X-ray Structural Analysis, and Ethylene Polymerization Studies of Group IV Metal Heterobimetallic Aluminum-Pyrrolyl Complexes. *Organometallics* **2012**, *31*, 6085–6094. [[CrossRef](#)]
83. Pasha, F.A.; Basset, J.-M.; Toulhoat, H.; de Bruin, T. DFT Study on the Impact of the Methylaluminoxane Cocatalyst in Ethylene Oligomerization Using a Titanium-Based Catalyst. *Organometallics* **2015**, *34*, 426–431. [[CrossRef](#)]
84. McGuinness, D.S. Olefin Oligomerization via Metallacycles: Dimerization, Trimerization, Tetramerization, and Beyond. *Chem. Rev.* **2011**, *111*, 2321–2341. [[CrossRef](#)]
85. Linnolahti, M.; Collins, S. Formation, Structure, and Composition of Methylaluminoxane. *ChemPhysChem* **2017**, *18*, 3369–3374. [[CrossRef](#)]
86. Tyumkina, T.V.; Islamov, D.N.; Kovyazin, P.V.; Parfenova, L.V. Chain and cluster models of methylaluminoxane as activators of zirconocene hydride, alkyl and metallacyclopropane intermediates in alkene transformations. *Mol. Catal.* **2021**, *512*, 111768. [[CrossRef](#)]
87. Barr, J.L.; Kumar, A.; Lionetti, D.; Cruz, C.A.; Blakemore, J.D. Understanding the Roles of Triethylaluminum in Phosphinimide-Supported Titanium Catalyst Systems for Ethylene Polymerization. *Organometallics* **2019**, *38*, 2150–2155. [[CrossRef](#)]
88. Kumar, A.; Barr, J.L.; Cruz, C.A.; Blakemore, J.D. Heterobimetallic [Ti, Al] Complexes: Divergent Synthesis, Redox Properties, and Ethylene Polymerization Catalysis. *Organometallics* **2021**, *40*, 2139–2148. [[CrossRef](#)]
89. Porri, L.; Giarrusso, A. 5-Conjugated Diene Polymerization. In *Comprehensive Polymer Science and Supplements*; Allen, G., Bevington, J.C., Eds.; Pergamon Press: Oxford, UK, 1989; pp. 53–108. [[CrossRef](#)]
90. Pragliola, S.; Botta, A.; Longo, P. Solvent effect in 1,3-butadiene polymerization by cyclopentadienyl titanium trichloride ($CpTiCl_3$)/methylaluminoxane (MAO) and pentamethylcyclopentadienyl titanium trichloride (Cp^*TiCl_3)/MAO catalysts. *Eur. Polym. J.* **2019**, *111*, 20–27. [[CrossRef](#)]

91. Poláček, J.; Antropiusová, H.; Hanuš, V.; Petrusová, L.; Mach, K. Titanium-catalyzed cyclotrimerization of butadiene: I. Arenetitanium(II) chloro- and bromo-alane complexes. *J. Mol. Catal.* **1985**, *29*, 165–180. [[CrossRef](#)]
92. Poláček, J.; Antropiusová, H.; Petrusová, L.; Mach, K. Titanium-catalyzed cyclotrimerization of butadiene: Part II. The $(C_6H_6)Ti^{II}(AlCl_4)_2-Et_xAlCl_{3-x}$ ($x = 1-3$) systems. *J. Mol. Catal.* **1990**, *58*, 53–73. [[CrossRef](#)]
93. Troyanov, S.I.; Poláček, J.; Antropiusová, H.; Mach, K. The crystal structure of $(\eta^6-C_6Me_6)Ti[(\mu-Cl)_2(AlClEt)]_2$ and the catalytic activity of the $(C_6Me_6)TiAl_2Cl_{8-x}Et_x$ ($x = 0-4$) complexes towards butadiene. *J. Organomet. Chem.* **1992**, *430*, 317–325. [[CrossRef](#)]
94. Thewalt, U.; Österle, F. Strukturchemie titanorganischer Verbindungen: Die Struktur von $\pi-(CH_3)_6C_6Ti(Cl_2AlCl_2)_2 \cdot C_6H_6$. *J. Organomet. Chem.* **1979**, *172*, 317–324. [[CrossRef](#)]
95. Thewalt, U.; Stollmaier, F. Strukturchemie titanorganischer verbindungen: Die structur von $\eta^6-C_6H_6Ti(Cl_2AlCl_2)_2$. *J. Organomet. Chem.* **1982**, *228*, 149–152. [[CrossRef](#)]
96. Wilke, G. Fifty Years of Ziegler Catalysts: Consequences and Development of an Invention. *Angew. Chem. Int. Ed.* **2003**, *42*, 5000–5008. [[CrossRef](#)]
97. Cossee, P. Ziegler-Natta catalysis I. Mechanism of polymerization of α -olefins with Ziegler-Natta catalysts. *J. Catal.* **1964**, *3*, 80–88. [[CrossRef](#)]
98. Arlman, E.J.; Cossee, P. Ziegler-Natta catalysis III. Stereospecific polymerization of propene with the catalyst system $TiCl_3-AlEt_3$. *J. Catal.* **1964**, *3*, 99–104. [[CrossRef](#)]
99. Rodriguez, L.A.M.; van Looy, H.M. Studies on Ziegler-Natta catalysts. Part V. Stereospecificity of the active center. *J. Polym. Sci. Part A-1 Polym. Chem.* **1966**, *4*, 1971–1992. [[CrossRef](#)]
100. Ziegler, K.; Holzkamp, E.; Breil, H.; Martin, H. Polymerisation von Äthylen und anderen Olefinen. *Angew. Chem.* **1955**, *67*, 426. [[CrossRef](#)]
101. Natta, G. Stereospezifische Katalysen und isotaktische Polymere. *Angew. Chem.* **1956**, *68*, 393–403. [[CrossRef](#)]
102. Kumawat, J.; Gupta, V.K.; Vanka, K. The Nature of the Active Site in Ziegler–Natta Olefin Polymerization Catalysis Systems—A Computational Investigation. *Eur. J. Inorg. Chem.* **2014**, *2014*, 5063–5076. [[CrossRef](#)]
103. Credendino, R.; Liguori, D.; Fan, Z.; Morini, G.; Cavallo, L. Toward a Unified Model Explaining Heterogeneous Ziegler–Natta Catalysis. *ACS Catal.* **2015**, *5*, 5431–5435. [[CrossRef](#)]
104. Bahri-Laleh, N. Interaction of different poisons with $MgCl_2/TiCl_4$ based Ziegler-Natta catalysts. *Appl. Surf. Sci.* **2016**, *379*, 395–401. [[CrossRef](#)]
105. Potapov, A.G. Titanium-magnesium Ziegler-Natta catalysts: New insight on the active sites precursor. *Mol. Catal.* **2017**, *432*, 155–159. [[CrossRef](#)]
106. Nifant'ev, I.E.; Smetannikov, O.V.; Tavtorkin, A.N.; Chinova, M.S.; Ivchenko, P.V. Titanium–Magnesium Nanocatalysts of Polymerization (Review). *Pet. Chem.* **2016**, *56*, 480–490. [[CrossRef](#)]
107. Klaue, A.; Kruck, M.; Friederichs, N.; Bertola, F.; Wu, H.; Morbidelli, M. Insight into the Synthesis Process of an Industrial Ziegler–Natta Catalyst. *Ind. Eng. Chem. Res.* **2019**, *58*, 886–896. [[CrossRef](#)]
108. Zorve, P.; Linnolahti, M. Adsorption of Titanium Tetrachloride on Magnesium Dichloride Clusters. *ACS Omega* **2018**, *3*, 9921–9928. [[CrossRef](#)] [[PubMed](#)]
109. Correa, A.; Piemontesi, F.; Morini, G.; Cavallo, L. Key Elements in the Structure and Function Relationship of the $MgCl_2/TiCl_4$ /Lewis Base Ziegler–Natta Catalytic System. *Macromolecules* **2007**, *40*, 9181–9189. [[CrossRef](#)]
110. Correa, A.; Credendino, R.; Pater, J.T.M.; Morini, G.; Cavallo, L. Theoretical Investigation of Active Sites at the Corners of $MgCl_2$ Crystallites in Supported Ziegler–Natta Catalysts. *Macromolecules* **2012**, *45*, 3695–3701. [[CrossRef](#)]
111. Kashiwa, N.; Yoshitake, J. The influence of the valence state of titanium in $MgCl_2$ -supported titanium catalysts on olefin polymerization. *Makromol. Chem.* **1984**, *185*, 1133–1138. [[CrossRef](#)]
112. Piovano, A.; Signorile, M.; Braglia, L.; Torelli, P.; Martini, A.; Wada, T.; Takasao, G.; Taniike, T.; Groppo, E. Electronic Properties of Ti Sites in Ziegler–Natta Catalysts. *ACS Catal.* **2021**, *11*, 9949–9961. [[CrossRef](#)]
113. Potapov, A.G.; Terskikh, V.V.; Zakharov, V.A.; Bukatov, G.D. ^{27}Al NMR MAS study of the surface Al complexes formed in reaction of organoaluminium compounds with supported $TiCl_4/MgCl_2$ catalyst. *J. Mol. Catal. A Chem.* **1999**, *145*, 147–152. [[CrossRef](#)]
114. Linnolahti, M.; Pakkanen, T.A.; Bazhenova, A.S.; Denifl, P.; Leinonen, T.; Pakkanen, A. Alkylation of titanium tetrachloride on magnesium dichloride in the presence of Lewis bases. *J. Catal.* **2017**, *353*, 89–98. [[CrossRef](#)]
115. Yu, Y.; McKenna, T.F.L.; Boisson, C.; Lacerda Miranda, M.S.; Martins Jr., O. Engineering Poly(ethylene-co-1-butene) through Modulating the Active Species by Alkylaluminum. *ACS Catal.* **2020**, *10*, 7216–7229. [[CrossRef](#)]
116. Vittoria, A.; Meppelder, A.; Friederichs, N.; Busico, V.; Cipullo, R. Demystifying Ziegler–Natta Catalysts: The Origin of Stereoselectivity. *ACS Catal.* **2017**, *7*, 4509–4518. [[CrossRef](#)]
117. Abazari, M.; Jamjah, R.; Bahri-Laleh, N.; Hanifpour, A. Synthesis and evaluation of a new three-metallic high-performance Ziegler–Natta catalyst for ethylene polymerization: Experimental and computational studies. *Polym. Bull.* **2022**, *79*, 7265–7280. [[CrossRef](#)]
118. Masoori, M.; Nekoomanesh, M.; Posada-Pérez, S.; Rashedi, R.; Bahri-Laleh, N. Exploring cocatalyst type effect on the Ziegler–Natta catalyzed ethylene polymerizations: Experimental and DFT studies. *J. Polym. Res.* **2022**, *29*, 1–11. [[CrossRef](#)]
119. Kaminsky, W.; Funck, A.; Hähnsen, H. New application for metallocene catalysts in olefin polymerization. *Dalton Trans.* **2009**, *41*, 8803–8810. [[CrossRef](#)]
120. Kaminsky, W. Production of Polyolefins by Metallocene Catalysts and Their Recycling by Pyrolysis. *Macromol. Symp.* **2016**, *360*, 10–22. [[CrossRef](#)]

121. Busico, V. Metal-catalysed olefin polymerisation into the new millennium: A perspective outlook. *Dalton Trans.* **2009**, *41*, 8794–8802. [[CrossRef](#)]
122. Beck, S.; Brintzinger, H.H. Alkyl exchange between aluminium trialkyls and zirconocene dichloride complexes—A measure of electron densities at the Zr center. *Inorg. Chim. Acta* **1998**, *270*, 376–381. [[CrossRef](#)]
123. Laine, A.; Linnolahti, M.; Pakkanen, T.A. Alkylation and activation of metallocene polymerization catalysts by reactions with trimethylaluminum: A computational study. *J. Organomet. Chem.* **2012**, *716*, 79–85. [[CrossRef](#)]
124. Kumawat, J.; Gupta, V.K. Catalyst Activation and Chain Transfer Agents in Metallocene Catalysts for Ethylene Polymerization: A Computational Investigation. *Eur. J. Inorg. Chem.* **2021**, *2021*, 3332–3343. [[CrossRef](#)]
125. Eilertsen, J.L.; Støvneng, J.A.; Ystenes, M.; Rytter, E. Activation of Metallocenes for Olefin Polymerization As Monitored by IR Spectroscopy. *Inorg. Chem.* **2005**, *44*, 4843–4851. [[CrossRef](#)] [[PubMed](#)]
126. Parfenova, L.V.; Kovyazin, P.V.; Gabdrakhmanov, V.Z.; Istomina, G.P.; Ivchenko, P.V.; Nifant'ev, I.E.; Khalilov, L.M.; Dzhemilev, U.M. Ligand exchange processes in zirconocene dichloride–trimethylaluminum bimetallic systems and their catalytic properties in reaction with alkenes. *Dalton Trans.* **2018**, *47*, 16918–16937. [[CrossRef](#)]
127. Harlan, C.J.; Bott, S.G.; Barron, A.R. Three-Coordinate Aluminum Is Not a Prerequisite for Catalytic Activity in the Zirconocene-Alumoxane Polymerization of Ethylene. *J. Am. Chem. Soc.* **1995**, *117*, 6465–6474. [[CrossRef](#)]
128. Götz, C.; Rau, A.; Luft, G. Ternary metallocene catalyst systems based on metallocene dichlorides and $\text{AlBu}_3^i/[\text{PhNMe}_2\text{H}][\text{B}(\text{C}_6\text{F}_5)_4]$: NMR investigations of the influence of Al/Zr ratios on alkylation and on formation of the precursor of the active metallocene species. *J. Mol. Catal. A Chem.* **2002**, *184*, 95–110. [[CrossRef](#)]
129. Baldwin, S.M.; Bercaw, J.E.; Brintzinger, H.H. Alkylaluminum-Complexed Zirconocene Hydrides: Identification of Hydride-Bridged Species by NMR Spectroscopy. *J. Am. Chem. Soc.* **2008**, *130*, 17423–17433. [[CrossRef](#)]
130. Negishi, E.; Yoshida, T. A novel zirconium-catalyzed hydroalumination of olefins. *Tetrahedron Lett.* **1980**, *21*, 1501–1504. [[CrossRef](#)]
131. Parfenova, L.V.; Pechatkina, S.V.; Khalilov, L.M.; Dzhemilev, U.M. Mechanism of Cp_2ZrCl_2 -catalyzed olefin hydroalumination by alkylalanes. *Russ. Chem. Bull.* **2005**, *54*, 316–327. [[CrossRef](#)]
132. Parfenova, L.V.; Balaev, A.V.; Gubaidullin, I.M.; Abzalilova, L.R.; Pechatkina, S.V.; Khalilov, L.M.; Spivak, S.I.; Dzhemilev, U.M. Kinetic model of olefin hydroalumination by HAlBu_2^i and AlBu_3^i in the presence of Cp_2ZrCl_2 catalyst. *Int. J. Chem. Kinet.* **2007**, *39*, 333–339. [[CrossRef](#)]
133. Parfenova, L.V.; Vil'danova, R.F.; Pechatkina, S.V.; Khalilov, L.M.; Dzhemilev, U.M. New effective reagent $[\text{Cp}_2\text{ZrH}_2 \cdot \text{ClAlEt}_2]$ for alkene hydrometallation. *J. Organomet. Chem.* **2007**, *692*, 3424–3429. [[CrossRef](#)]
134. Parfenova, L.V.; Kovyazin, P.V.; Nifant'ev, I.E.; Khalilov, L.M.; Dzhemilev, U.M. Role of Zr,Al Hydride Intermediate Structure and Dynamics in Alkene Hydroalumination with XAlBu_2^i (X = H, Cl, Bui), Catalyzed by $\text{Zr} \eta^5$ Complexes. *Organometallics* **2015**, *34*, 3559–3570. [[CrossRef](#)]
135. Pankratyev, E.Y.; Tyumkina, T.V.; Parfenova, L.V.; Khalilov, L.M.; Khursan, S.L.; Dzhemilev, U.M. DFT Study on Mechanism of Olefin Hydroalumination by XAlBu_2^i in the Presence of Cp_2ZrCl_2 Catalyst. I. Simulation of Intermediate Formation in Reaction of HAlBu_2^i with Cp_2ZrCl_2 . *Organometallics* **2009**, *28*, 968–977. [[CrossRef](#)]
136. Nurislamova, L.F.; Gubaydullin, I.M.; Koledina, K.F. Kinetic model of isolated reactions of the catalytic hydroalumination of olefins. *Reac. Kinet. Mech. Catal.* **2015**, *116*, 79–93. [[CrossRef](#)]
137. Nurislamova, L.F.; Gubaydullin, I.M.; Koledina, K.F.; Safin, R.R. Kinetic model of the catalytic hydroalumination of olefins with organoaluminum compounds. *Reac. Kinet. Mech. Catal.* **2015**, *117*, 1–14. [[CrossRef](#)]
138. Pankratyev, E.Y.; Tyumkina, T.V.; Parfenova, L.V.; Khalilov, L.M.; Khursan, S.L.; Dzhemilev, U.M. DFT and *Ab Initio* Study on Mechanism of Olefin Hydroalumination by XAlBu_2^i in the Presence of Cp_2ZrCl_2 Catalyst. II. Olefin Interaction with Catalytically Active Centers. *Organometallics* **2011**, *30*, 6078–6089. [[CrossRef](#)]
139. Pankratyev, E.Y.; Khursan, S.L.; Dzhemilev, U.M. DFT and *ab initio* study on mechanism of olefin hydroalumination by XAlBu_2^i in the presence of Cp_2ZrCl_2 catalyst. III. Efficiency of transmetallation in $\text{Cp}_2\text{ZrRCl}-\text{XAlBu}_2^i$ system. *J. Organomet. Chem.* **2012**, *718*, 117–123. [[CrossRef](#)]
140. Culver, D.B.; Corieri, J.; Lief, G.; Conley, M.P. Reactions of Triisobutylaluminum with Unbridged or Bridged Group IV Metallocene Dichlorides. *Organometallics* **2022**, *41*, 892–899. [[CrossRef](#)]
141. Van Horn, D.E.; Negishi, E. Selective carbon-carbon bond formation via transition metal catalysts. 8. Controlled carbometalation. Reaction of acetylenes with organoalane-zirconocene dichloride complexes as a route to stereo- and regio-defined trisubstituted olefins. *J. Am. Chem. Soc.* **1978**, *100*, 2252–2254. [[CrossRef](#)]
142. Xu, S.; Negishi, E. Zirconium-Catalyzed Asymmetric Carboalumination of Unactivated Terminal Alkenes. *Acc. Chem. Res.* **2016**, *49*, 2158–2168. [[CrossRef](#)]
143. Kondakov, D.Y.; Negishi, E. Zirconium-catalyzed enantioselective methylalumination of monosubstituted alkenes. *J. Am. Chem. Soc.* **1995**, *117*, 10771–10772. [[CrossRef](#)]
144. Kondakov, D.Y.; Negishi, E. Zirconium-Catalyzed Enantioselective Alkylalumination of Monosubstituted Alkenes Proceeding via Noncyclic Mechanism. *J. Am. Chem. Soc.* **1996**, *118*, 1577–1578. [[CrossRef](#)]
145. Parfenova, L.V.; Zakirova, I.V.; Kovyazin, P.V.; Karchevsky, S.G.; Istomina, G.P.; Khalilov, L.M.; Dzhemilev, U.M. Intramolecular mobility of η^5 -ligands in chiral zirconocene complexes and the enantioselectivity of alkene functionalization by organoaluminum compounds. *Dalton Trans.* **2016**, *45*, 12814–12826. [[CrossRef](#)] [[PubMed](#)]

146. Negishi, E.; Kondakov, D.Y.; Choueiry, D.; Kasai, K.; Takahashi, T. Multiple Mechanistic Pathways for Zirconium-Catalyzed Carboalumination of Alkynes. Requirements for Cyclic Carbometalation Processes Involving C-H Activation. *J. Am. Chem. Soc.* **1996**, *118*, 9577–9588. [[CrossRef](#)]
147. Kaminsky, W.; Kopf, J.; Thirase, G. Notiz über die Röntgenstrukturanalyse von Al,Zr- μ -Chloro-1-[bis(cyclopentadienyl)zirkonio(IV)]-2,2-bis(diäthylaluminio)äthan. *Eur. J. Org. Chem.* **1974**, 1531–1533. [[CrossRef](#)]
148. Khalilov, L.M.; Parfenova, L.V.; Rusakov, S.V.; Ibragimov, A.G.; Dzhemilev, U.M. Synthesis and conversions of metallocycles. 22. NMR studies of the mechanism of Cp₂ZrCl₂-catalyzed cycloalumination of olefins with triethylaluminum to form aluminacyclopentanes. *Bull. Acad. Sci. USSR Div. Chem. Sci.* **2000**, *49*, 2051–2058. [[CrossRef](#)]
149. Rusakov, S.V.; Khalilov, L.M.; Parfenova, L.V.; Ibragimov, A.G.; Ponomarev, O.A.; Dzhemilev, U.M. Synthesis and transformations of metallocycles. 27. Quantum-chemical study of the mechanism of styrene catalytic cyclometallation with triethylaluminum in the presence of Cp₂ZrCl₂. *Bull. Acad. Sci. USSR Div. Chem. Sci.* **2001**, *50*, 2336–2345. [[CrossRef](#)]
150. Tyumkina, T.V.; Islamov, D.N.; Parfenova, L.V.; Whitby, R.J.; Khalilov, L.M.; Dzhemilev, U.M. Mechanistic aspects of chemo- and regioselectivity in Cp₂ZrCl₂-catalyzed alkene cycloalumination by AlEt₃. *J. Organomet. Chem.* **2016**, *822*, 135–143. [[CrossRef](#)]
151. Tyumkina, T.V.; Islamov, D.N.; Parfenova, L.V.; Karchevsky, S.G.; Khalilov, L.M.; Dzhemilev, U.M. Mechanism of Cp₂ZrCl₂-Catalyzed Olefin Cycloalumination with AlEt₃: Quantum Chemical Approach. *Organometallics* **2018**, *37*, 2406–2418. [[CrossRef](#)]
152. Parfenova, L.V.; Kovyazin, P.V.; Mukhamadeeva, O.V.; Ivchenko, P.V.; Nifant'ev, I.E.; Khalilov, L.M.; Dzhemilev, U.M. Zirconocene dichlorides as catalysts in alkene carbo- and cyclometalation by AlEt₃: Intermediate structures and dynamics. *Dalton Trans.* **2021**, *50*, 15802–15820. [[CrossRef](#)] [[PubMed](#)]
153. Erker, G.; Noe, R.; Wingbermühle, D. Seven-Membered Heterodimetallic Ring Systems from (Conjugated Diene) Group 4 Metallocene Complexes and Organoaluminum Reagents. *Eur. J. Inorg. Chem.* **1994**, *127*, 805–811. [[CrossRef](#)]
154. Hartner Jr., F. W.; Schwartz, J.; Clift, S.M. Synthesis of carbene complexes of Group IV metals from alkylidene-bridged heterobimetallic precursors. *J. Am. Chem. Soc.* **1983**, *105*, 640–641. [[CrossRef](#)]
155. Hartner, F.M.; Clift, S.M.; Schwartz, J.; Tulip, T.H. Synthesis and characterization of alkylidene-bridged zirconium-aluminum complexes. *Organometallics* **1987**, *6*, 1346–1350. [[CrossRef](#)]
156. Pédeutour, J.-N.; Cramail, H.; Deffieux, A. Influence of X ligand nature in the activation process of racEt(Ind)₂ZrX₂ by methylaluminoxane. *J. Mol. Catal. A Chem.* **2001**, *176*, 87–94. [[CrossRef](#)]
157. Pédeutour, J.-N.; Cramail, H.; Deffieux, A. The negative role of chloride counter-anion in the activation process of zirconocene dichloride by methylaluminoxane. *J. Mol. Catal. A Chem.* **2001**, *174*, 81–87. [[CrossRef](#)]
158. Franceschini, F.C.; Tavares, T.T.R.; dos Santos, J.H.Z.; Ferreira, M.L.; Soares, J.B.P. Ethylene and Propylene Polymerization Using In Situ Supported Me₂Si(Ind)₂ZrCl₂ Catalyst: Experimental and Theoretical Study. *Macromol. Mater. Eng.* **2006**, *291*, 279–287. [[CrossRef](#)]
159. Parfenova, L.V.; Kovyazin, P.V.; Tyumkina, T.V.; Islamov, D.N.; Lyapina, A.R.; Karchevsky, S.G.; Ivchenko, P.V. Reactions of bimetallic Zr,Al-hydride complexes with methylaluminoxane: NMR and DFT study. *J. Organomet. Chem.* **2017**, *851*, 30–39. [[CrossRef](#)]
160. Stahl, N.G.; Salata, M.R.; Marks, T.J. B(C₆F₅)₃- vs Al(C₆F₅)₃-Derived Metallocenium Ion Pairs. Structural, Thermochemical, and Structural Dynamic Divergences. *J. Am. Chem. Soc.* **2005**, *127*, 10898–10909. [[CrossRef](#)]
161. Velthoen, M.E.Z.; Munoz-Murillo, A.; Bouhmadi, A.; Cecius, M.; Diefenbach, S.; Weckhuysen, B.M. The multifaceted role of methylaluminoxane in metallocene-based olefin polymerization catalysis. *Macromolecules* **2018**, *51*, 343–355. [[CrossRef](#)]
162. Velthoen, M.E.Z.; Boereboom, J.M.; Buló, R.E.; Weckhuysen, B.M. Insights into the activation of silica-supported metallocene olefin polymerization catalysts by methylaluminoxane. *Catal. Today* **2019**, *334*, 223–230. [[CrossRef](#)]
163. Baldwin, S.M.; Bercaw, J.E.; Henling, L.M.; Day, M.W.; Brintzinger, H.H. Cationic Alkylaluminum-Complexed Zirconocene Hydrides: NMR-Spectroscopic Identification, Crystallographic Structure Determination, and Interconversion with Other Zirconocene Cations. *J. Am. Chem. Soc.* **2011**, *133*, 1805–1813. [[CrossRef](#)] [[PubMed](#)]
164. Lenton, T.N.; Bercaw, J.E.; Panchenko, V.N.; Zakharov, V.A.; Babushkin, D.E.; Soshnikov, I.E.; Talsi, E.P.; Brintzinger, H.H. Formation of Trivalent Zirconocene Complexes from *ansa*-Zirconocene-Based Olefin-Polymerization Precatalysts: An EPR- and NMR-Spectroscopic Study. *J. Am. Chem. Soc.* **2013**, *135*, 10710–10719. [[CrossRef](#)]
165. Thorn, M.G.; Diefenbach, S.P. *Book of Abstracts; Advances in Polyolefins X*: Santa Rosa, CA, USA; American Chemical Society, Division of Polymer Chemistry, Inc.: Blacksburg, VA, USA, 2015.
166. Thorn, M.G.; Marcel, L. *SPE International Polyolefins Conference 2016*; Global Interdependence: Houston, TX, USA; SPE South Texas Section, Society of Plastics Engineers: Bethel, CT, USA, 2016.
167. Slaugh, L.H.; Schoenthal, G.W. Vinylidene Olefin Process. U.S. Patent 4658078, 14 April 1987.
168. Thiele, S.; Erker, G. Adjusting the Features of Active Metallocene Ziegler Systems for Their Potential Use as Carbon–Carbon Coupling Catalysts in Organic Synthesis. *Eur. J. Inorg. Chem.* **1997**, *130*, 201–207. [[CrossRef](#)]
169. Janiak, C.; Blank, F. Metallocene Catalysts for Olefin Oligomerization. *Macromol. Symp.* **2006**, *236*, 14–22. [[CrossRef](#)]
170. Janiak, C.; Lange, K.C.H.; Marquardt, P. α -Olefin oligomers with narrow molar mass distributions from zirconocene/methylaluminoxane catalysts—An examination of the structure-reactivity relationship. *Macromol. Rapid Commun.* **1995**, *16*, 643–650. [[CrossRef](#)]
171. Kissin, Y.V.; Schwab, F.C. Post-Oligomerization of α -Olefin Oligomers: A Route to Single-Component and Multicomponent Synthetic Lubricating Oils. *J. Appl. Polym. Sci.* **2009**, *111*, 273–280. [[CrossRef](#)]

172. Kissin, Y.V. Detailed Kinetics of 1-Hexene Oligomerization Reaction with (*n*-Bu-Cp)₂ZrCl₂-MAO Catalyst. *Macromol. Chem. Phys.* **2009**, *210*, 1241–1246. [[CrossRef](#)]
173. Boccia, A.C.; Costabile, C.; Pragliola, S.; Longo, P. Selective Dimerization of γ -Branched α -Olefins in the Presence of C_{2v} Group-4 Metallocene-Based Catalysts. *Macromol. Chem. Phys.* **2004**, *205*, 1320–1326. [[CrossRef](#)]
174. Salmela, M.; Lehtinen, T.; Efimova, E.; Santala, S.; Santala, V. Towards bioproduction of poly- α -olefins from lignocellulose. *Green Chem.* **2020**, *22*, 5067–5076. [[CrossRef](#)]
175. Bagheri, V.; Moore, L.D.; Di Giacinto, P.M.; Sanchezrivas, M. Low Viscosity Oligomer Oil Product, Process and Composition. U.S. Patent 20130225459, 29 August 2013.
176. Sato, H.; Kamimura, H. Process for Producing Saturated Aliphatic Hydrocarbon Compound, and Lubricant Composition. U.S. Patent 8373011, 12 February 2013.
177. Patil, A.; Lewis, K.G.; Bodige, S.; Zushma, S. Ester Compounds, Lubricating Oil Composition Containing Same and Process for Making Same. U.S. Patent 2019062663, 28 February 2019.
178. Sato, H.; Kashiwamura, T.; Okamoto, T.; Yokota, K. Carbonyl Compound Containing Long-Chain Branched Alkyl Group. U.S. Patent 7402610, 22 July 2008.
179. Harvey, B.G.; Quintana, R.L. Synthesis of renewable jet and diesel fuels from 2-ethyl-1-hexene. *Energy Environ. Sci.* **2010**, *3*, 352–357. [[CrossRef](#)]
180. Nifant'ev, I.E.; Minyaev, M.E.; Tavtorkin, A.N.; Vinogradov, A.A.; Ivchenko, P.V. Branched alkylphosphinic and disubstituted phosphinic and phosphonic acids: Effective synthesis based on α -olefin dimers and applications in lanthanide extraction and separation. *RSC Adv.* **2017**, *7*, 24122–24128. [[CrossRef](#)]
181. Nifant'ev, I.E.; Vinogradov, A.A.; Vinogradov, A.A.; Ivchenko, P.V. Production Method of Vinylidene Olefins. RU Patent RU2652118, 25 April 2018.
182. Takeuchi, K.; Fujikawa, S. Base Oil for Oil Drilling Fluid and Oil Drilling Fluid Composition. U.S. Patent 2011251445, 13 October 2011.
183. Fujikawa, S.; Okamoto, T.; Yokota, K. Process for Producing Unsaturated Hydrocarbon Compound. U.S. Patent 8119850, 21 February 2012.
184. Kovyazin, P.V.; Bikmeeva, A.K.; Islamov, D.N.; Yanybin, V.M.; Tyumkina, T.V.; Parfenova, L.V. Ti Group Metallocene-Catalyzed Synthesis of 1-Hexene Dimers and Tetramers. *Molecules* **2021**, *26*, 2775. [[CrossRef](#)] [[PubMed](#)]
185. Parfenova, L.V.; Kovyazin, P.V.; Bikmeeva, A.K. Bimetallic Zr,Zr-Hydride Complexes in Zirconocene Catalyzed Alkene Dimerization. *Molecules* **2020**, *25*, 2216. [[CrossRef](#)] [[PubMed](#)]
186. Park, J.H.; Jang, Y.E.; Jeon, J.Y.; Go, M.J.; Lee, J.; Kim, S.K.; Lee, S.-I.; Lee, B.Y. Preparation of *ansa*-metallocenes for production of poly(α -olefin) lubricants. *Dalton Trans.* **2014**, *43*, 10132–10138. [[CrossRef](#)]
187. Nifant'ev, I.E.; Vinogradov, A.A.; Vinogradov, A.A.; Bezzubov, S.I.; Ivchenko, P.V. Catalytic oligomerization of α -olefins in the presence of two-stage activated zirconocene catalyst based on 6,6-dimethylfulvene 'dimer'. *Mendeleev Commun.* **2017**, *27*, 35–37. [[CrossRef](#)]
188. Jiang, H.; Yu, K. Catalytic polymerization of 1-decene using a silicon-bridged metallocene system. *Petrol. Sci. Technol.* **2017**, *35*, 1451–1456. [[CrossRef](#)]
189. Dong, S.Q.; Mi, P.K.; Xu, S.; Zhang, J.; Zhao, R.D. Preparation and Characterization of Single-Component Poly- α -olefin Oil Base Stocks. *Energy Fuels* **2019**, *33*, 9796–9804. [[CrossRef](#)]
190. Nifant'ev, I.E.; Vinogradov, A.A.; Vinogradov, A.A.; Sedov, I.V.; Dorokhov, V.G.; Lyadov, A.S.; Ivchenko, P.V. Structurally uniform 1-hexene, 1-octene, and 1-decene oligomers: Zirconocene/MAO-catalyzed preparation, characterization, and prospects of their use as low-viscosity low-temperature oil base stocks. *Appl. Catal. A Gen.* **2018**, *549*, 40–50. [[CrossRef](#)]
191. Shao, H.; Wang, R.; Li, H.; Guo, X.; Jiang, T. Synthesis of low-molecular-weight poly- α -olefins using silicon-bridged zirconocene catalyst for lubricant basestock. *Arab. J. Chem.* **2020**, *13*, 2715–2721. [[CrossRef](#)]
192. Jalali, A.; Nekoomanehs-Haghighi, M.; Dehghani, S.; Bahri-Laleh, N. Effect of metal type on the metallocene-catalyzed oligomerization of 1-hexene and 1-octene to produce poly- α -olefin-based synthetic lubricants. *Appl. Organomet. Chem.* **2020**, *34*, e5338. [[CrossRef](#)]
193. Lamb, J.V.; Buffet, J.-C.; Turner, Z.R.; Khamnaen, T.; O'Hare, D. Metallocene Polyethylene Wax Synthesis. *Macromolecules* **2020**, *53*, 5847–5856. [[CrossRef](#)]
194. Tritto, I.; Boggioni, L.; Sacchi, M.C.; Dall'Occo, T. Novel aluminum based cocatalysts for metallocene catalyzed olefin polymerization. *J. Mol. Catal. A Chem.* **2003**, *204*, 305–314. [[CrossRef](#)]
195. Hagen, H.; Boersma, J.; van Koten, G. Homogeneous vanadium-based catalysts for the Ziegler–Natta polymerization of α -olefins. *Chem. Soc. Rev.* **2002**, *31*, 357–364. [[CrossRef](#)]
196. Gambarotta, S. Vanadium-based Ziegler–Natta: Challenges, promises, problems. *Coord. Chem. Rev.* **2003**, *237*, 229–243. [[CrossRef](#)]
197. Redshaw, C. Vanadium procatalysts bearing chelating aryloxides: Structure–activity trends in ethylenepolymerisation. *Dalton Trans.* **2010**, *39*, 5595–5604. [[CrossRef](#)]
198. Wu, J.-Q.; Li, Y.-S. Well-defined vanadium complexes as the catalysts for olefin polymerization. *Coord. Chem. Rev.* **2011**, *255*, 2303–2314. [[CrossRef](#)]
199. Nomura, K.; Zhang, S. Design of Vanadium Complex Catalysts for Precise Olefin Polymerization. *Chem. Rev.* **2011**, *111*, 2342–2362. [[CrossRef](#)]
200. Zambelli, A.; Sessa, I.; Grisi, F.; Fusco, R.; Accomazzi, P. Syndiotactic Polymerization of Propylene: Single-Site Vanadium Catalysts in Comparison with Zirconium and Nickel. *Macromol. Rapid Commun.* **2001**, *22*, 297–310. [[CrossRef](#)]

201. Feghali, K.; Harding, D.J.; Reardon, D.; Gambarotta, S.; Yap, G.; Wang, Q. Stability of Metal–Carbon Bond versus Metal Reduction during Ethylene Polymerization Promoted by a Vanadium Complex: The Role of the Aluminum Cocatalyst. *Organometallics* **2002**, *21*, 968–976. [[CrossRef](#)]
202. Liguori, D.; Centore, R.; Csok, Z.; Tuzi, A. Polymerization of Propene and 1,3-Butadiene with Vanadyl(V) Monoamidinate Precatalysts and MAO or Dialkylaluminum Chloride Cocatalysts. *Macromol. Chem. Phys.* **2004**, *205*, 1058–1063. [[CrossRef](#)]
203. Wang, W.; Nomura, K. Notable Effects of Aluminum Alkyls and Solvents for Highly Efficient Ethylene (Co)polymerizations Catalyzed by (Arylimido)-(aryloxo)vanadium Complexes. *Adv. Synth. Catal.* **2006**, *348*, 743–750. [[CrossRef](#)]
204. Soshnikov, I.E.; Semikolenova, N.V.; Shubin, A.A.; Bryliakov, K.P.; Zakharov, V.A.; Redshaw, C.; Talsi, E.P. EPR Monitoring of Vanadium(IV) Species Formed upon Activation of Vanadium(V) Polyphenolate Precatalysts with AlR₂Cl and AlR₂Cl/Ethyltrichloroacetate (R = Me, Et). *Organometallics* **2009**, *28*, 6714–6720. [[CrossRef](#)]
205. Xu, B.-C.; Hu, T.; Wu, J.-Q.; Hu, N.-H.; Li, Y.-S. Novel vanadium(III) complexes with bidentate *N,N*-chelating iminopyrrolide ligands: Synthesis, characterization and catalytic behaviour of ethylene polymerization and copolymerization with 10-undecen-1-ol. *Dalton Trans.* **2009**, *41*, 8854–8863. [[CrossRef](#)] [[PubMed](#)]
206. Mu, J.-S.; Shi, X.-C.; Li, Y.-S. Ethylene homopolymerization and copolymerization by vanadium(III) complexes containing tridentate or tetradentate iminopyrrolyl ligands. *J. Polym. Sci. A Polym. Chem.* **2011**, *49*, 2700–2708. [[CrossRef](#)]
207. Zhang, S.-W.; Lu, L.-P.; Li, B.-X.; Li, Y.-S. Synthesis, structural characterization, and olefin polymerization behavior of vanadium(III) complexes bearing bidentate phenoxy-phosphine ligands. *J. Polym. Sci. A Polym. Chem.* **2012**, *50*, 4721–4731. [[CrossRef](#)]
208. Kurmaev, D.A.; Kolosov, N.A.; Gagieva, S.C.; Borissova, A.O.; Tuskaev, V.A.; Bravaya, N.M.; Bulychiev, B.M. Coordination compounds of chromium (+3) and vanadium (+3) and (+5) with 2,6-bis(diphenylhydroxymethyl)pyridyl ligand: Synthesis and study of catalytic activity in the polymerization of ethylene. *Inorg. Chim. Acta* **2013**, *396*, 136–143. [[CrossRef](#)]
209. Wu, J.-Q.; Pan, L.; Hu, N.-H.; Li, Y.-S. Synthesis, Structural Characterization, and Ethylene Polymerization Behavior of the Vanadium(III) Complexes Bearing Salicylaldiminato Ligands. *Organometallics* **2008**, *27*, 3840–3848. [[CrossRef](#)]
210. Wu, J.-Q.; Pan, L.; Li, Y.-G.; Liu, S.-R.; Li, Y.-S. Synthesis, Structural Characterization, and Olefin Polymerization Behavior of Vanadium(III) Complexes Bearing Tridentate Schiff Base Ligands. *Organometallics* **2009**, *28*, 1817–1825. [[CrossRef](#)]
211. Wang, Y.; Zuo, M.; Li, Y. Theoretical investigation of the mechanism of ethylene polymerization with salicylaldiminato vanadium(III) complexes. *Chin. J. Catal.* **2015**, *36*, 657–666. [[CrossRef](#)]
212. Bialek, M.; Bisz, E. Dichlorovanadium(IV) diamine-bis(phenolate) complexes for ethylene (co)polymerization and 1-olefin isospecific polymerization. *J. Catal.* **2018**, *362*, 65–73. [[CrossRef](#)]
213. Soshnikov, I.E.; Semikolenova, N.V.; Bryliakov, K.P.; Zakharov, V.A.; Talsi, E.P. Vanadium olefin polymerization catalysts: NMR spectroscopic characterization of V(III) intermediates. *J. Organomet. Chem.* **2018**, *867*, 4–13. [[CrossRef](#)]
214. Yi, J.; Nakatani, N.; Nomura, K.; Hada, M. Time-dependent DFT study of the K-edge spectra of vanadium and titanium complexes: Effects of chloride ligands on pre-edge features. *Phys. Chem. Chem. Phys.* **2020**, *22*, 674–682. [[CrossRef](#)] [[PubMed](#)]
215. Yi, J.; Nakatani, N.; Nomura, K. Solution XANES and EXAFS analysis of active species of titanium, vanadium complex catalysts in ethylene polymerisation/dimerisation and syndiospecific styrene polymerisation. *Dalton Trans.* **2020**, *49*, 8008–8028. [[CrossRef](#)] [[PubMed](#)]
216. Nomura, K.; Izawa, I.; Kuboki, M.; Inoue, K.; Aoki, H.; Tsutsumi, K. Solution XAS Analysis for Reactions of Phenoxide-Modified (Arylimido)vanadium(V) Dichloride and (Oxo)vanadium(V) Complexes with Al Alkyls: Effect of Al Cocatalyst in Ethylene (Co)polymerization. *Catalysts* **2022**, *12*, 198. [[CrossRef](#)]
217. Liu, K.; Liu, Z.; Cheng, R.; He, X.; Liu, B. Mechanistic study on the effects of co-catalyst on ethylene polymerization over supported vanadocene catalyst. *Mol. Catal.* **2020**, *486*, 110852. [[CrossRef](#)]
218. Do, L.H.; Labinger, J.A.; Bercaw, J.E. Mechanistic Studies of Ethylene and α -Olefin Co-Oligomerization Catalyzed by Chromium–PNP Complexes. *Organometallics* **2012**, *31*, 5143–5149. [[CrossRef](#)]
219. Zilbershtein, T.M.; Kardash, V.A.; Suvorova, V.V.; Golovko, A.K. Decene formation in ethylene trimerization reaction catalyzed by Cr-pyrrole system. *Appl. Catal. A Gen.* **2014**, *475*, 371–378. [[CrossRef](#)]
220. Gong, M.; Liu, Z.; Li, Y.; Ma, Y.; Sun, Q.; Zhang, J.; Liu, B. Selective Co-Oligomerization of Ethylene and 1-Hexene by Chromium–PNP Catalysts: A DFT Study. *Organometallics* **2016**, *35*, 972–981. [[CrossRef](#)]
221. Dixon, J.T.; Green, M.J.; Hess, F.M.; Morgan, D.H. Advances in selective ethylene trimerization—A critical overview. *J. Organomet. Chem.* **2004**, *689*, 3641–3668. [[CrossRef](#)]
222. Wass, D.F. Chromium-catalysed ethene trimerisation and tetramerization—Breaking the rules in olefin oligomerisation. *Dalton Trans.* **2007**, *8*, 816–819. [[CrossRef](#)] [[PubMed](#)]
223. Van Leeuwen, P.W.; Clément, N.D.; Tschan, M.J.-L. New processes for the selective production of 1-octene. *Coord. Chem. Rev.* **2011**, *255*, 1499–1517. [[CrossRef](#)]
224. Belov, G.P. Tetramerization of Ethylene to Octene-1 (A Review). *Pet. Chem.* **2012**, *52*, 139–154. [[CrossRef](#)]
225. Agapie, T. Selective ethylene oligomerization: Recent advances in chromium catalysis and mechanistic investigations. *Coord. Chem. Rev.* **2011**, *255*, 861–880. [[CrossRef](#)]
226. Forestière, A.; Olivier-Bourbigou, H.; Saussine, L. Oligomerization of Monoolefins by Homogeneous Catalysts. *Oil. Gas Sci. Technol.* **2009**, *64*, 649–667. [[CrossRef](#)]
227. Belov, G.P.; Matkovsky, P.E. Processes for the Production of Higher Linear α -Olefins. *Pet. Chem.* **2010**, *50*, 296–302. [[CrossRef](#)]
228. Reagen, W.K. Process for Olefin Polymerization. European Patent 0417477, 9 August 1990.
229. Knudsen, R.D.; Freeman, J.W.; Lashier, M.E. Olefin Production. U.S. Patent 5563312, 8 October 1996.

230. Lashier, M.E. Process for the Oligomerization of Olefins. European Patent 0780353, 25 June 1997.
231. Freeman, J.W.; Buster, J.L.; Knudsen, R.D. Olefin Production. U.S. Patent 5856257, 5 January 1999.
232. Tanaka, E.; Urata, H.; Oshiki, T.; Aoshima, T.; Kawashima, R.; Iwade, S.; Nakamura, H.; Katsuki, S.; Okano, T. Process for Producing Alpha-Olefin Oligomer Compositions. European Patent 0611743, 24 August 1994.
233. Yoshitaka, A.; Hirofumi, N.; Yoshaki, N.; Takeshi, O. Process for Producing Alpha-Olefin Oligomer. U.S. Patent 5856612, 5 January 1999.
234. Van Rensburg, W.J.; Grové, C.; Steynberg, J.P.; Stark, K.B.; Huysen, J.J.; Steynberg, P.J. A DFT Study toward the Mechanism of Chromium-Catalyzed Ethylene Trimerization. *Organometallics* **2004**, *23*, 1207–1222. [[CrossRef](#)]
235. Jabri, A.; Mason, C.B.; Sim, Y.; Gambarotta, S.; Burchell, T.J.; Duchateau, R. Isolation of Single-Component Trimerization and Polymerization Chromium Catalysts: The Role of the Metal Oxidation State. *Angew. Chem. Int. Ed.* **2008**, *47*, 9717–9721. [[CrossRef](#)]
236. Vidyaratne, I.; Nikiforov, G.B.; Gorelsky, S.I.; Gambarotta, S.; Duchateau, R.; Korobkov, I. Isolation of a self-activating ethylene trimerization catalyst. *Angew. Chem. Int. Ed.* **2009**, *48*, 6552–6566. [[CrossRef](#)]
237. Budzelaar, P.H.M. Ethene trimerization at CrI/CrIII – A density functional theory (DFT) study. *Can. J. Chem.* **2009**, *87*, 832–837. [[CrossRef](#)]
238. Yang, Y.; Liu, Z.; Cheng, R.; He, X.; Liu, B. Mechanistic DFT Study on Ethylene Trimerization of Chromium Catalysts Supported by a Versatile Pyrrole Ligand System. *Organometallics* **2014**, *33*, 2599–2607. [[CrossRef](#)]
239. Venderbosch, B.; Oudsen, J.-P.H.; Wolzak, L.A.; Martin, D.J.; Korstanje, T.J.; Tromp, M. Spectroscopic Investigation of the Activation of a Chromium-Pyrrolyl Ethene Trimerization Catalyst. *ACS Catal.* **2019**, *9*, 1197–1210. [[CrossRef](#)] [[PubMed](#)]
240. Carter, A.; Cohen, S.A.; Cooley, N.A.; Murphy, A.; Scutt, J.; Wass, D.F. High activity ethylene trimerisation catalysts based on diphosphine ligands. *Chem. Commun.* **2002**, *8*, 858–859. [[CrossRef](#)]
241. Kim, T.H.; Lee, H.M.; Park, H.S.; Kim, S.D.; Kwon, S.J.; Tahara, A.; Nagashima, H.; Lee, B.Y. MAO-free and extremely active catalytic system for ethylene tetramerization. *Appl. Organomet. Chem.* **2019**, *33*, e4829. [[CrossRef](#)]
242. Jabri, A.; Crewdson, P.; Gambarotta, S.; Korobkov, I.; Duchateau, R. Isolation of a Cationic Chromium(II) Species in a Catalytic System for Ethylene Tri- and Tetramerization. *Organometallics* **2006**, *25*, 715–718. [[CrossRef](#)]
243. Müller, B.H.; Fritz, P.M.; Bölt, H.; Wöhl, A.; Müller, W.; Winkler, F.; Wellenhoffer, A.; Rosenthal, U.; Hapke, M.; Peulecke, N.; et al. Catalyst Composition and Process for Di-, Tri- and/or Tetramerization of Ethylene. WO Patent 2009006979, 15 January 2009.
244. Peitz, S.; Peulecke, N.; Aluri, B.R.; Hansen, S.; Müller, B.H.; Spannenberg, A.; Rosenthal, U.; Al-Hazmi, M.H.; Mosa, F.M.; Wöhl, A.; et al. A Selective Chromium Catalyst System for the Trimerization of Ethene and Its Coordination Chemistry. *Eur. J. Inorg. Chem.* **2010**, *2010*, 1167–1171. [[CrossRef](#)]
245. Müller, B.H.; Peulecke, N.; Peitz, S.; Aluri, B.R.; Rosenthal, U.; Al-Hazmi, M.H.; Mosa, F.M.; Wöhl, A.; Müller, W. Activity Enhancement of a Catalyst System for the Selective Trimerization of Ethene to 1-Hexene by Modification of the Chromium to Chloride to Aluminium Ratio. *Chem. Eur. J.* **2011**, *17*, 6935–6938. [[CrossRef](#)]
246. Peitz, S.; Peulecke, N.; Müller, B.H.; Spannenberg, A.; Drexler, H.-J.; Rosenthal, U.; Al-Hazmi, M.H.; Al-Eidan, K.E.; Wöhl, A.; Müller, W. Heterobimetallic Al-Cl-Cr Intermediates with Relevance to the Selective Catalytic Ethene Trimerization Systems Consisting of CrCl₃(THF)₃, the Aminophosphorus Ligands Ph₂PNP(Ph)NH, and Triethylaluminum. *Organometallics* **2011**, *30*, 2364–2370. [[CrossRef](#)]
247. Bartlett, S.A.; Moulin, J.; Tromp, M.; Reid, G.; Dent, A.J.; Cibir, G.; McGuinness, D.S.; Evans, J. Activation of [CrCl₃{PPh₂N(ⁱPr)PPh₂}] for the selective oligomerisation of ethene: A Cr K-edge XAFS study. *Cat. Sci. Technol.* **2016**, *6*, 6237–6246. [[CrossRef](#)]
248. Nifant'ev, I.E.; Vinogradov, A.A.; Vinogradov, A.A.; Roznyatovsky, V.A.; Grishin, Y.K.; Ivanyukl, A.V.; Sedov, I.V.; Churakov, A.V.; Ivchenko, P.V. 5,6-Dihydrodibenzo[c,e][1,2]azaphosphinine-based PNP ligands, Cr coordination and Cr(III) precatalysts for ethylene oligomerization. *Organometallics* **2018**, *37*, 2660–2664. [[CrossRef](#)]
249. Lee, D.G.; Baek, J.W.; Lee, J.H.; Lee, H.J.; Seo, Y.H.; Lee, J.; Lee, C.G.; Lee, B.Y. Replacement of the Common Chromium Source CrCl₃(thf)₃ with Well-Defined [CrCl₂(μ-Cl)(thf)₂]₂. *Molecules* **2021**, *26*, 1167. [[CrossRef](#)]
250. Albahily, K.; Koç, E.; Al-Baldawi, D.; Savard, D.; Gambarotta, S.; Burchell, T.J.; Duchateau, R. Chromium Catalysts Supported by a Nonspectator NPN Ligand: Isolation of Single-Component Chromium Polymerization Catalysts. *Angew. Chem. Int. Ed.* **2008**, *47*, 5816–5819. [[CrossRef](#)] [[PubMed](#)]
251. McGuinness, D.S.; Brown, D.B.; Tooze, R.P.; Hess, F.M.; Dixon, J.T.; Slawin, A.M.Z. Ethylene Trimerization with Cr-PNP and Cr-SNS Complexes: Effect of Ligand Structure, Metal Oxidation State, and Role of Activator on Catalysis. *Organometallics* **2006**, *25*, 3605–3610. [[CrossRef](#)]
252. Temple, C.; Jabri, A.; Crewdson, P.; Gambarotta, S.; Korobkov, I.; Duchateau, R. The Question of the Cr Oxidation State in the {Cr(SNS)} Catalyst for Selective Ethylene Trimerization: An Unanticipated Re-Oxidation Pathway. *Angew. Chem. Int. Ed.* **2006**, *45*, 7050–7053. [[CrossRef](#)] [[PubMed](#)]
253. Albahily, K.; Gambarotta, S.; Duchateau, R. Ethylene Oligomerization Promoted by a Silylated-SNS Chromium System. *Organometallics* **2011**, *30*, 4655–4664. [[CrossRef](#)]
254. Zhang, J.; Li, A.; Andy Hor, T.S. Crystallographic Revelation of the Role of AlMe₃ (in MAO) in Cr [NNN] Pyrazolyl Catalyzed Ethylene Trimerization. *Organometallics* **2009**, *28*, 2935–2937. [[CrossRef](#)]
255. Thapa, I.; Gambarotta, S.; Korobkov, I.; Duchateau, R.; Kulangara, S.V.; Chevalier, R. Switchable Chromium(II) Complexes of a Chelating Amidophosphine (N-P) for Selective and Nonselective Ethylene Oligomerization. *Organometallics* **2010**, *29*, 4080–4089. [[CrossRef](#)]

256. Kulangara, S.V.; Mason, C.; Juba, M.; Yang, Y.; Thapa, I.; Gambarotta, S.; Korobkov, I.; Duchateau, R. Synthesis and Catalytic Oligomerization Activity of Chromium Catalysts of Ligand Systems with Switchable Connectivity. *Organometallics* **2012**, *31*, 6438–6449. [[CrossRef](#)]
257. Alzamly, A.; Gambarotta, S.; Korobkov, I. Polymer-Free Ethylene Oligomerization Using a Pyridine-Based Pincer PNP-Type of Ligand. *Organometallics* **2013**, *32*, 7204–7212. [[CrossRef](#)]
258. Alzamly, A.; Gambarotta, S.; Korobkov, I. Synthesis, Structures, and Ethylene Oligomerization Activity of Bis(phosphanylamine)pyridine Chromium/Aluminate Complexes. *Organometallics* **2013**, *32*, 7107–7115. [[CrossRef](#)]
259. Alzamly, A.; Gambarotta, S.; Korobkov, I.; Murugesu, M.; Le Roy, J.J.H.; Budzelaar, P.H.M. Isolation of a Hexanuclear Chromium Cluster with a Tetrahedral Hydridic Core and Its Catalytic Behavior for Ethylene Oligomerization. *Inorg. Chem.* **2014**, *53*, 6073–6081. [[CrossRef](#)] [[PubMed](#)]
260. Kulangara, S.V.; Haveman, D.; Vidjayacoumar, B.; Korobkov, I.; Gambarotta, S.; Duchateau, R. Effect of Cocatalysts and Solvent on Selective Ethylene Oligomerization. *Organometallics* **2015**, *34*, 1203–1210. [[CrossRef](#)]
261. Keim, W. Oligomerization of Ethylene to α -Olefins: Discovery and Development of the Shell Higher Olefin Process (SHOP). *Angew. Chem. Int. Ed.* **2013**, *52*, 12492–12496. [[CrossRef](#)] [[PubMed](#)]
262. Kuhn, P.; Sémeril, D.; Matt, D.; Chetcuti, M.J.; Lutz, P. Structure–reactivity relationships in SHOP-type complexes: Tunable catalysts for the oligomerisation and polymerisation of ethylene. *Dalton Trans.* **2007**, *5*, 515–528. [[CrossRef](#)]
263. Ittel, S.D.; Johnson, L.K.; Brookhart, M. Late-Metal Catalysts for Ethylene Homo- and Copolymerization. *Chem. Rev.* **2000**, *100*, 1169–1203. [[CrossRef](#)]
264. Qasim, M.; Bashir, M.S.; Iqbal, S.; Mahmood, Q. Recent advancements in α -diimine-nickel and -palladium catalysts for ethylene polymerization. *Eur. Polym. J.* **2021**, *160*, 110783. [[CrossRef](#)]
265. Wu, R.; Wu, W.K.; Stieglitz, L.; Gaan, S.; Rieger, B.; Heuberger, M. Recent advances on α -diimine Ni and Pd complexes for catalyzed ethylene (Co)polymerization: A comprehensive review. *Coord. Chem. Rev.* **2023**, *474*, 214844. [[CrossRef](#)]
266. Mu, H.; Pan, L.; Song, D.; Li, Y. Neutral Nickel Catalysts for Olefin Homo- and Copolymerization: Relationships between Catalyst Structures and Catalytic Properties. *Chem. Rev.* **2015**, *115*, 12091–12137. [[CrossRef](#)]
267. Mu, H.; Zhou, G.; Hu, X.; Jian, Z. Recent advances in nickel mediated copolymerization of olefin with polar monomers. *Coord. Chem. Rev.* **2021**, *435*, 213802. [[CrossRef](#)]
268. Wang, F.; Chen, C. A continuing legend: The Brookhart-type α -diimine nickel and palladium catalysts. *Polym. Chem.* **2019**, *10*, 2354–2369. [[CrossRef](#)]
269. Bogdanović, B. Catalysis and Organic Syntheses. Selectivity Control in Nickel-Catalyzed Olefin Oligomerization. In *Advances in Organometallic Chemistry*; Stone, F.G.A., West, R., Eds.; Elsevier: Amsterdam, The Netherlands, 1979; Volume 17, pp. 105–140. [[CrossRef](#)]
270. Corker, J.M.; Evans, J. EXAFS studies of the activation of homogeneous nickel catalysts for propene dimerisation by aluminium reagents. *J. Chem. Soc. Chem. Commun.* **1991**, *16*, 1104–1106. [[CrossRef](#)]
271. De Souza, R.F.; Simon, L.C.; do Carmo, M.; Alves, M. XAS study of the nickel(α -diimine) catalyst for olefin polymerization. *J. Catal.* **2003**, *214*, 165–168. [[CrossRef](#)]
272. Chai, W.; Yu, J.; Wang, L.; Hu, X.; Redshaw, C.; Sun, W.-H. Synthesis, characterization and ethylene oligomerization behavior of *N*-(2-alkyl-5,6,7-trihydroquinolin-8-ylidene)arylamino nickel(II) dichlorides. *Inorg. Chim. Acta* **2012**, *385*, 21–26. [[CrossRef](#)]
273. He, F.; Hao, X.; Cao, X.; Redshaw, C.; Sun, W.-H. Nickel halide complexes bearing 2-benzimidazolyl-*N*-arylquinoline-8-carboxamide derived ligands: Synthesis, characterization and catalytic behavior towards ethylene oligomerization and the vinyl polymerization of norbornene. *J. Organomet. Chem.* **2012**, *712*, 46–51. [[CrossRef](#)]
274. Boudier, A.; Breuil, P.-A.R.; Magna, L.; Olivier-Bourbigou, H.; Braunstein, P. Nickel(II) complexes with imino-imidazole chelating ligands bearing pendant donor groups (SR, OR, NR₂, PR₂) as precatalysts in ethylene oligomerization. *J. Organomet. Chem.* **2012**, *718*, 31–37. [[CrossRef](#)]
275. Sun, W.-H.; Song, S.; Li, B.; Redshaw, C.; Hao, X.; Li, Y.-S.; Wang, F. Ethylene polymerization by 2-iminopyridylnickel halide complexes: Synthesis, characterization and catalytic influence of the benzhydryl group. *Dalton Trans.* **2012**, *41*, 11999–12010. [[CrossRef](#)]
276. Song, K.; Yang, W.; Li, B.; Liu, Q.; Redshaw, C.; Li, Y.; Sun, W.-H. Nickel(II) complexes bearing 4,5-bis(arylimino)-pyrenylidene: Synthesis, characterization, and ethylene polymerization behaviour. *Dalton Trans.* **2013**, *42*, 9166–9175. [[CrossRef](#)]
277. Soshnikov, I.E.; Semikolenova, N.V.; Bryliakov, K.P.; Antonov, A.A.; Talsi, E.P. Ni(I) Intermediates Formed upon Activation of a Ni(II) α -Diimine Ethylene Polymerization Precatalyst with AlR₃ (R = Me, Et, and ^tBu), AlR₂Cl (R = Me, Et), and MMAO: A Comparative Study. *Organometallics* **2022**, *41*, 1015–1024. [[CrossRef](#)]
278. Obuah, C.; Omondi, B.; Nozaki, K.; Darkwa, J. Solvent and co-catalyst dependent pyrazolylpyridinamine and pyrazolylpyrroleamine nickel(II) catalyzed oligomerization and polymerization of ethylene. *J. Mol. Catal. A Chem.* **2014**, *382*, 31–40. [[CrossRef](#)]
279. Singh, A.; Maji, A.; Mohanty, A.; Ghosh, K. Design and synthesis of base-metal nickel(II) based catalysts: Studies on nearly selective formation of 1-butene from ethylene. *J. Organomet. Chem.* **2021**, *934*, 121631. [[CrossRef](#)]
280. Leone, G.; Losio, S.; Piovani, D.; Sommazzi, A.; Ricci, G. Living copolymerization of ethylene with 4-methyl-1-pentene by an α -diimine Ni(II)/Et₂AlCl catalyst: Synthesis of diblock copolymers via sequential monomer addition. *Polym. Chem.* **2012**, *3*, 1987–1990. [[CrossRef](#)]